ATLAS ITk

Outer EndCap of the Pixel detector

Design Validation and Performance

OEC Global Mechanical FEA Studies

Doc. v.2.0

Mauro Monti
Istituto Nazionale di Fisica Nucleare – Sezione di Milano

OEC FEA studies - introduction

A new Finite Element Model (v.3.0) of the overall Outer Endcap (OEC) has been built in *ANSYS,* to evaluate the mechanical performances of the global structures:

1. to perfom a detailed stress analysis of the L2, built using *ANSYS ACP* to simulate the composite structures;
2. to respond to actions/recommendations raised in the Report of the ITk Pixel Global Mechanics and Integration Final Design Review (May 14–16, 2024): *https://edms.cern.ch/document/3104932*.

The requirements placed on the Endcap Global Supports are summarized in the *ITk Pixel Global Supports Design Specifications - AT2-IP-ES-0007 Rev. 4* [1].

All the Thermo-Mechanical FEA results of the overall OEC are collected on EDMS: *OEC FEM Simulations - AT2-IP-EN-0054 v.1,* *https://edms.cern.ch/document/3086330/1*.

GM&I FDR (May 14–16, 2024) – FEA outcomes

The report of the GM&I FDR (see *https://edms.cern.ch/document/3104932*) identified a number of points of attention or aspects that should be further investigated and worked out by FEA. The Actions or Recommendations, to be addressed by the OEC Collaboration are:

A-10: *Results of a preliminary FEA simulation, showing only small deformations (inside the envelopes) as a consequence of gravity and cool-down, are very encouraging. Still, a full stress analysis needs to be completed as soon as possible.*

A-12: *FEA work on the stress on clips and mounting lugs still needs to be finalized.*

R-11: *The presented FEA results consider a uniform cool-down to −55 °C without any thermal gradient. In reality, temperature gradients are expected, mainly in the vertical direction (convection). The functional form of such gradients is unknown, but the sensitivity should be investigated. One could start with linear gradients of 10 ℃ degrees to get a feel for possible effects. If the sensitivity turns out to be very large, further studies are required.*

R-29: *For all FEA simulations, the inclination of the ATLAS detector by 0.708° should be implemented (even if it is probably irrelevant for all practical purposes).*

OEC performance specifications

Concerning the stress analysis, the specification *AT2-IP-ES-007 Rev. 4 section 4.5* [1] provides the Table below, which summarizes the detector masses to be used, and the following guidelines:

Sub-system	Item	Structure Mass Estimate (kg)			Design Values* (kg)		
		Structure	Services	Total	Structure	Services	Total
Inner System	Endcap A			59.6			71.52
	Barrel						
	Endcap C						
	Global Structure						
IST		6.4	0	6.4	7.68		7.68
Outer Barrel	Local Supports longerons(including modules and Type-0 services and PP0)	41.75	112.54	260.26	50.1	135.0	312.3
	Inclined Units (including cooling manifolds, Type-0 and PP0)	36.44			43.7		
	Global structures (shells, support points…)	39.61			47.5		
	Cooling Manifolds	29.92			35.9		
Outer Endcap A	CF end flanges, cylinders and rings (including Module and Type0)	21.6	27.6	53.7	25.92	33.12	64.44
	Cooling Manifolds	4.5			5.4		
Outer Endcap C	CF end flanges, cylinders and rings (including Module and Type0)	21.6	27.6	53.7	25.92	33.12	64.44
	Cooling Manifolds	4.5			5.4		
Beam Pipe		3.65	0	3.65	4.38	0	4.38
IPT		0.8	0	0.8	0.96	0	0.96
Pixel Detector with Beam Pipe		210.77	167.74	438.11	252.924	201.288	525.732

Table 1: Dector mass inventory.

1. *The design values include a 1.2 safety factor to account for uncertainties in the mass estimates.*
2. *The design values included in the previous table shall be used to verify that the performance of the global structures of the pixel detector complies with the requirements defined in section 5 of the specification.* ***However, an additional safety factor of 1.2 shall be considered to verify the safety of the global structures and assemblies.***
3. *Maximum stress level must be less than 1/10 of the yield (section 4.7).*

Overall OEC FEM model

The **FEM model v. 3.0** (fig.1) **includes all relevant structures involved in the structural and thermo-mechanical response of the OEC to the performance specifications**. It is based on the currently most up-to-dated OEC Master CAD model: ***np49-04-100_asm_17-07-2024.stp***, **https://edms.cern.ch/document/2052151/3**.

After a long process of geometries preparation, to make the model suitable for the FEA environment, it ultimately includes 2,149 active bodies:

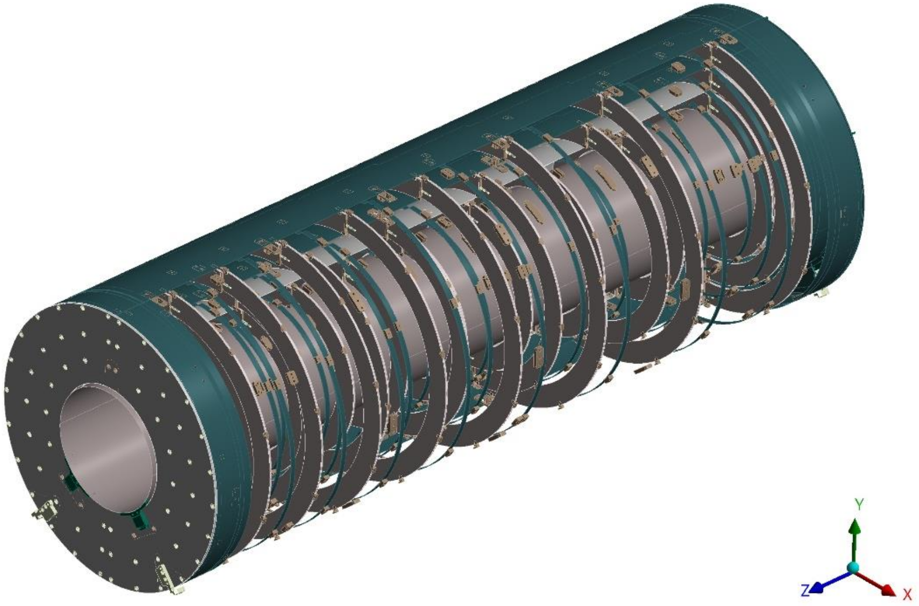

Figure 1: overall OEC FEM model v.3.0.

- L2, L3, L4 half-shells/end flanges
- Interlinks, mounting lugs
- Front and rear supports
- Half-Rings (22xL2, 16xL3, 18xL4)
- C-supports of type-1 services
- VEE and FLAT sliders
- IST adjustable saddle supports
- IST (portion).

L2 composite Global Structures

Composite Global Structures of the L2 (fig.2) **and Front/Rear supports have been built using *ANSYS ACP*, in order to perform the stress analysis ply by ply:**

- Half-shells & front/rear flanges: M55J/EX1515 $[90/45/-45/0]_s$ – t. 0.6 mm
- Front support: CFRP parts M55J/EX1515 $[90/45/-45/0]_s$ – t. 0.6 mm
- Rear support: CFRP parts M55J/EX1515 $[90/45/-45/0]_{5s}$ – t. 3.0 mm.

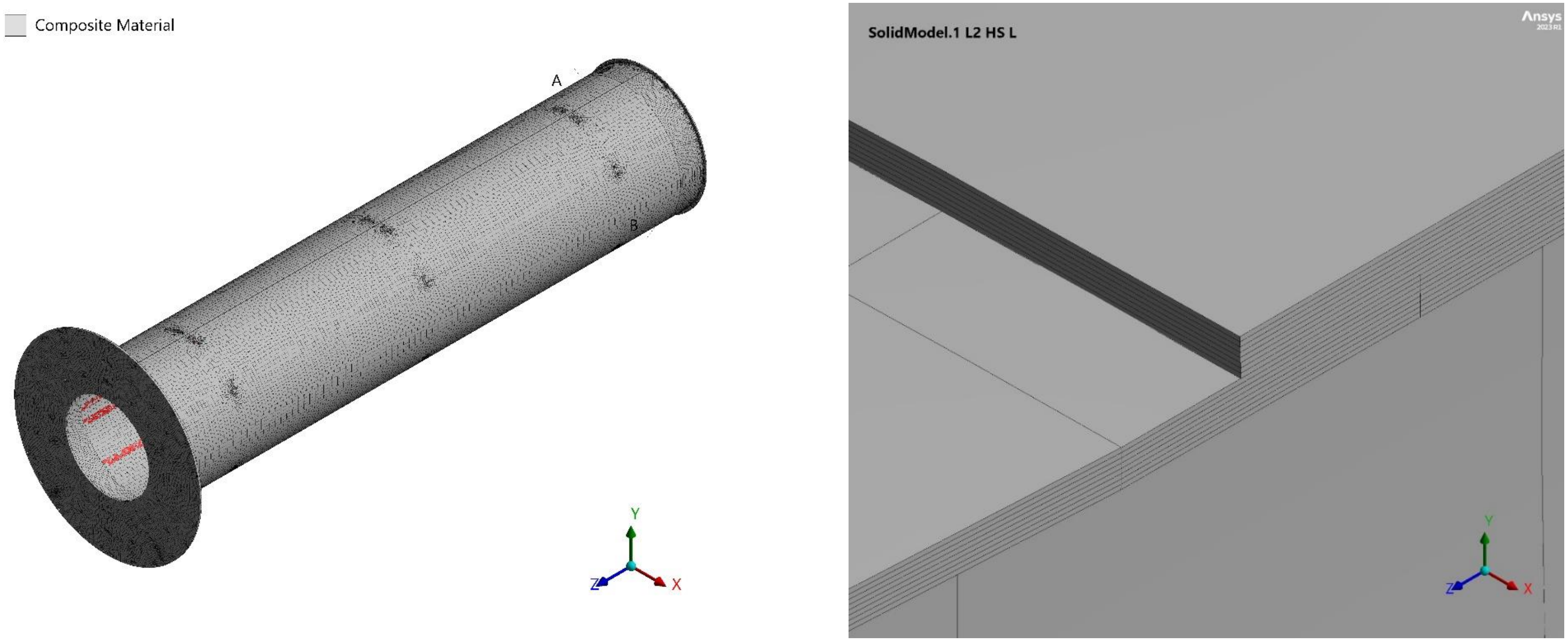

Figure 2: L2 composite Global Structures in the FEM model v.3.0.

Overall OEC FEM model: mesh

The **mesh of the OEC FEM model** (fig.3) **consists of:**

- ≈ 4 million of quadratic 3D bricks elements / quadratic shells
- ≈ **11.3 million of nodes**.

Mesh quality controlled by elements aspect ratio.

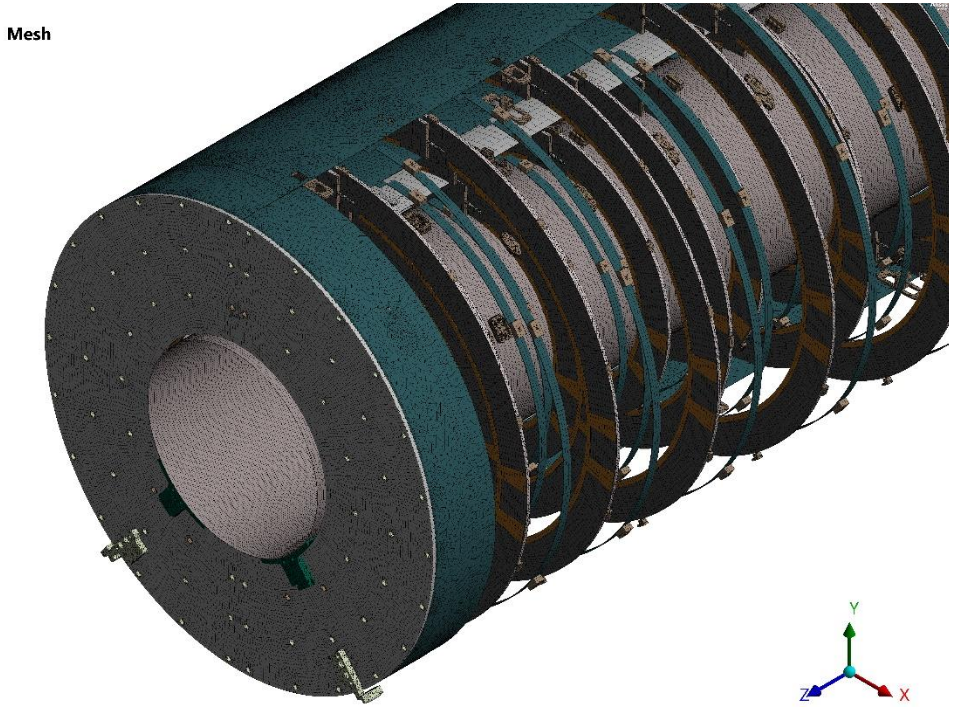

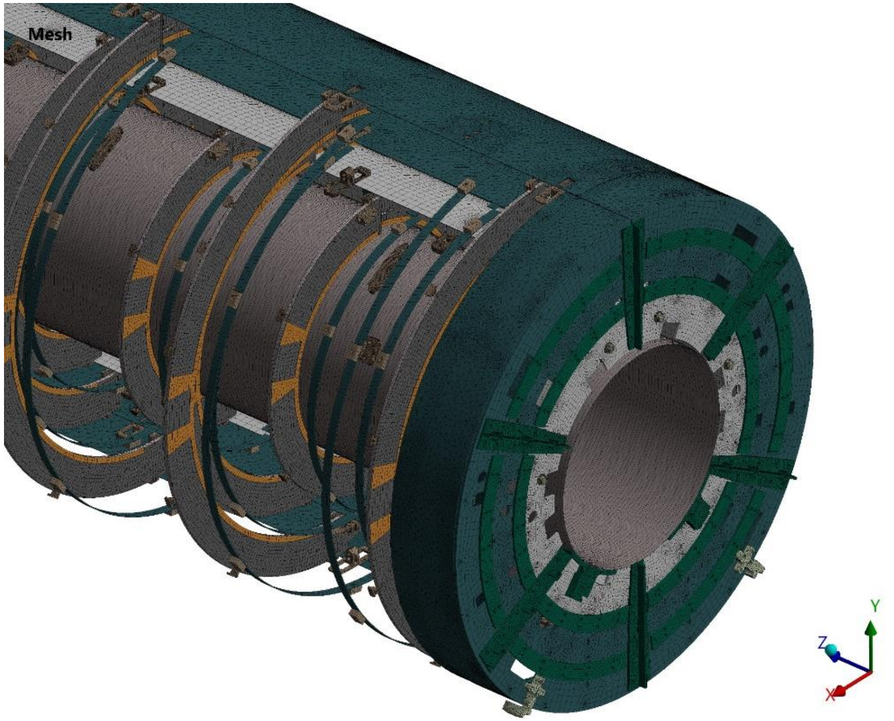

Figure 3: Mesh of the OEC FEM model v. 3.0.

Overall OEC FEM model: contacts

Connections between active bodies of the OEC FEM model: **4,619 contacts, all verified**. **All contacts are defined** to be rigidly ***bonded***, **except** the **contact regions between** the **IST** and the **saddle supports** (fig.4) on the front of the detector, **defined as «*no separation*»** (**IST free to move in Z**, to accommodate the CTE mismatch IST/OEC).

Support #	Location z [mm] and phi [deg]*	Ux	Uy	Uz
1	± 1111.5 and +39 ° ±5°	0	0	free
2	± 1111.5 and -39°±5° *	0	0	free
3	± 2984.5 and +39°±5°	0	0	0
4	± 2984.5 and -39°±5°	0	0	0

Table 2: Supports of IST /OEC interface [2].

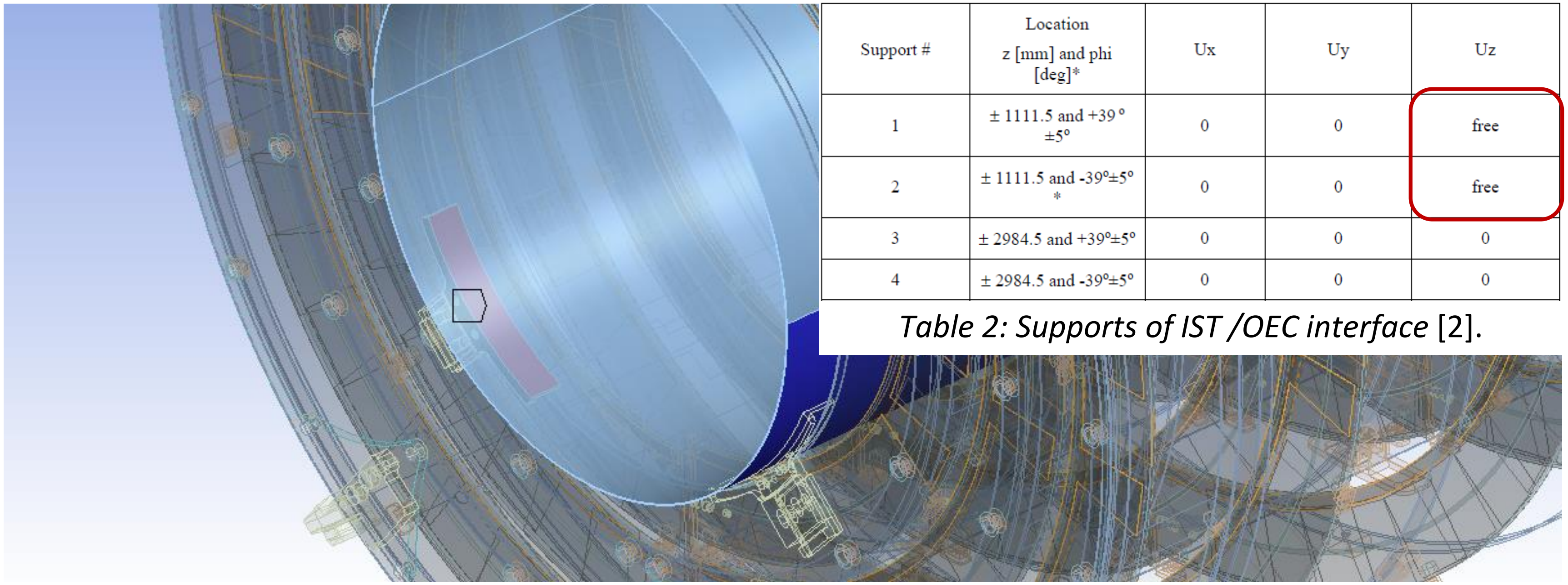

Figure 4: IST/OEC contacts at low Z.

Materials properties

Table 3, below, summarizes the material properties used in the OEC FEA.
Orthotropic properties of composites/laminates calculated using ***EsaComp*** software.

PART	MATERIAL	Density [Kg/m^3]	Young's Modulus [GPa]			Poisson's ratio	CTE [1e^{-6}/°C]		
			X	Y	Z	XY	X	Y	Z
Half-ring facings	CFRP K13C2U/EX-1515 [0/90/0] V.f. 48.9%	1645	295.5	150.5	150.5	0.0117	-0.713	0.153	0.153
Half-ring carbon foam	Looked Martin K9 δ=0.40 g/cm^3	400	0.293			0.33	1.0		
Half Ring cooling pipe & fittings VEE/FLAT sliders Supporting inserts	Titanium GR2	4500	105			0.34	8.6		
Half Ring electrical breaker	Ceramic 97.6% Alumina	3760	340			0.22	6.9		
Half-ring bus tape v.6	Laminate Copper/Kapton	4805	53.1			0.34	18.2		
Half-ring lugs/closeouts Interlinks/mounting lugs/spacers	ULTEM 1000	1270	3.2			0.36	50		
Half-shells/end flanges Front support Rear support Rear junction ring and plates	CFRP M55J/EX-1515 [90/45/-45/0]$_S$, CFRP M55J/EX-1515 [90/45/-45/0]$_{10S}$ CFRP M55J/EX-1515 [90/45/-45/0]$_{5S}$ V.f. 46.5% (all)	1514	89.85			0.324	0.261		
Front support core	Honeycomb	80	1.00E-03	1.00E-03	2.55E-01	0.49	-	-	-

Table 3: Materials properties used in the OEC FEA studies.

Materials properties

The material properties of the L2 composite Global Structures are based on the properties of the pre-preg MJ55/EX1515, Vf. 46.5%, 80 gsm, CPT 75 µm, listed in the table 4 below (*ANSYS material database*).

Properties of Outline Row 4: Pre-preg M55J EX-1515 80gsm 46.5%vf CPT_75.0 um

	A	B		
1	Property	Value		
2	Material Field Variables	Table		
3	Density	1.514E-06	kg mm^-3	
4	Orthotropic Instantaneous Coefficient of Thermal Expansion	Tabular		
5	Properties Row 4: Orthotropic Instantaneous Coefficient of Thermal Expansion			

	A	B	C		D
6	A	B	C		D
7	Temperature (C)	Coefficient of Thermal Expansion X direction (C^-1)	Coefficient of Thermal Expansion Y direction (C^-1)		Coefficient of Thermal Expansion Z direction (C^-1)
8	-55	-1.05E-06	3.47E-05	[11]	3.47E-05
9	20	-1.05E-06	6.1E-05	[9]	6.1E-05
10					

	A	B		
11	Orthotropic Elasticity			
12	Young's Modulus X direction	2.5897E+05	[9]	MPa
13	Young's Modulus Y direction	4491.7	[9]	MPa
14	Young's Modulus Z direction	4491.7	[9]	MPa
15	Poisson's Ratio XY	0.25	[9]	
16	Poisson's Ratio YZ	0.27	[9]	
17	Poisson's Ratio XZ	0.25	[9]	
18	Shear Modulus XY	2466.1	[9]	MPa
19	Shear Modulus YZ	1773	[9]	MPa
20	Shear Modulus XZ	2466.1	[9]	MPa
21	Orthotropic Stress Limits			
22	Tensile X direction	1469	[10]	MPa
23	Tensile Y direction	46	[11]	MPa
24	Tensile Z direction	46	[11]	MPa
25	Compressive X direction	-566	[10]	MPa
26	Compressive Y direction	-89.8	EsaComp calculation	MPa
27	Compressive Z direction	-89.8	EsaComp calculation	MPa
28	Shear XY	32.06	EsaComp calculation	MPa
29	Shear YZ	32.06	EsaComp calculation	MPa
30	Shear XZ	32.06	EsaComp calculation	MPa
31	Ply Type			
32	Type	Regular		

Table 4: Properties of pre-preg M55J/EX15151 used in the OEC FEA studies.

Distributed masses

Table 5 below summarizes the distributed masses of non-explicitly modeled geometries, applied in the OEC FEA:

- **IS+IST+Beam pipe masses**: applied on to the lower half of IST.
- **OB Type-1 services mass**: on to the outer surface of L4 half-shells (R= 325.1 mm).
- **Pixel modules masses**: on to half-rings CFRP footprints.

Sub-system	*Item*	*ATLAS Project Document No:*	*Note*	*Mass (kg)*
Inner System	Endcap A, Barrel, Endcap C, Global Structure	*EDMS: AT2-IP-ES-0007 Rev.4.0*	Design Value	***35.760***
IST		*EDMS: AT2-IP-ES-0007 Rev.4.0*	Design Value	***2.160***
Beam Pipe		*EDMS: AT2-IP-ES-0007 Rev.4.0*	Design Value	***2.19***
Outer Barrel	Type-1 services (Side A or Side C)	*EDMS: AT2-IP-EN-0024 Rev.1.0*	-	***53.60***
Outer Endcap (A or C)	Pixel Modules - L4 Half-rings	*EDMS: AT2-IP-ES-0005 Rev.5.1*	Estimated Module Mass per unit of active area EMM = 0.3 g/cm^2	***2.279***
	Pixel Modules - L3 Half-rings	*EDMS: AT2-IP-ES-0005 Rev.5.1*		***1.714***
	Pixel Modules - L2 Half-rings	*EDMS: AT2-IP-ES-0005 Rev.5.1*		***1.714***
	Electrical Services Type-1 (total x 3 layers)	*EDMS: AT2-IP-EN-0024 Rev.1.0*	Design Value	***24.300***
	Electrical Services Type-1 - Layer 2		*Design value divided layer by layeraccording to the number of the half-rings*	***9.546***
	Electrical Services Type-1 - Layer 3			***6.943***
	Electrical Services Type-1 - Layer 4			***7.811***
	Cooling Services Type-1 (total x 3 layers)	*EDMS: AT2-IP-EN-0024 Rev.1.0*	Design Value	***4.700***
	Liquid CO_2 inside cooling pipes (total x 3 layers)	-	Estimated	***2.116***

Table 5: Distributed masses applied in the OEC FEA.

OEC Type-1 services

Type-1 electrical services are bundled into four identical annular volumes, whilst the **Type-1 cooling structures** are grouped together into a fifth annular volume. Type-1 services are not modeled explicitly, but the relevant bundle surfaces have been imprinted on the inner wall of the half-shells and divided up into as many sections as the half-rings (fig.5). The distributed masses have been applied on to the footprints.

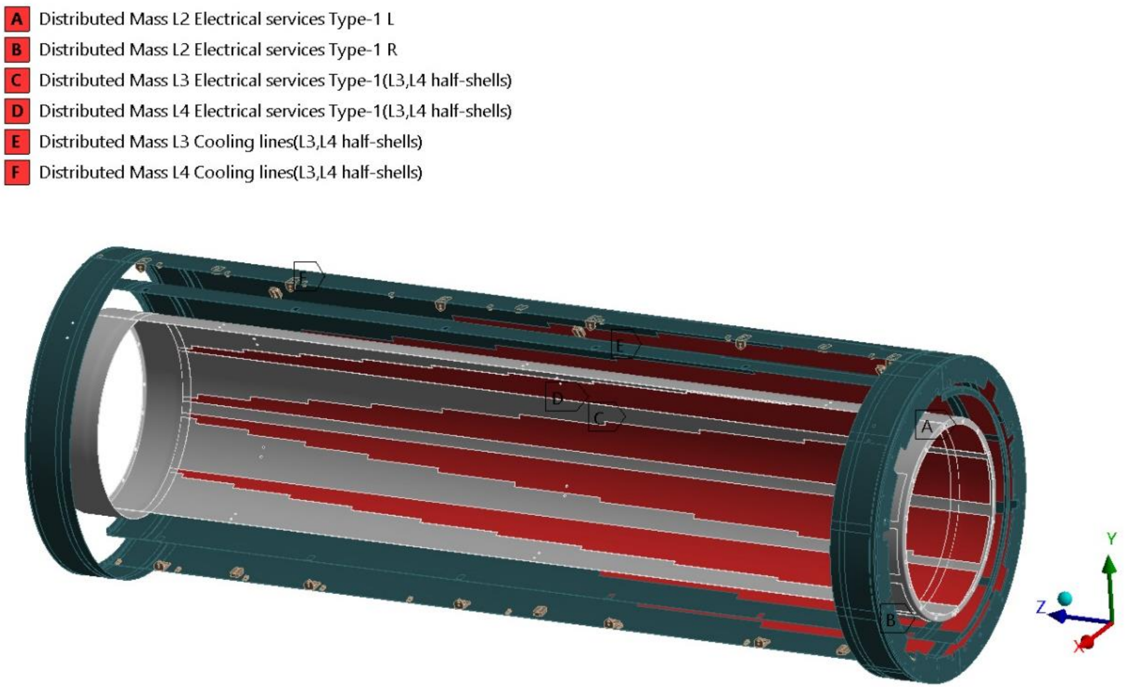

Figure 5: Type-1 services footprints on half-shells.

OEC Cooling manifolds: reaction forces/moments

Type-1 cooling lines are not modeled explicitly in the OEC FEM model, but the forces/moments exerted by the outlet cooling pipes on the electrical breaker fittings of the L2 half-rings have been evaluated @-55°C by a separate FEA study (L. Cunningham) and then applied in the structural FEA of the L2 , to evaluate their effects.

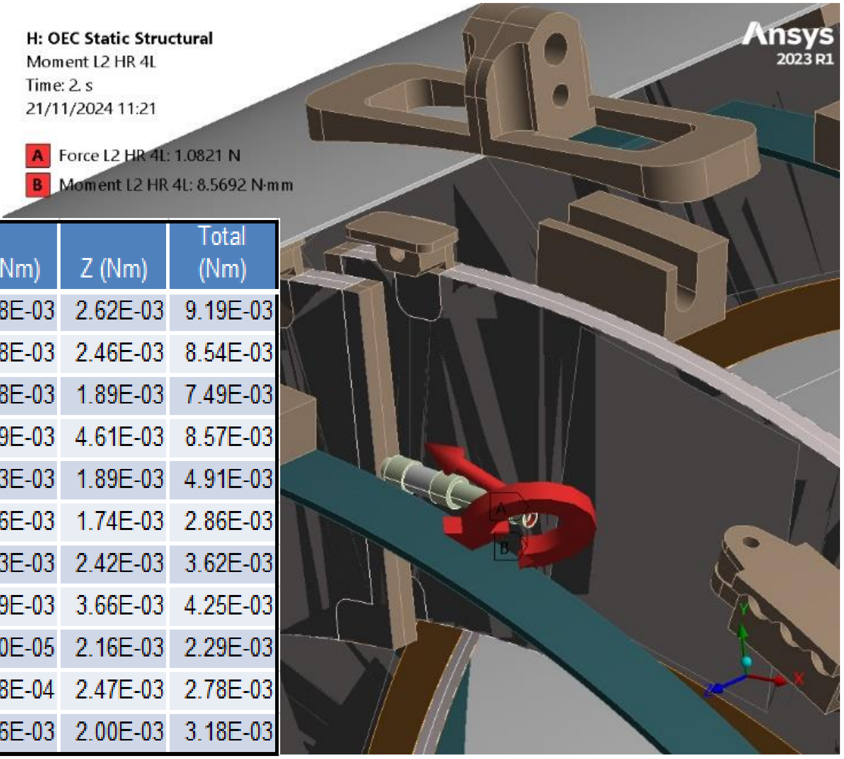

Load	Ring no	X (N)	Y (N)	Z (N)	Total (N)	X (Nm)	Y (Nm)	Z (Nm)	Total (Nm)
-55°C	1	-0.43	0.63	0.73	1.06	5.85E-03	-6.58E-03	2.62E-03	9.19E-03
	2	-0.42	0.57	0.68	0.98	5.35E-03	-6.18E-03	2.46E-03	8.54E-03
	3	-0.4	0.51	0.66	0.92	4.75E-03	-5.48E-03	1.89E-03	7.49E-03
	4	-0.42	0.72	0.69	1.08	4.45E-03	-5.69E-03	4.61E-03	8.57E-03
	5	-0.17	0.61	0.57	0.86	2.83E-03	-3.53E-03	1.89E-03	4.91E-03
	6	-0.41	0.54	0.73	1	2.52E-04	-2.26E-03	1.74E-03	2.86E-03
	7	-0.15	0.52	0.39	0.67	9.00E-04	-2.53E-03	2.42E-03	3.62E-03
	8	-0.17	0.45	0.37	0.61	-1.06E-03	-1.89E-03	3.66E-03	4.25E-03
	9	-0.27	0.29	0.14	0.42	-7.72E-04	6.10E-05	2.16E-03	2.29E-03
	10	-0.07	0.21	0.11	0.25	9.91E-04	8.08E-04	2.47E-03	2.78E-03
	11	-0.04	0.21	0.11	0.24	-2.42E-04	2.46E-03	2.00E-03	3.18E-03

Table 6: Forces/moments of the Type-1 cooling lines on the L2 half-rings.

1. OEC thermo-mechanical FEA: Layer 2

Structural FEA of the fully integrated OEC Layer 2, mounted on T-trolley, thermally cycled in climate chamber.

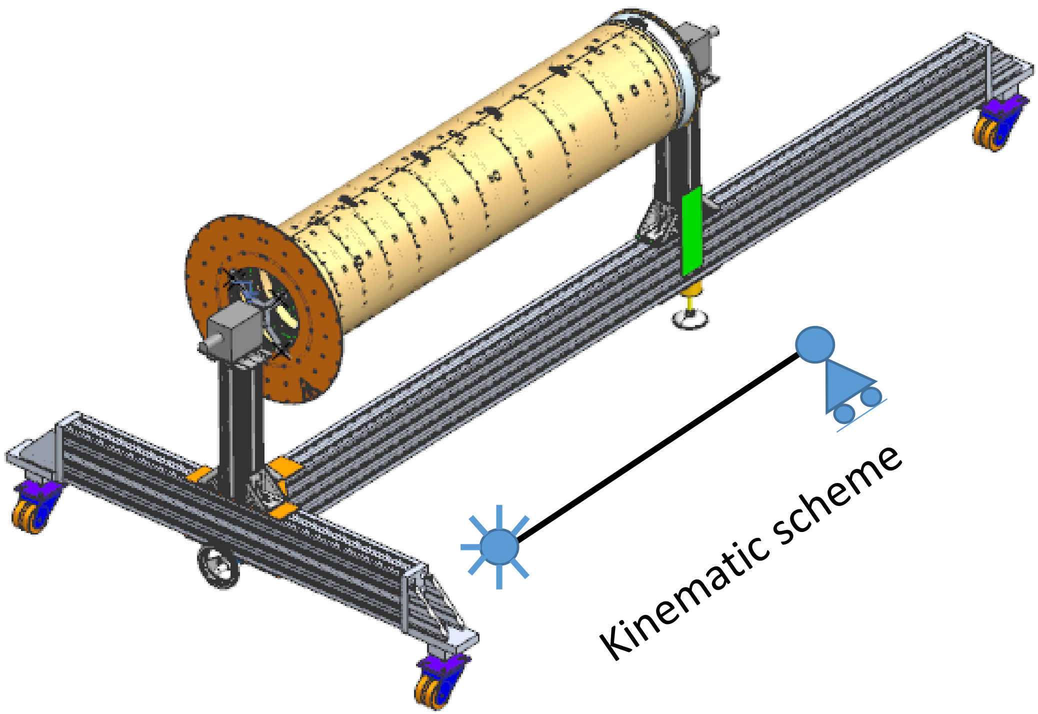

Support with spherical flange bearing on both sides

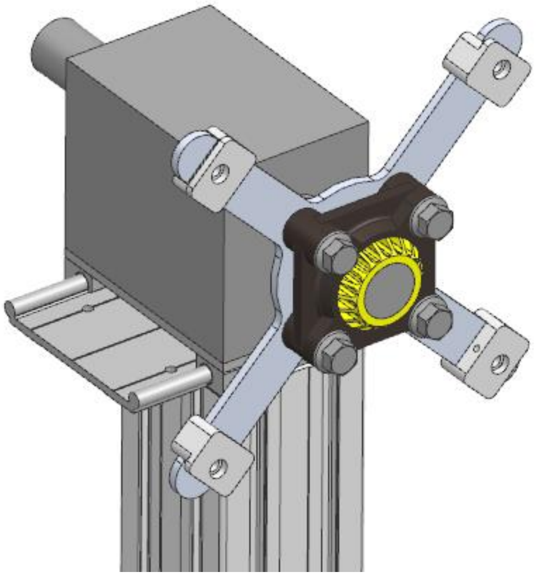

Figure 6: Supporting scheme of the fully integrated Layer 2 of the OEC.

OEC thermo-mechanical FEA: Layer 2

Kinematics of the T-trolley supports implemented in the FEM model as **constraints conditions on the hole of the cruciform supports** (remote displacements).

Front support

UX = 0
UY = 0
UZ = 0
ROTX = free
ROTY = free
ROTZ = 0

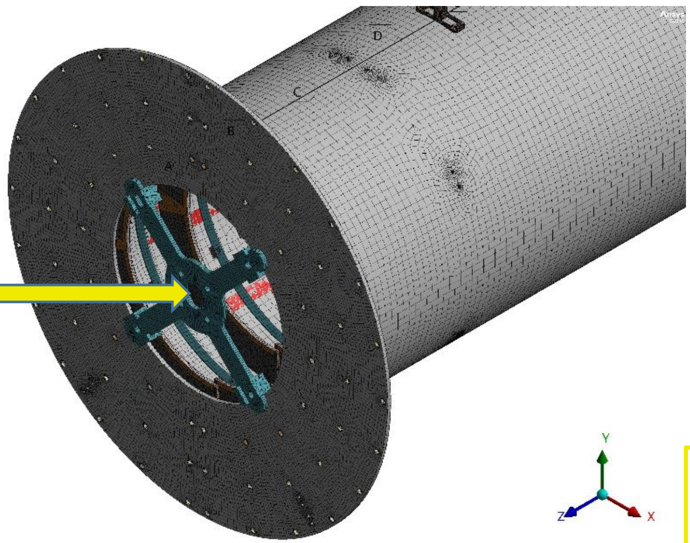

Rear support

UX = 0
UY = 0
UZ = free
ROTX = free
ROTY = free
ROTZ = free

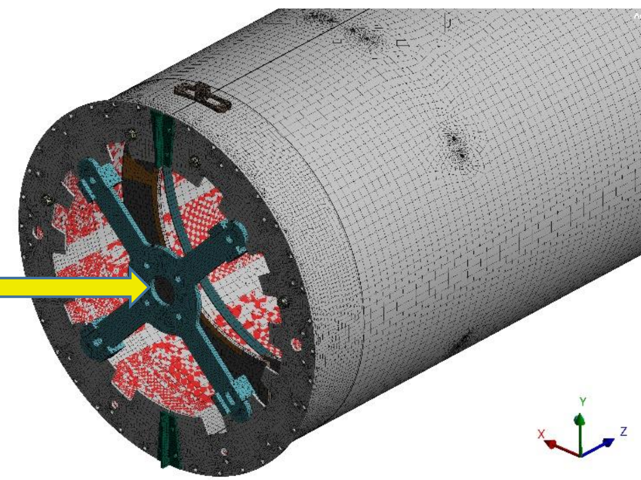

Figure 7: Constraint conditions of the fully integrated Layer 2 of the OEC.

OEC thermo-mechanical FEA: Layer 2

- **Load step 1**: Gravity x 1.2 safety factor.
- **Load step 2**: Cooling down from +20°C to – 55°C (plus forces and moments exerted by the cooling lines on the EB fittings of the half-rings). Max ΔT = -75°C.

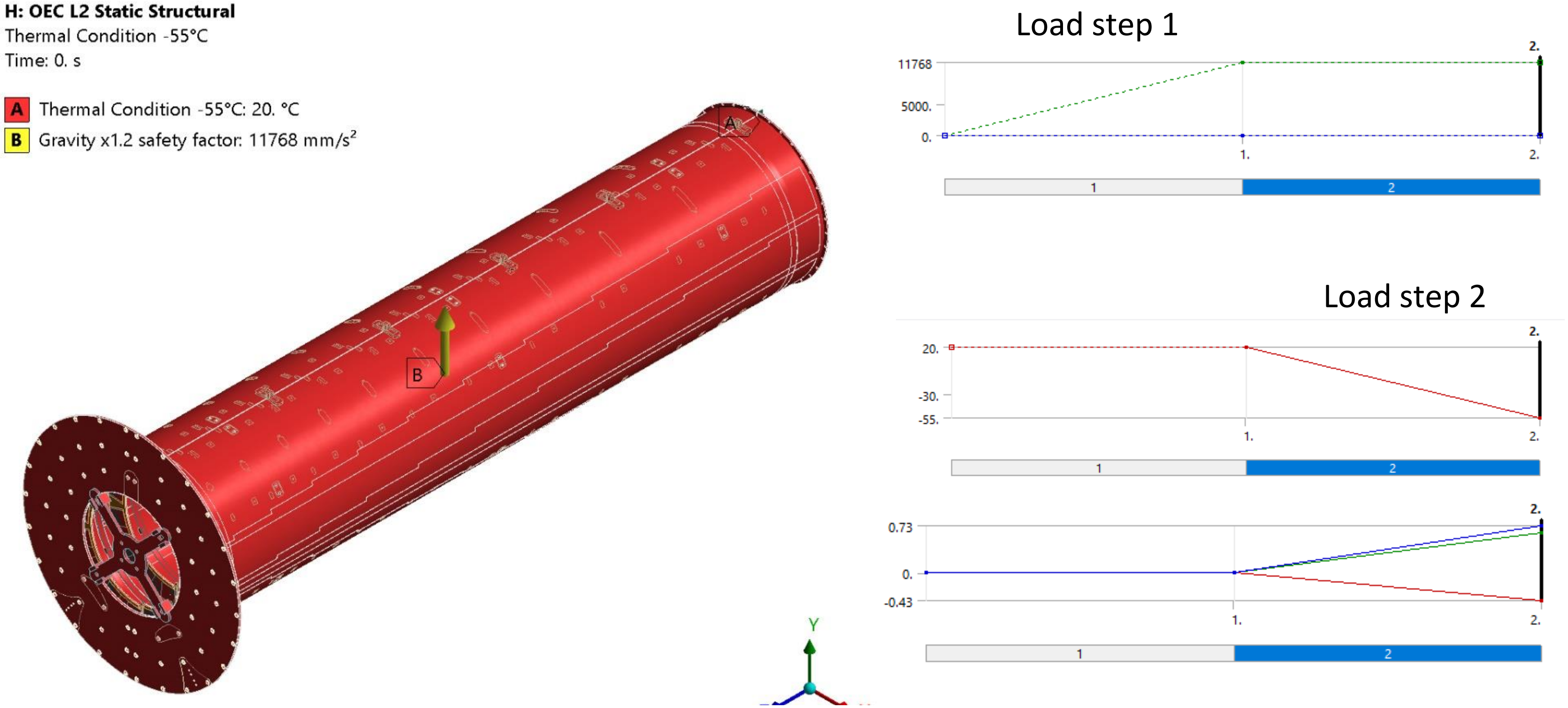

Figure 8: Load steps applied in the FEA of the Layer 2 of the OEC.

OEC thermo-mechanical FEA: Layer 2

Criteria for stress analysis of the composite Global Structures

The c**omposite Global Structures of the L2 have been built using ANSYS ACP, in order to perform the stress analysis ply by ply.**

Different failure criteria could be used to evaluate the strength of composite structures , depending on the available material properties.

After careful evaluations, it has been decided to proceed using the **Maximum Stress Failure Criterion, evaluating the maximum (+) tensile / minimum (-) compressive S_1 stress of the plies along fibers direction**. This because we can rely on Toray datasheet [10], which provides the tensile strength and the compressive strength along fibers direction of the prepreg M55J/EX1515 60% fiber volume.

LAMINATE DATA - TORAY M55J (78 Msi/538 GPa) PAN GRAPHITE/EX-1515

Property	Condition	Method	Results	
Tensile Strength 0°	RTD	ASTM D 3039	1896 MPa	275 ksi
Tensile Modulus 0°	RTD	ASTM D 3039	354 GPa	50 Msi
Compressive Strength 0°	RTD	ASTM D 6641	731 MPa	106 ksi
Compressive Modulus 0°	RTD	ASTM D 6641	310 GPa	45 Msi
Flexural Strength 0°	RTD	ASTM D 7264	1089 MPa	158 ksi
Flexural Modulus 0°	RTD	ASTM D 7264	317 GPa	46 Msi
Interlaminar Shear Strength	RTD	ASTM D 2344	62 MPa	9 ksi
Standard 121°C (250°F) Autoclave cure 85 psi, normalized to 60% fiber volume.				

Table 7: Toray datasheet, prepreg M55J/EX1515 Vf 60%.

OEC thermo-mechanical FEA: Layer 2

Toray datasheet refers to 60% fiber volume fraction pre-preg, so **the strength values of the table 7 have been scaled to 46.5% fiber volume fraction.** The details of this calculation are collected in two backup slides. The reference values calculated are:

1. **Tensile strength: $F_{1t,(46.5\%)}$ = 1469 MPa;**
2. **Compressive strength: $F_{1c,(46.5\%)}$ = -566 MPa.**

Evaluating the strength of composite structures using the Maximum Stress Failure Criterion, **the First Ply Failure (FPF) will occur when S_1 stress exceeds the corresponding strength of the ply along the fiber direction.**

Failure under tension of continuous-fiber composites is due to rupture of the fibers, while failure under longitudinal compression is associated with microbuckling of the fibers within the matrix.

Clearly, **the compressive strength is the most critical strength parameter**.

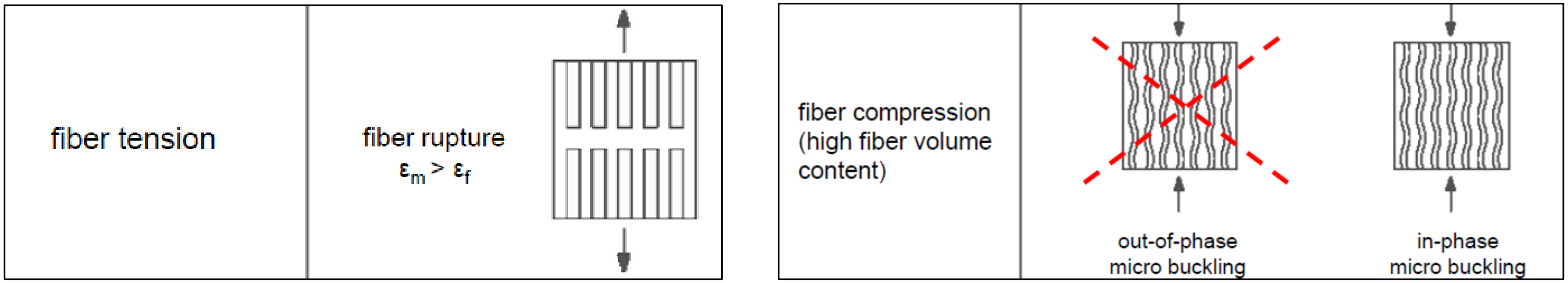

Figure 9: Fibers failure modes under tensile and compressive stress.

OEC thermo-mechanical FEA: Layer 2

A **Safety Factor (SF)** can be defined as follow:

SF = Ultimate strength / Maximum S_1 stress.

The **expected average S_1 stress should be** [1]:

1. **Tensile stress:** $S_{1t,av} < F_{1t}/10$ = 1469/10 = **146.9 MPa** => SF > 10
2. **Compressive stress:** $S_{1c,av} > F_{1c}/10$ = -566/10 = -**56.6 MPa** => SF > 10

Local peaks of stress should be evaluated each time, to establish weather they are due to a real effect rather than to a singularity (edge effect, mesh defeact, etc.). **The most important example of edge effect concerns the Shear Stress. It is proven that the peaks of Shear Stress on the edges increase as the mesh density increases, but they are fake if the edges are shared with free surfaces, on which the Shear Stress must be equal to zero** (Figure 10).

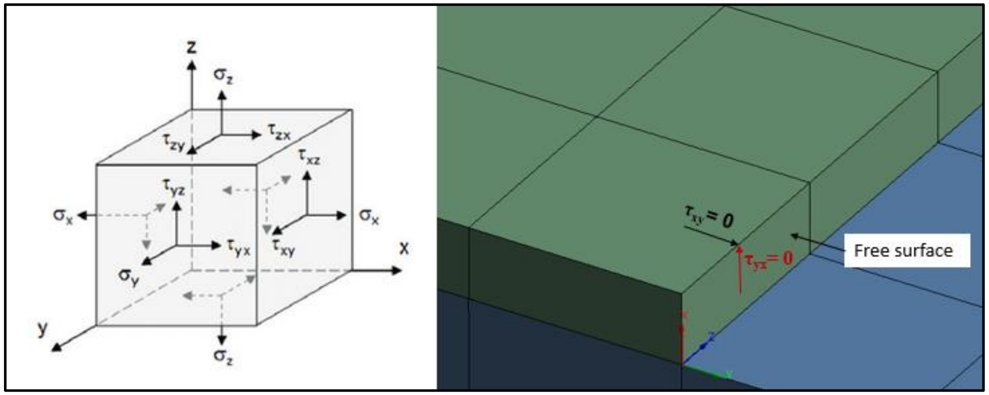

Figure 10: left ,tri-axial stress state of a solid; right, shear stress equal to zero on external free surface.

OEC thermo-mechanical FEA: Layer 2

Criteria for stress analysis of isotropic components

Stress analysis of isotropic parts can be performed evaluating Von Mises equivalent stress.

For a ductile material, starting from the Yield Stress value (σ_y), in a classic structural analysis a safety factor 1.5 defines the maximum admissible stress:

$$\boldsymbol{\sigma_{adm} = \sigma_y/1.5}$$

However, **the expected average Von Mises stress**, according to the specification [1], **should be**:

$$\boldsymbol{\sigma_{eq,av} < \sigma_y/10}.$$

- **ULTEM 1000,** unreinforced amorphous polyetherimide (PEI) resin (**interlinks, mounting lugs, inserts** of the Front Support):
  - **Yield Stress: σ_y = 105 MPa @ T = +20°C** (not irradiated).
  - Maximum Admissible Stress: $\boldsymbol{\sigma_{adm}} = \sigma_y/SF = 105/1.5$ **= 70 MPa.**
  - Expected average Von Mises stress: $\boldsymbol{\sigma_{eq,av}} < \sigma_y/10 = 105/10$ **= 10.5 MPa**.
- **Titanium grade II annealed** (**inserts** of the Front Support):
  - **Yield Stress: σ_y = 340 MPa @ T = +20°C**.
  - Maximum Admissible Stress: $\boldsymbol{\sigma_{adm}} = \sigma_y/SF = 340/1.5$ **= 226 MPa.**
  - Expected average Von Mises stress: $\boldsymbol{\sigma_{eq,av}} < \sigma_y/10 = 340/10$ **= 34 MPa**.

OEC thermo-mechanical FEA: Layer 2 results

Load step 1: Gravity x 1.2 safety factor

Vertical (Y axis) deformation

$|UY_{min}|$ = 31.3 µm < 0.5 mm (Spec. Range [1]).

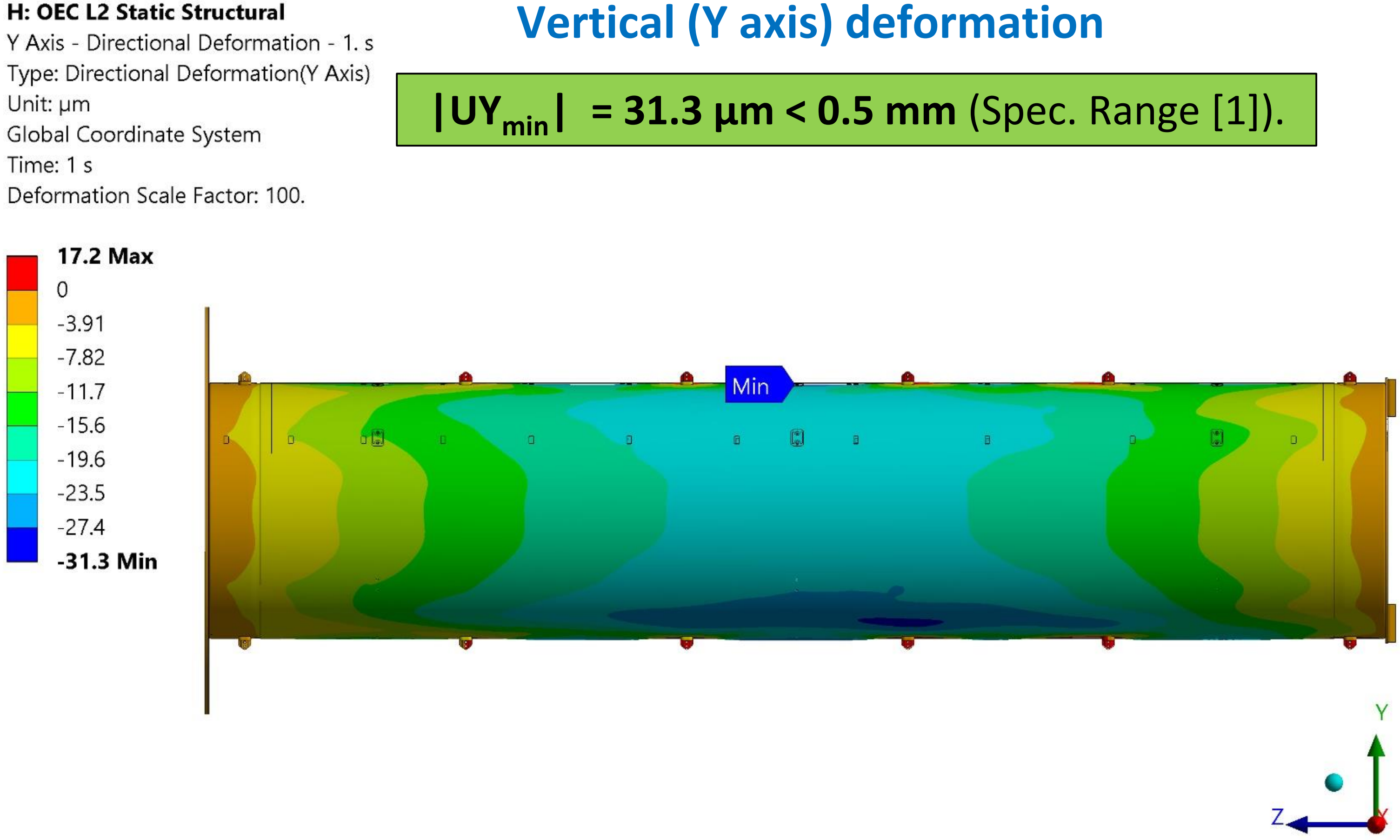

Figure 11: OEC L2 – Vertical deformation of the Global Structures under gravity.

OEC thermo-mechanical FEA: Layer 2 results

Load step 1: Gravity x 1.2 safety factor

Load step 1 produces small stresses on the composite Global structures, <u>everywhere</u>:

$S_{1,max} \leq 5$ MPa
$S_{1,min} \geq -4.8$ MPa
SF > 10

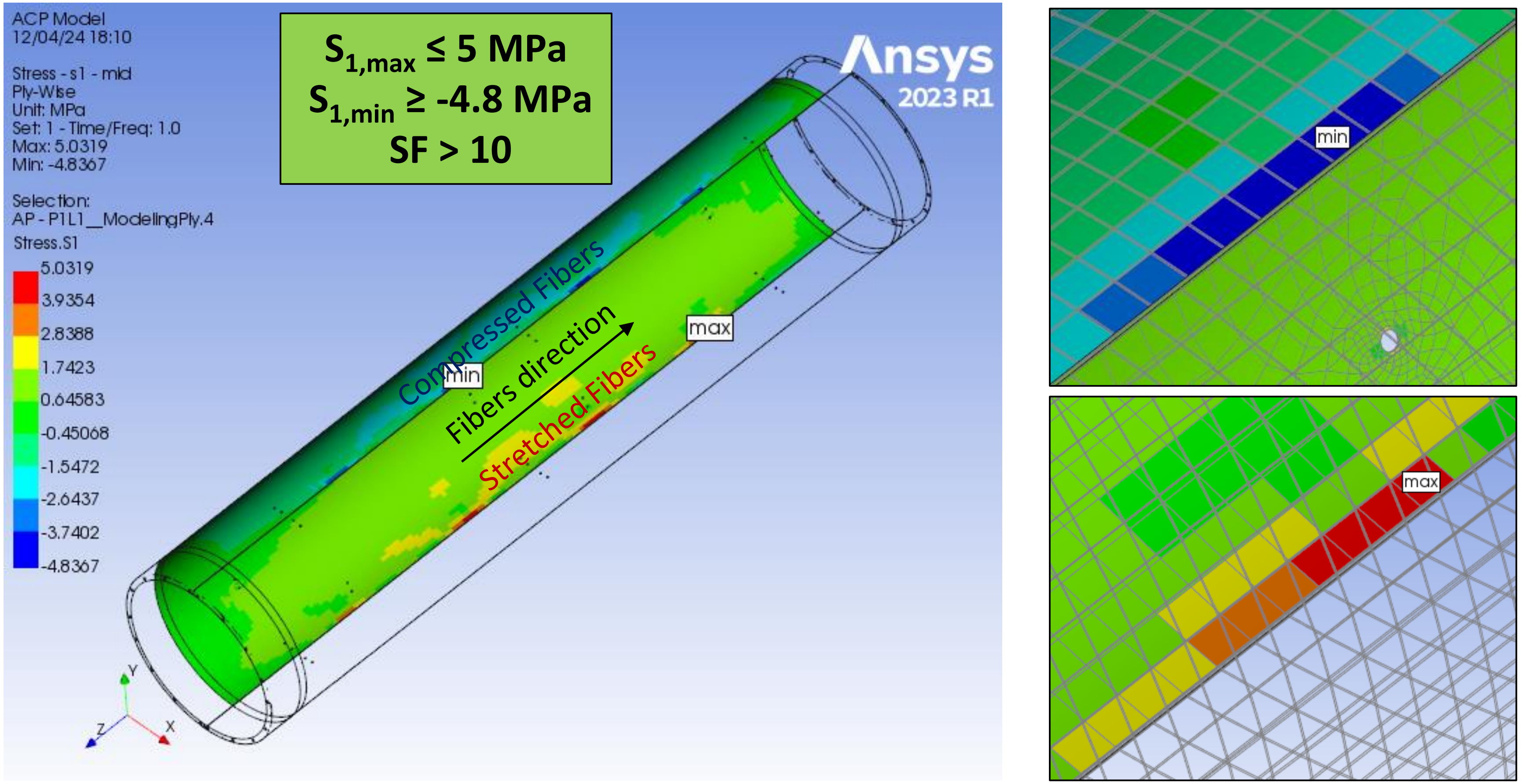

Figure 12: Max/Min S_1 stress found on Global Structures under load step 1(Left hand half-shell, 0° ply).

OEC thermo-mechanical FEA: Layer 2 results

Load step 2: Cooling down from +20°C to – 55°C

Total deformation

$USUM_{max}$ = 906 µm

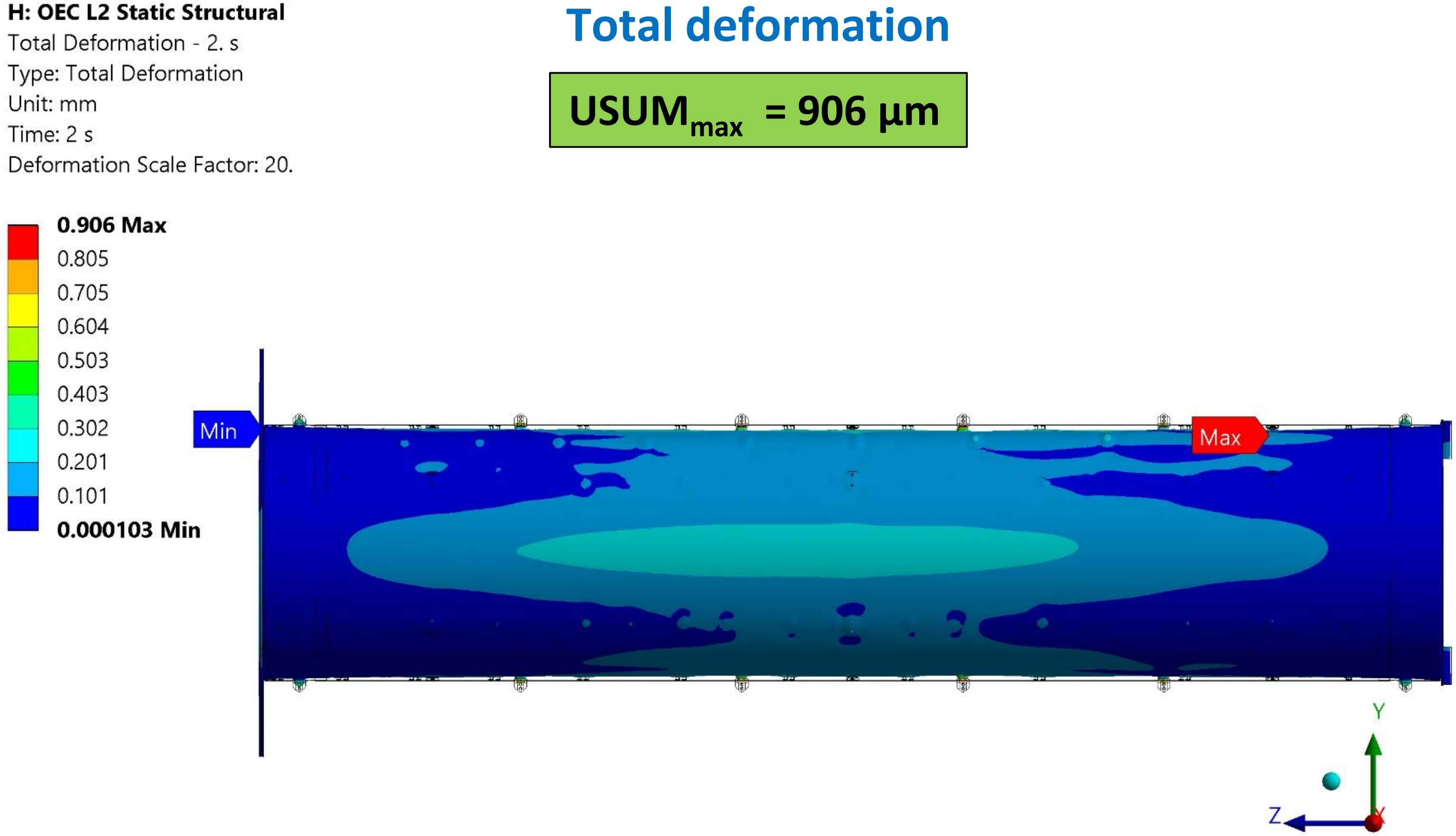

Figure 13: OEC L2 – Total deformation after cooling down (ΔT=-75°C).

OEC thermo-mechanical FEA: Layer 2 results

Load step 2: Cooling down from +20°C to – 55°C

Table 8, below, collects S_1 stress results calculated ply by ply, at the end of the load step 2 (T=-55°C) for L2 half-shells, front and rear flanges.

Ply		Half-shell left		Half-shell right	
		Max s1 tensile stress	Min s1 compressive stress	Max s1 tensile stress	Min s1 compressive stress
		MPa	MPa	MPa	MPa
1-bottom	90	98.8	-141.4	99.1	-147.1
2	45	101.7	-116.4	108.8	-123.3
3	-45	82.4	-101.9	80.5	-103.0
4	0	29.0	-98.4	29.6	-91.7
5	0	5.0	-84.0	7.9	-83.7
6	45	24.9	-112.5	21.4	-112.1
7	-45	38.2	-137.0	52.5	-131.2
8-top	90	54.2	-149.1	51.9	-145.4

Ply		Front flange left		Front flange right	
		Max s1 tensile stress	Min s1 compressive stress	Max s1 tensile stress	Min s1 compressive stress
		MPa	MPa	MPa	MPa
1-top	90	85.5	-179.6	83.1	-182.2
2	45	51.4	-150.6	51.4	-150.3
3	-45	36.6	-133.0	33.1	-125.8
4	0	17.3	-96.4	8.5	-103.7
5	0	25.4	-100.7	27.0	-103.7
6	45	61.2	-132.5	55.1	-127.6
7	-45	75.9	-126.1	64.6	-133.8
8-bottom	90	108.9	-133.9	83.4	-142.1

Ply		Rear flange left		Rear flange right	
		Max s1 tensile stress	Min s1 compressive stress	Max s1 tensile stress	Min s1 compressive stress
		MPa	MPa	MPa	MPa
1-top	90	85.1	-177.7	86.9	-179.9
2	45	55.4	-150.1	56.3	-149.7
3	-45	37.7	-125.1	37.1	-125.4
4	0	10.0	-70.6	11.6	-70.7
5	0	3.1	-59.0	2.8	-59.6
6	45	12.2	-88.0	11.5	-87.9
7	-45	17.7	-105.3	18.1	-104.9
8-bottom	90	24.9	-135.0	25.2	-133.7

Table 8: Half-shells/flanges, Max/Min S1 stress along fiber direction, ply by ply, @-55°C.

$S_{1t,max}$ = 108.8 MPa

Max Tensile stress: SF>10

$S_{1c,min}$ = -182.2 MPa

Min compressive stress: SF>3

Let's have a look at this peak, in detail (next slide).

OEC thermo-mechanical FEA: Layer 2 results

Load step 2: Cooling down from +20°C to – 55°C

Figure 14 shows small regions on the right-hand front flange where S_1 compressive stress has local peeks on the top ply (90° ply), while the rest of the composite structure is above -56.6 MPa, with SF > 10.

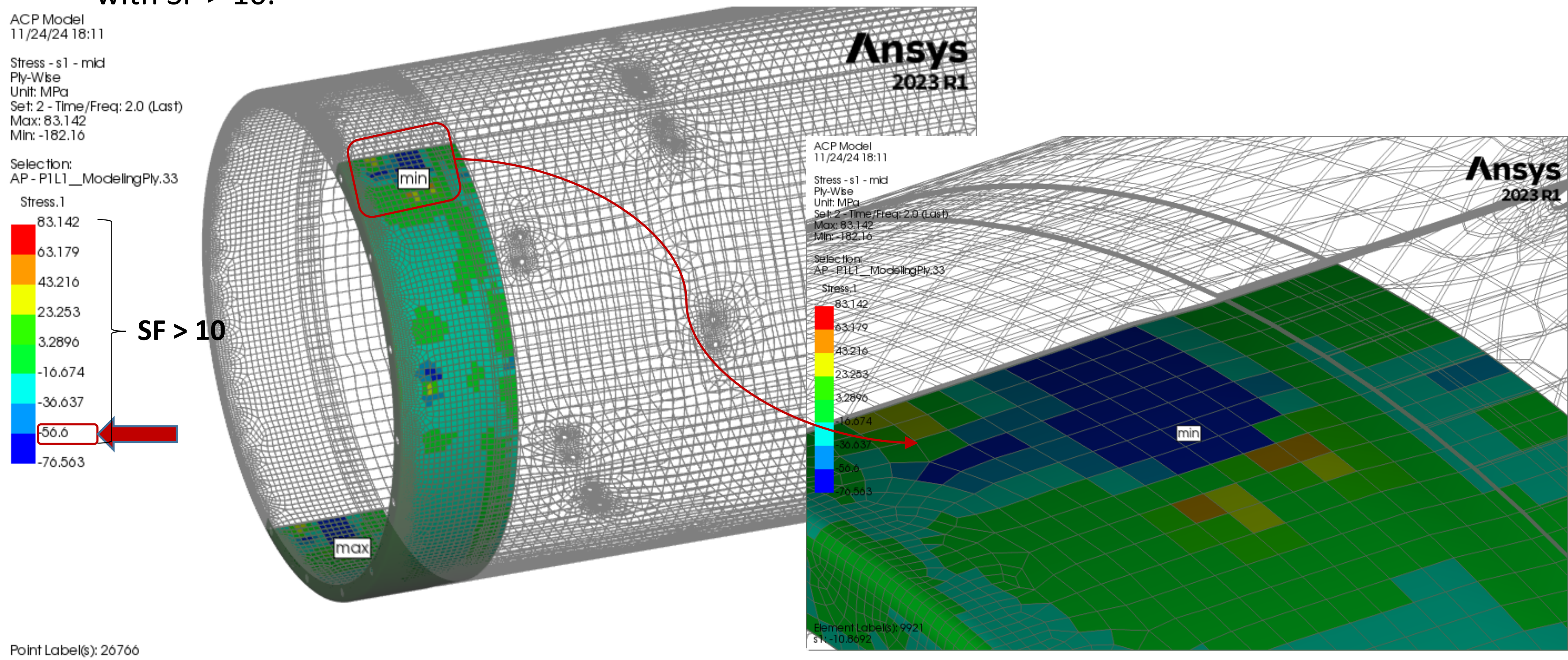

Figure 14: S_1 stress of the top ply of the right-hand front flange @-55°C.

OEC thermo-mechanical FEA: Layer 2 results

Load step 2: Cooling down from +20°C to – 55°C

Figure 15 shows that S_1 compressive stress also presents peaks on the half-shells, on the top ply (90° ply), in small regions where the interlinks (or other components made in ULTEM 1000) are glued.

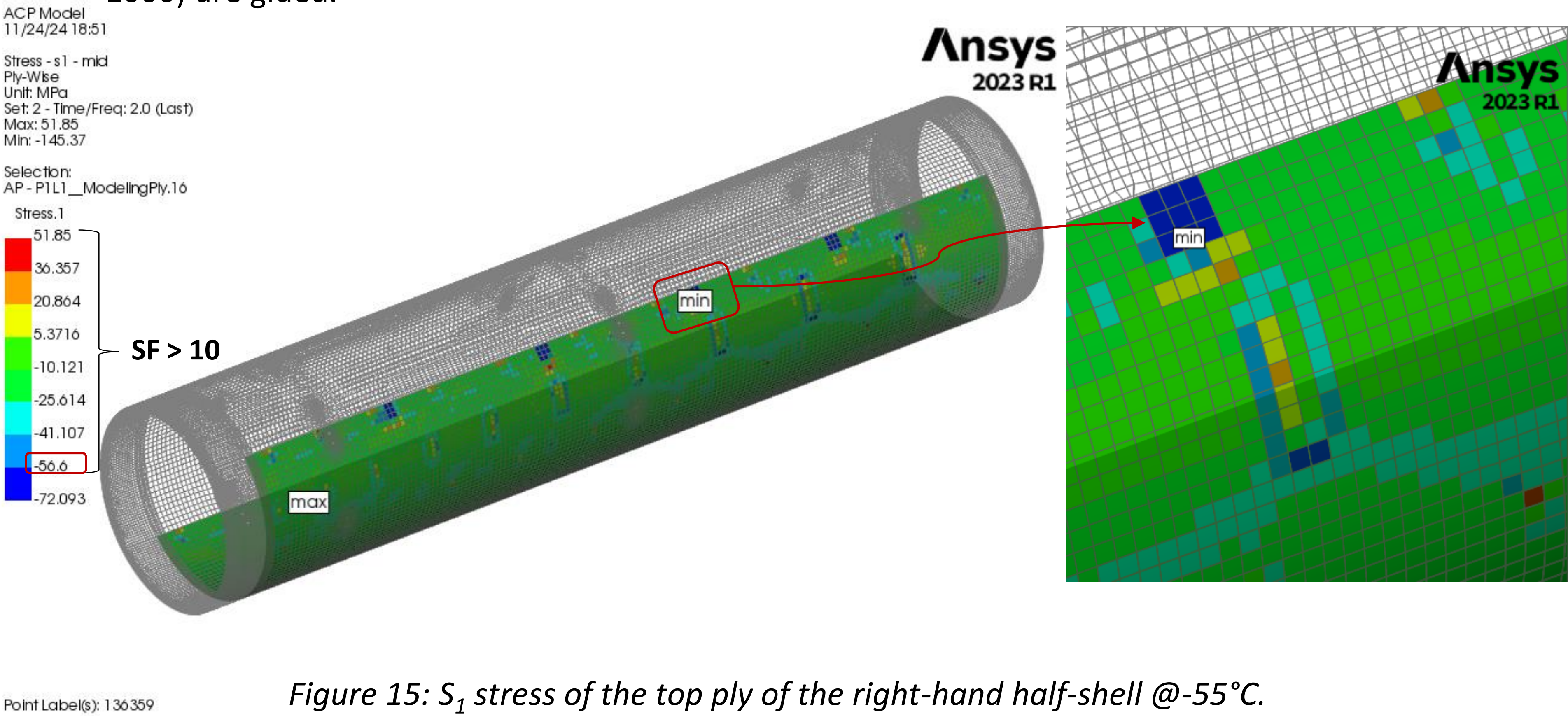

Figure 15: S_1 stress of the top ply of the right-hand half-shell @-55°C.

OEC thermo-mechanical FEA: Layer 2 results

Load step 2: Cooling down from +20°C to – 55°C

Figure 16 shows that the Shear stress on the glued region of the top ply is similar to that on the interlink bottom. CTE mismatch between ULTEM/composite generates the local peak of stress.

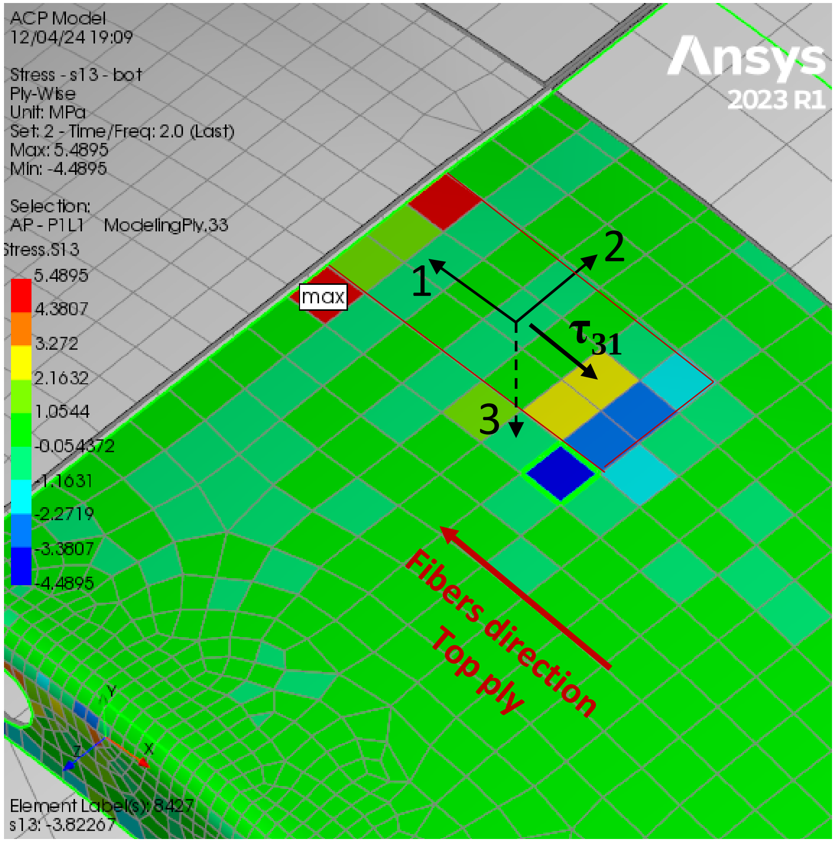

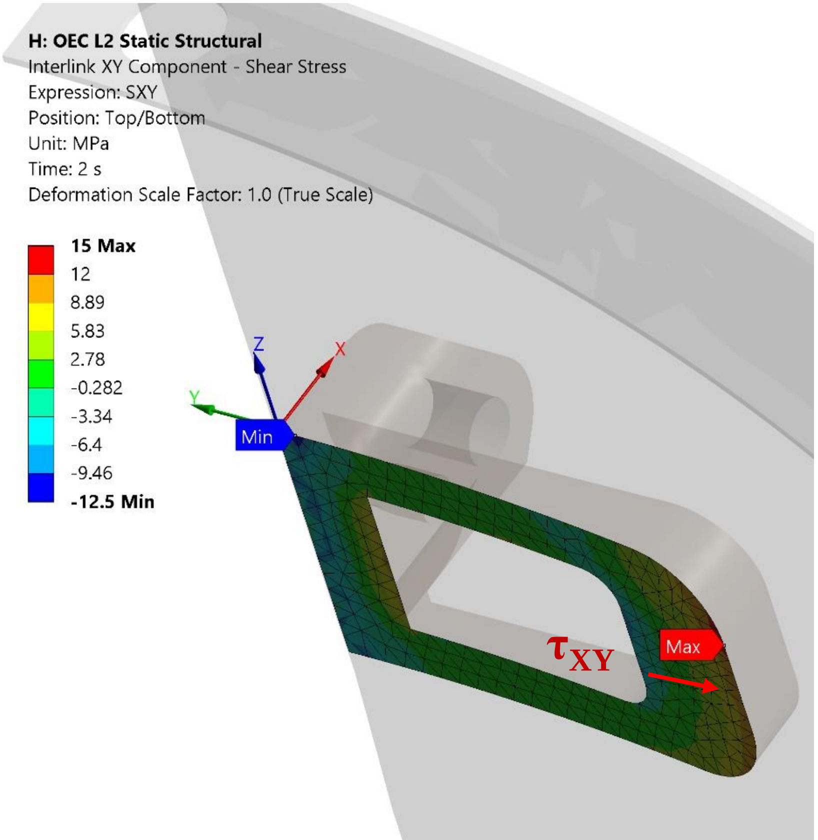

Figure 16: Comparison of Shear stresses (composite vs. interlink bonded area).

OEC thermo-mechanical FEA: Layer 2 results

Load step 2: Cooling down from +20°C to – 55°C

S_1 stress analysis along fibers direction of the composite Global Structures at the end of the load step 2 (T=-55°C), performed with ANSYS ACP, **show that:**

- **The plies of the half-shells work mainly in compression, except local small regions.**
- **The maximum tensile stress S_1 of the composite plies is lower than 109 MPa, so the related SF > 10 everywhere.**
- **The (negative) compressive stress S_1 of the composite plies is largely over -56.6 MPa, that means SF > 10, except local regions. The minimum safety factor (SF_{min} = 3.1) affects a small region on the top of the right-hand front flange, where $S_{1,c,min}$ = -182.2 MPa, but similar values occur in the other regions of the L2 composite structures where ULTEM parts (interlinks, mounting lugs etc.) are glued on.** This is **due to the CTE mismatch between ULTEM 1000 (50 ppm/K) and the composite shell (0.26 ppm/K)**.

OEC thermo-mechanical FEA: Layer 2 results

Load step 2: Cooling down from +20°C to – 55°C

Front Support - Total deformation

CFRP Layup $[90/45/-45/0]_s$ t=0.6 mm

$USUM_{max}$ = 116 µm

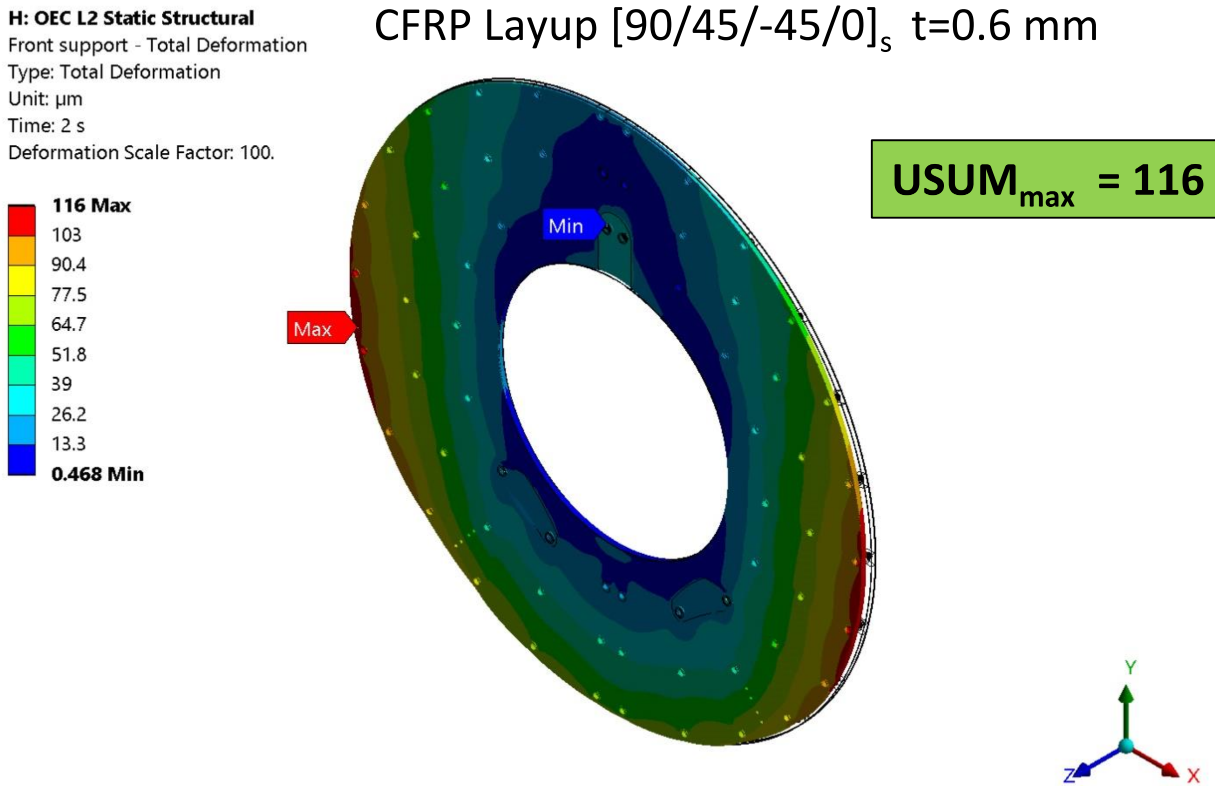

Figure 17: Front Support - Total deformation @-55°C.

OEC thermo-mechanical FEA: Layer 2 results

Load step 2: Cooling down from +20°C to – 55°C

Front Support - S_1 stress of the plies

Minimum S_1 compressive stress on first ply in contact with inserts (titanium/ULTEM), due to CTE mismatch between CFRP (0.26 ppm/K), Titanium (8.6 ppm/K), ULTEM (50 ppm/K).

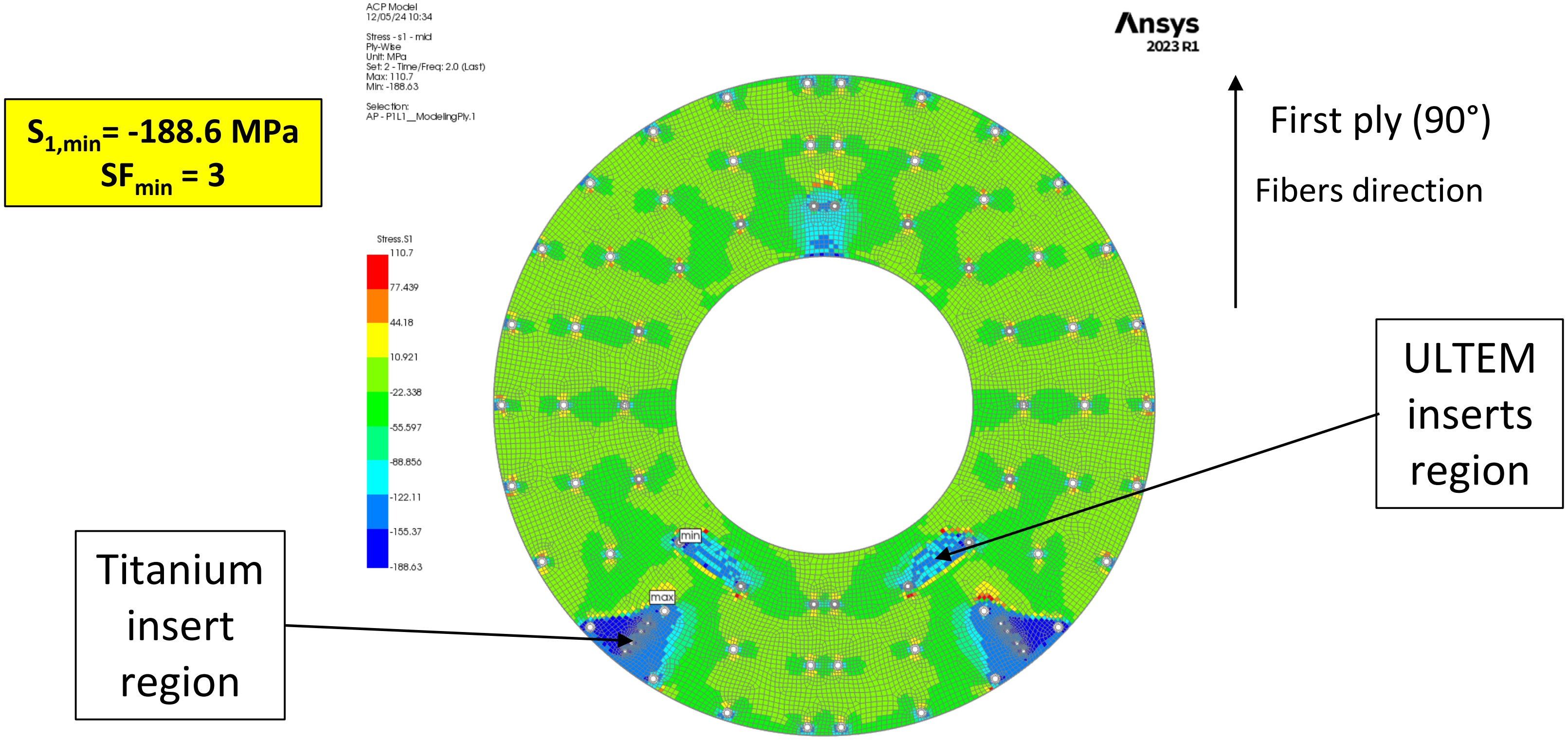

Figure 18: Front Support - S_1 stress @-55°C (first ply).

OEC thermo-mechanical FEA: Layer 2 results

Load step 2: Cooling down from +20°C to – 55°C

Front Support ULTEM inserts - Von Mises stress

Excluding local peaks on the edges (singularities), Von Mises stress is below 25 MPa => SF = 4.2
Average Von Mises stress: $\sigma_{eq,av}$ = 15 MPa => SF_{av} = 7.

$\sigma_{eq,max}$ = 25 MPa
SF_{min} = 4.2

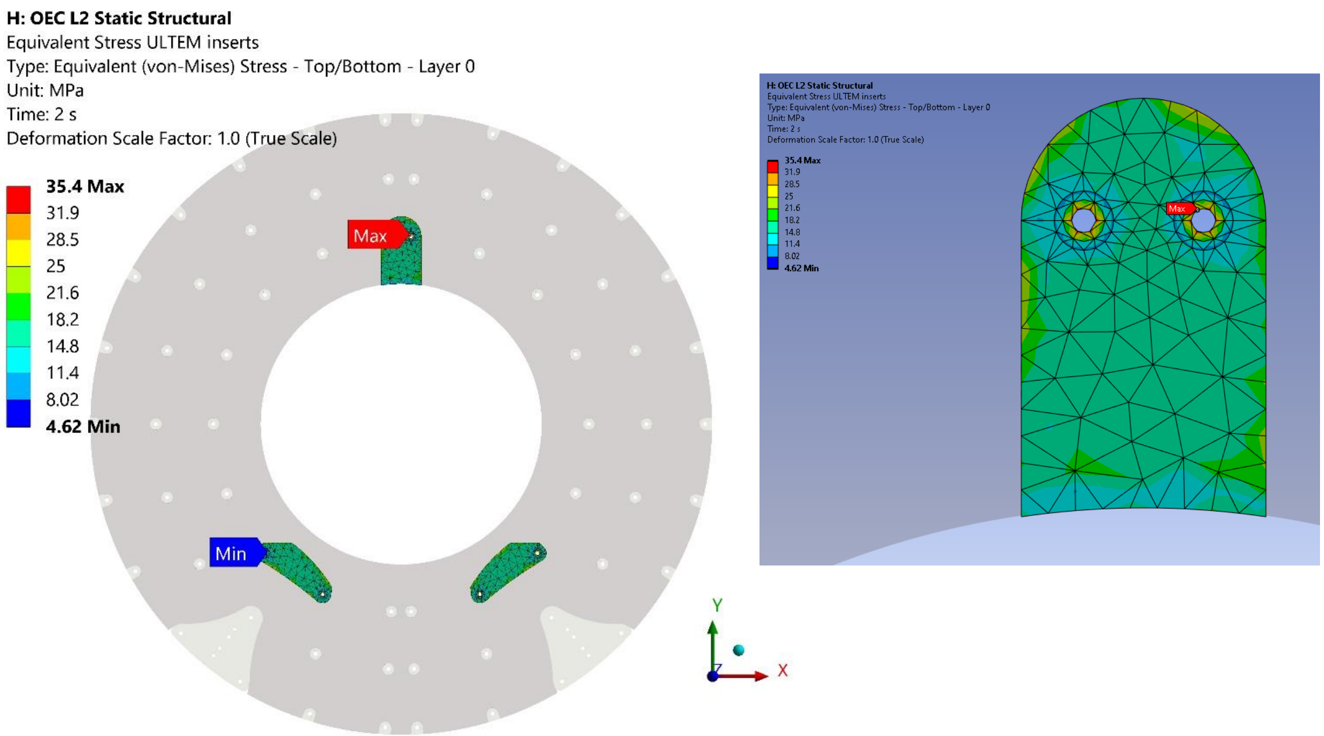

Figure 19: Front Support ULTEM inserts – Von Mises stress @-55°C.

OEC thermo-mechanical FEA: Layer 2 results

Load step 2: Cooling down from +20°C to – 55°C

Front Support ULTEM inserts - Von Mises stress

Excluding local peaks on the edges (singularities), Von Mises stress is below 42 MPa => SF = 8

Average Von Mises stress: $\sigma_{eq,av}$ = 19.9 MPa => SF_{av} > 10.

$\sigma_{eq,max}$ = 42 MPa
SF_{min} = 8

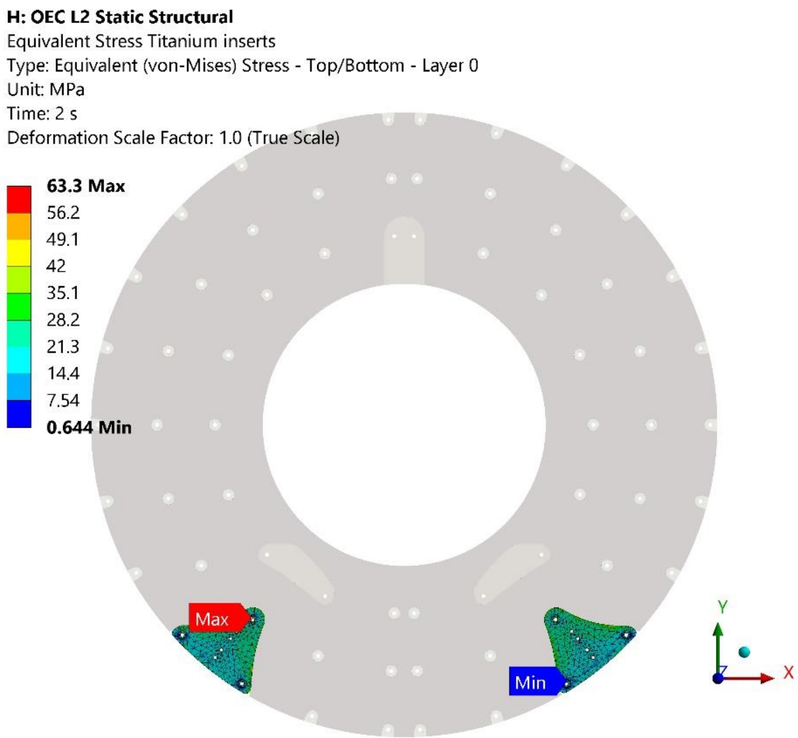

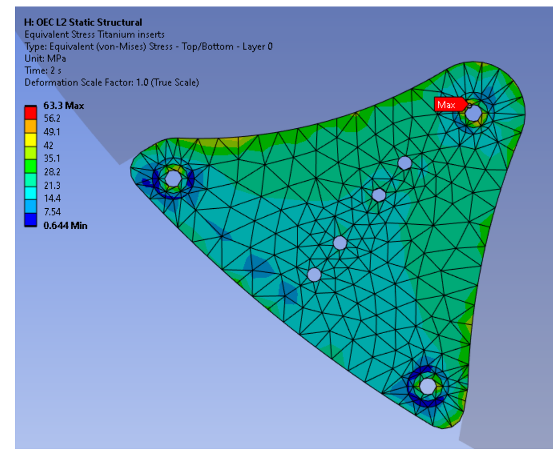

Figure 20: Front Support Titanium inserts – Von Mises stress @-55°C.

OEC thermo-mechanical FEA: Layer 2 results

Load step 2: Cooling down from +20°C to – 55°C

Rear Support - Total deformation

CFRP Layup $[90/45/-45/0]_{5s}$ t=3 mm

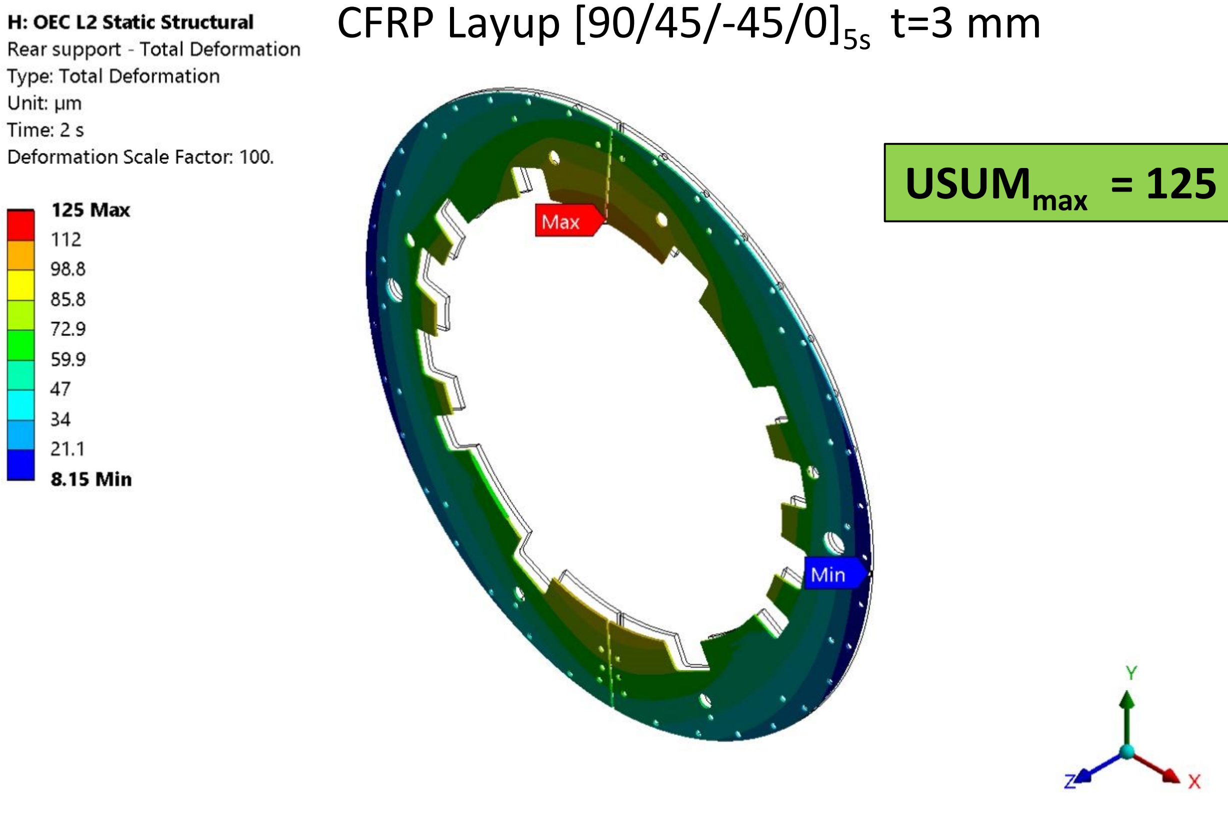

$USUM_{max}$ = 125 µm

Figure 21: L2 Rear Support - Total deformation @-55°C.

OEC thermo-mechanical FEA: Layer 2 results

Load step 2: Cooling down from +20°C to – 55°C

Rear Support - S_1 stress of the plies

S_1 compressive stress on first ply, in contact with half-shell flanges.

$S_{1,min}$= -28.3 MPa (1)
SF > 10

(1) excluding local peeks of stress on the edges of the holes.

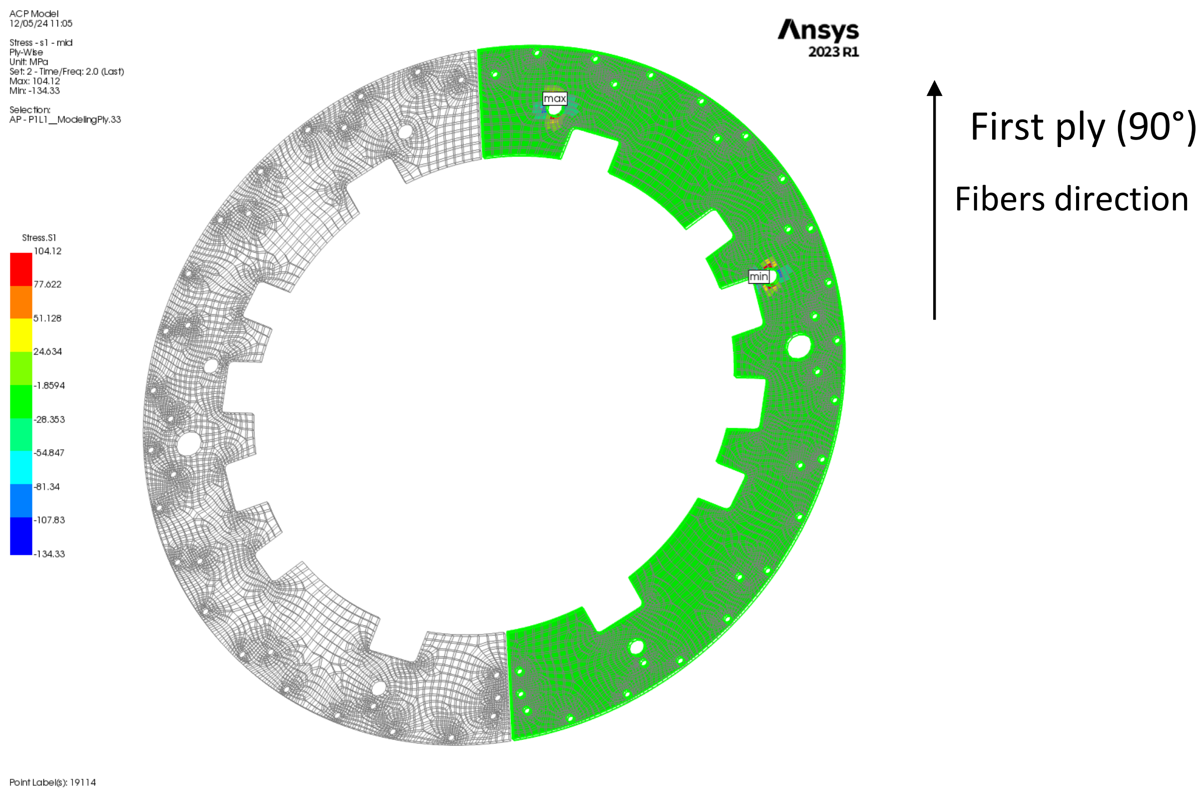

Figure 22: L2 Rear Support - S_1 stress @-55°C (first ply).

OEC thermo-mechanical FEA: Layer 2 results

Load step 2: Cooling down from +20°C to – 55°C

Coupling Rear Support/half-shells flanges - Radial deformation

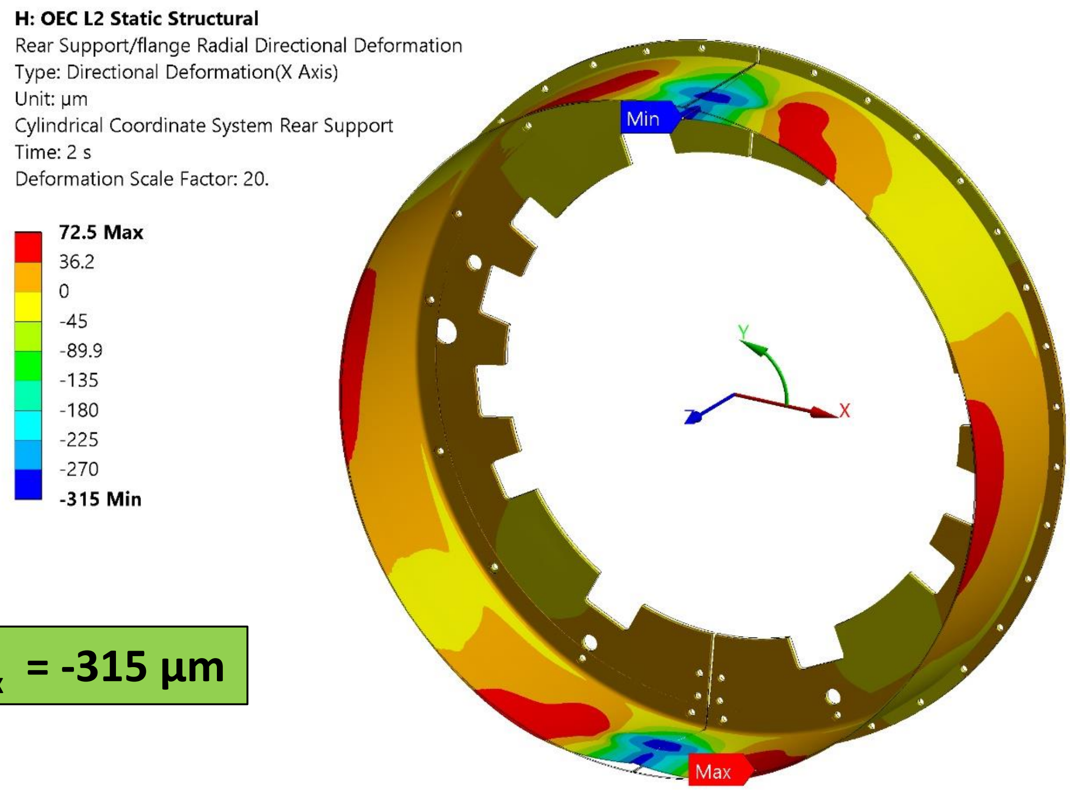

UR_{max} = -315 µm

Figure 23: L2 Coupling Rear Support/half shells flanges - Radial deformation @-55°C.

OEC thermo-mechanical FEA: Layer 2 results

Load step 2: Cooling down from +20°C to – 55°C

Stress analysis of the interlinks

Figure 24 is the plot of the **Von Mises Stress of all the L2 interlinks.** The maximum stress is located on the first interlinks pair, on the top of the detector. The overall average value is:

$$\boldsymbol{\sigma_{eq,av}} = \mathbf{5.84\ MPa} < \boldsymbol{\sigma_y/10} = 105/10 = \mathbf{10.5\ MPa}.$$

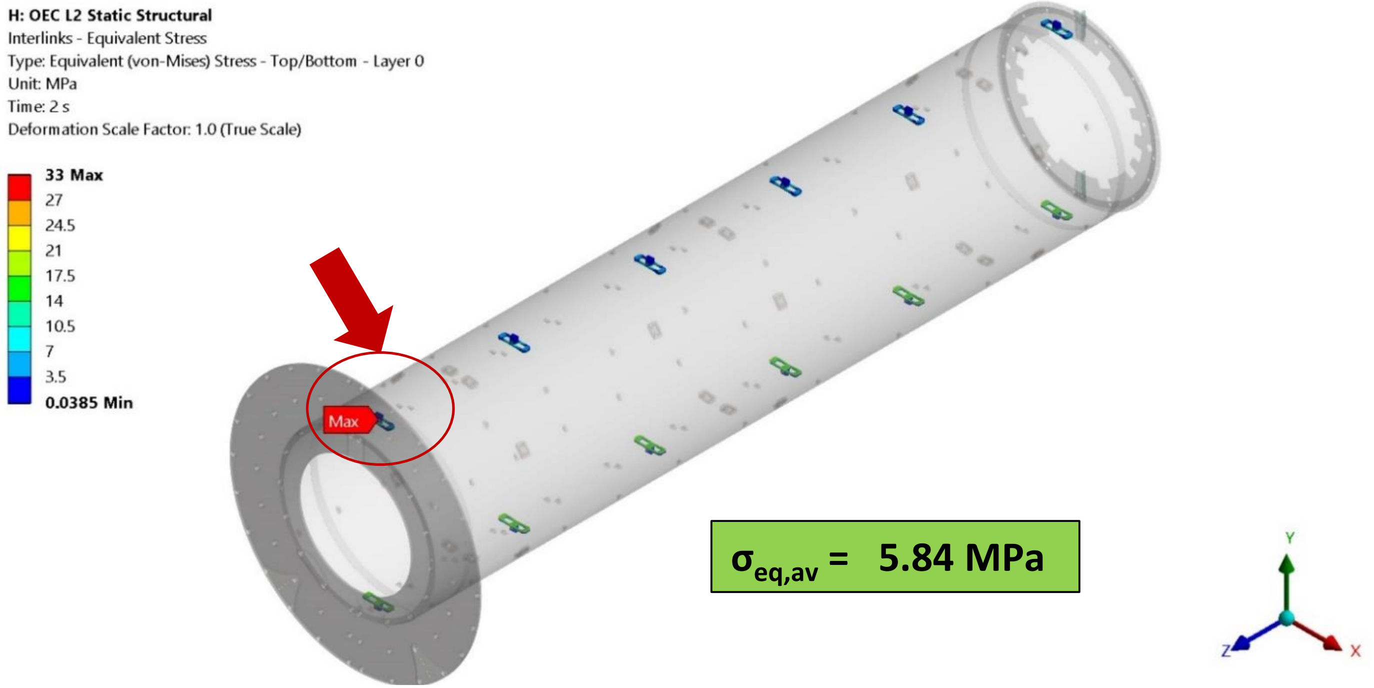

Figure 24: Von Mises stress of the L2 Interlinks @-55°C.

OEC thermo-mechanical FEA: Layer 2 results

Examining in detail the interlinks pair with the maximum ***Von Mises stress,* on the bottom glued surfaces the stress** is greater than 10.5 MPa, but it **is below 22 MPa everywhere (< $\boldsymbol{\sigma_{adm}}$= 70 MPa)**, **except for local peaks on the edges** (Fig.25). The Shear Stress is included in the Von Mises equation which calculates the equivalent stress:

$$\sigma_{\mathrm{VM}} = \sqrt{\frac{1}{2}\left[\left(\sigma_{xx}-\sigma_{yy}\right)^2+\left(\sigma_{yy}-\sigma_{zz}\right)^2+\left(\sigma_{zz}-\sigma_{xx}\right)^2\right]+3\left(\tau_{xy}^2+\tau_{yz}^2+\tau_{zx}^2\right)}$$

Being the peaks of Shear Stress on the edges false values in FEA (see slide #19), Von Mises stress over 22 MPa can be considered fake.

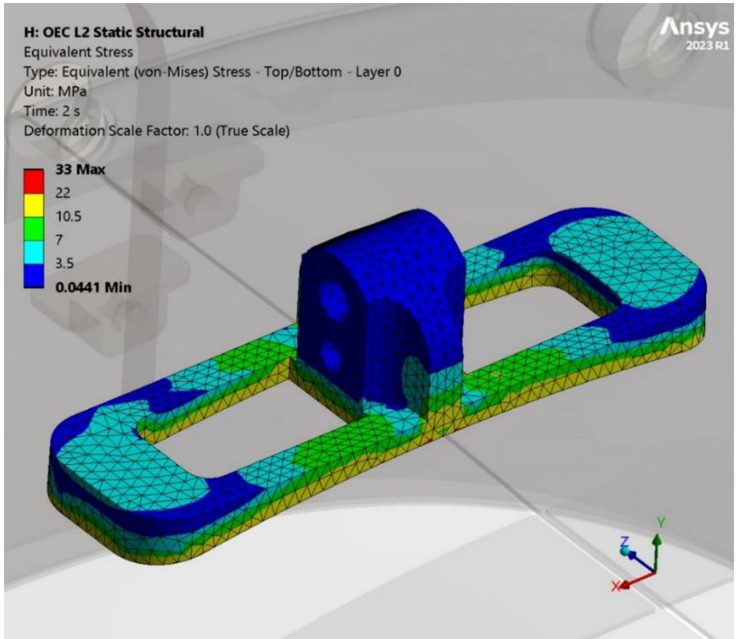

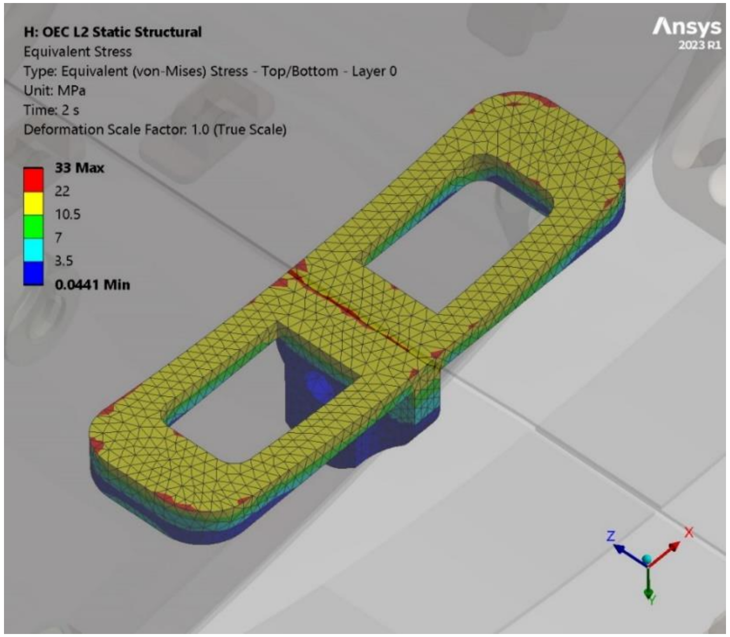

Figure 25: L2 Interlinks pair with Maximum Von Mises stress @-55°C.

OEC thermo-mechanical FEA: Layer 2 results

Von Mises stress between 10.5 MPa and 22 MPa, on the bottom surface of the interlinks, is mainly driven by the Shear stress (fig.26), **due to the CTE mismatch between ULTEM 1000 (50 ppm/K) and the half-shell (0.26 ppm/K)**, which mainly involves the strength of the adhesive layer (not modeled in the FEM model) rather than the strength of the interlinks (**in any case, $\sigma_{eq,max}$ = 22 MPa => SF 4.8**).

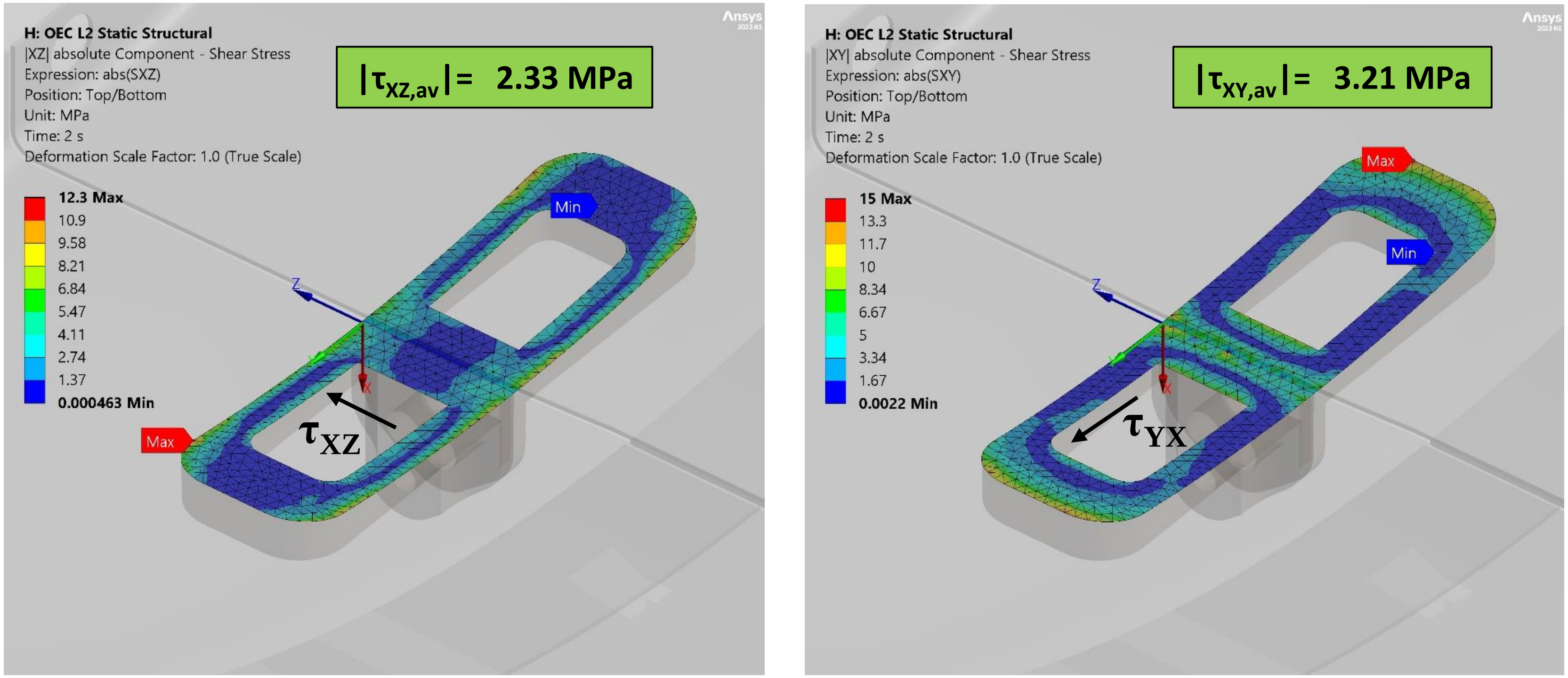

Figure 26: Shear stress (absolute value) on the glued surface of interlinks.

OEC thermo-mechanical FEA: Layer 2 results

Load step 2: Cooling down from +20°C to – 55°C

Stress analysis of the mounting lugs of the half-rings

Figure 27 is the plot of the **Von Mises Stress of all the L2 mounting lugs**. The maximum stress is located on a mounting lug of the sixth half-ring. The overall average value is:

$$\boldsymbol{\sigma_{eq,av} = 6.89\ \mathrm{MPa} < \sigma_y/10} = 105/10 = \mathbf{10.5\ MPa}.$$

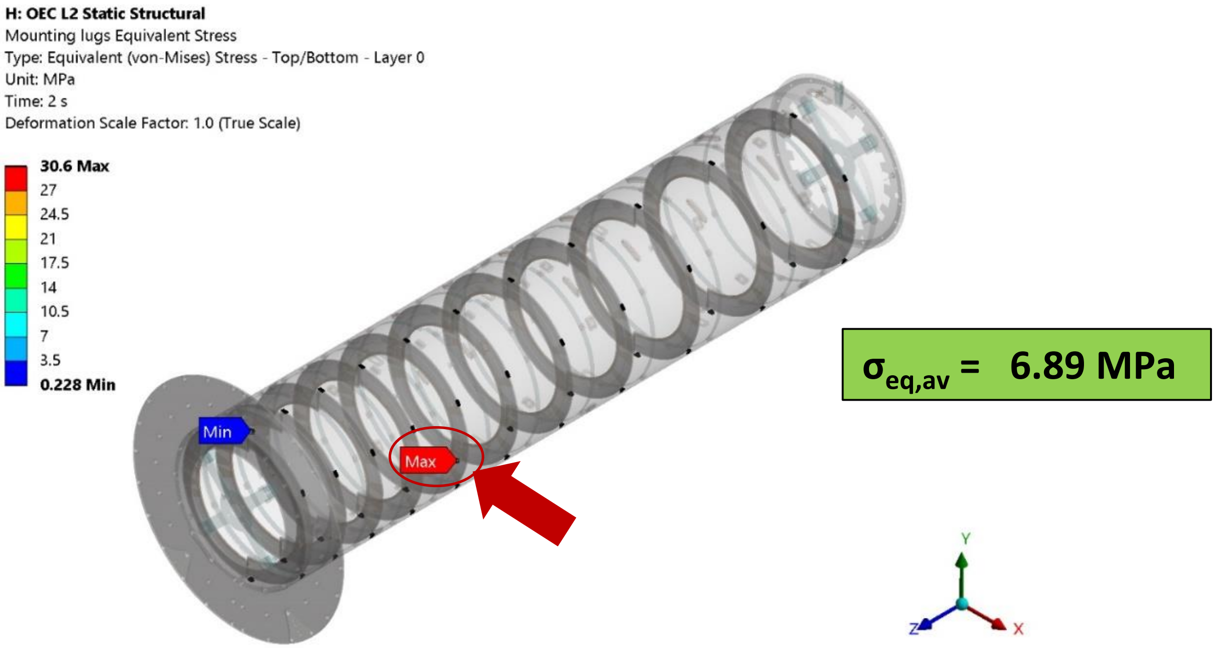

Figure 27: Von Mises stress of the L2 mounting lugs @-55°C.

OEC thermo-mechanical FEA: Layer 2 results

Examining in detail the mounting lug with the maximum **Von Mises stress**, on the bottom glued surface the stress is greater than 10.5 MPa, but it **is below 22 MPa everywhere** (< $\sigma_{adm} = 70$ MPa), **except local peaks on the edges** (Fig.28-left). **Stress values over 10.5 MPa are mainly driven by the Shear stress** on the glued surface (Fig.28-right), as already demonstrated for the interlinks (**in any case, $\sigma_{eq,max}$ = 22 MPa => SF 4.8)**.

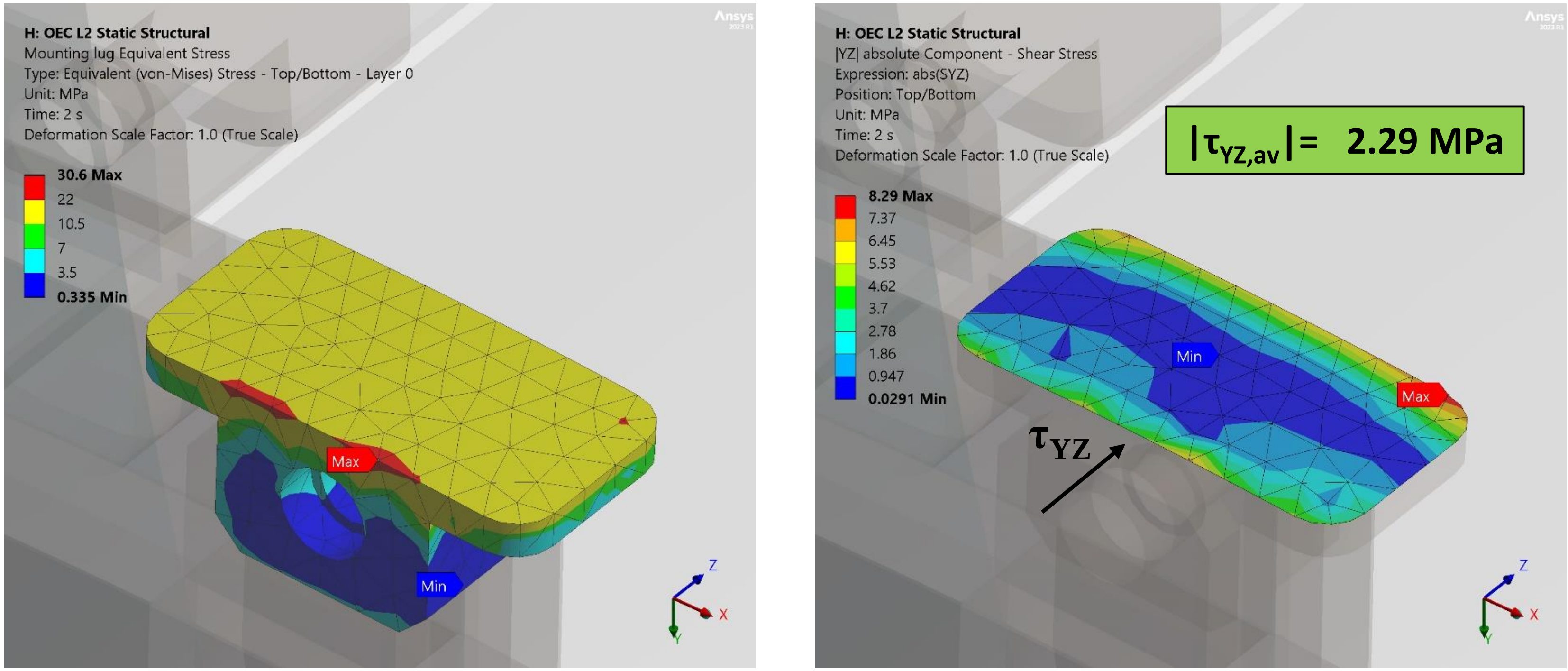

Figure 28: L2 mounting lug with Maximum Von Mises stress and related Shear stress @-55°C .

OEC thermo-mechanical FEA: Layer 2 results

Load step 2: Cooling down from +20°C to – 55°C

Stress of the adhesive layers

The adhesive layers between the composite Global Structures and the polymeric components (interlinks, mounting lugs, etc.), made of ULTEM, are not explicitly modeled in the FEM model 3.0, because they are too much expensive in terms of nodes/elements.
However, an evaluation of the Shear stress between the glued surfaces is useful, being it driven by the CTE mismatch during the cooling down.

Considering the **Epoxy adhesive Hysol EA 9396**, the reference Shear strength is **22.8 MPa @-55°C** (Henkel® datasheet). However, being the material of the adherends and the surface treatment also crucial for the joint strength (e.g. cohesive failure), we refer to the Double Lap Shear tests performed at the University of Manchester (March 17, 2023) **[4]**, according to ASTM D3528 − 96 (Standard Test Method for Strength Properties of Double Lap Shear Adhesive Joints by Tension Loading), where the adherends were the CFRPs of the half-rings. The resulting value of the joint Shear strength, for pure and not irradiate Hysol, was 17.39 MPa with STDEV 3.96 MPa, @+20°C (failure mode: mixed cohesive and adhesive shear). So, **the reference value to evaluate the joint strength is set to 13.43 MPa, to be compared with the Shear stress between the interfaces calculated by FEA**.

OEC thermo-mechanical FEA: Layer 2 results

The value of the average in-plane Shear stress: $\tau_{in-plane} = \sqrt[2]{(\tau_{XY}^2 + \tau_{XZ}^2)}$ of the bonded surfaces @-55°C (max = **4.49 MPa**), can be compared with the joint Shear strength, to calculate a minimum safety factor:

$$\mathbf{SF_{min} = 13.43\ MPa\ /\ 4.49\ MPa = 3}.$$

The peaks of Shear stress on free edges, calculated by FEA, are fake, so the concern in these regions could be the propagation of delamination due to microcracks or local defects (e.g. lack of glue).

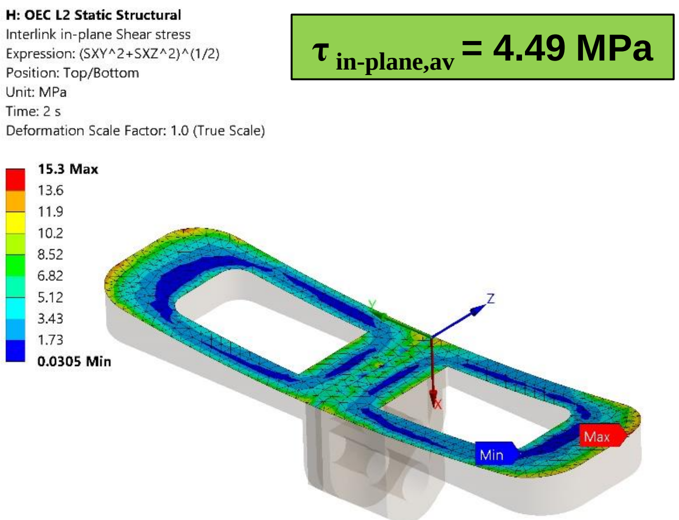

SF_{min} = 3

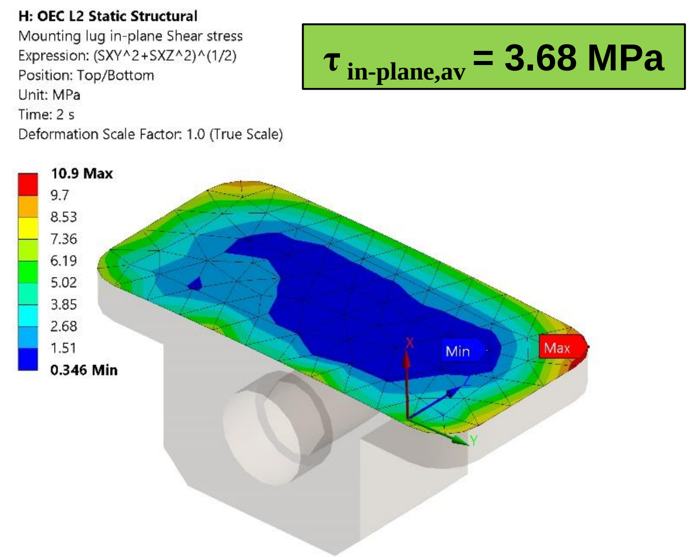

Figure 29: In-plane Shear stress on the bonded surface of interlinks and mounting lugs @-55°C.

OEC thermo-mechanical FEA: Layer 2

Conclusions of the stress analysis of the OEC L2

Responses of the structural thermo-mechanical FEA of the OEC L2, under gravity x 1.2 SF (load step 1) and cooled down to -55°C (load step 2):

- **Composite Global Structures (half-shells, flanges, Front supports faceplates, Rear support)**

  Failure Criterion: Maximum Stress along the fibers (S_1) ply by ply.

  Pre-preg M55J/EX1515 v.f. 46.5%: Tensile strength (1469 MPa), compressive strength (-566 MPa). Expected SF ≥ 10.

  - **Under gravitational loads** (load step 1): **SF > 10**.
  - **After cooling down to -55°C** (load step 2):
    - **Tensile stress: SF > 10 everywhere.**
    - **Compressive stress: SF ≥ 3 in small regions where polymeric/Titanium parts are glued on the structures** (due to the CTE mismatch)**. SF > 10 everywhere else.**

- **Isotropic parts**

  Von Mises stress compared with Yield stress σ_y:

  Expected SF ≥ 10 ($\sigma_{eq,max} < \sigma_y/10$);

  Maximum Admissible Stress (in a classic static structural analysis): $\sigma_{adm} = \sigma_y/1.5$.

OEC thermo-mechanical FEA: Layer 2

Conclusions of the stress analysis of the OEC L2

Interlinks and mounting lugs (ULTEM 1000):

- **After cooling down to -55°C** (load step 2):
  SF > 10 if calculated on average Von Mises stress. On bonded surfaces SF is reduced to 4.8.

Inserts of the Front Support (ULTEM 1000/Titanium grade II annealed):

- **After cooling down to -55°C** (load step 2):
  - **ULTEM parts: SF ≥ 4.2 (SF >7 if calculated on average Von Mises stress).**
  - **Titanium parts: SF ≥ 8 (SF >10 if calculated on average Von Mises stress).**

Adhesive layers of interlinks/mounting lugs:

Shear stress caused by the CTE mismatch ULTEM/CFRP (CTE: 50 ppm/K vs. 0.26 ppm/K).

Adhesive: epoxy Hysol EA 9396 (unirradiated). Shear strength 13.43 MPa (measurement).

- **After cooling down to -55°C** (load step 2):

  Average in-plane Shear stress: $\tau_{in\text{-}plane,av} \cong 4.5$ MPa, SF = 3.

  FEA can't exclude propagation of delamination starting from the borders, due to local defects.

2. Overall OEC FEA

Simulations of the overall OEC FEM model v. 3.0:

A. **Effects of a thermal gradient (10 °C) along the vertical axis of the detector** (-55°C on OEC bottom, -45°C on OEC top), to be compared with the simulation of the OEC at uniform temperature -55°, to evaluate deformations on envelope and stresses (half-shells).

   Ref.: *Recommendation R11 – Report of the GM&I FDR (see slide #3).*

B. **Effect of the pull force during insertion of the Pixel Outer System into the Strip detector.**
   This simulation helps address the *Recommendation R29 of the Report of the GM&I FDR (see slide #3).*

Overall OEC FEA constraints

ITk Pixel Global Supports Design Specifications - AT2-IP-ES-0007 Rev. 4.0 [1] provides the **supporting scheme of the OEC** (fig.30): it sits in the PST on four sliding contact points resting on the PST rails. Table 9 summarizes the nature of the four supports.

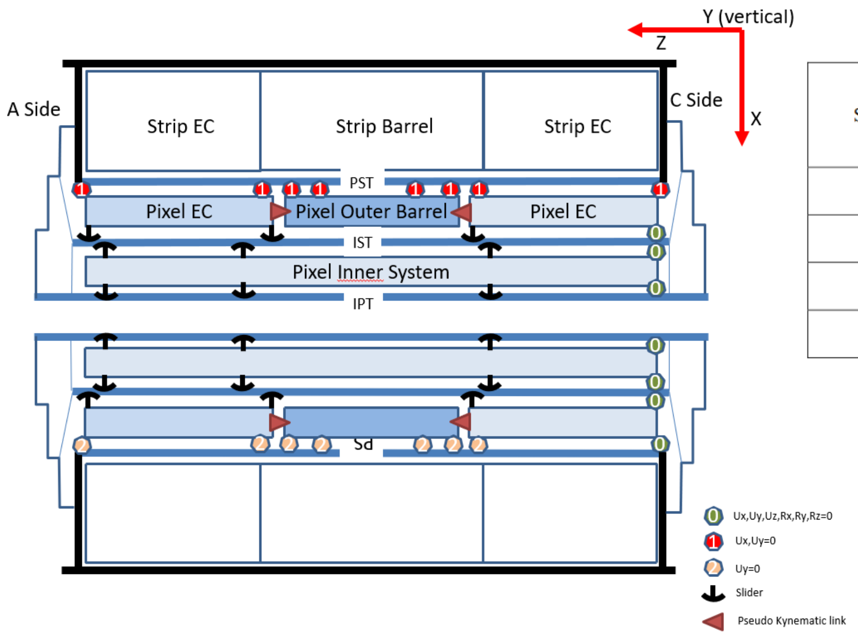

Figure 30: Supporting scheme of the OEC.

Support #	Location z [mm] and phi [deg]*	Ux	Uy	Uz
1	± 1111.5 and +39°	free	0	free
2	± 1111.5 and -39°	0	0	free
3	± 2984.5 and +39°	free	0	free
4	± 2984.5 and -39°	0	0	0**

Table 9: OEC supports locations onto the PST rails. *Ref.: AT2-IP-MG-0013 rev. 0.3.* [2].

Overall OEC FEA constraints

The prescriptions of the table 9 have been **implemented** as **constraints conditions on to the sliders of the FEA model** (all in ATLAS Cartesian CSYS, except IST in ATLAS cylindrical CSYS).

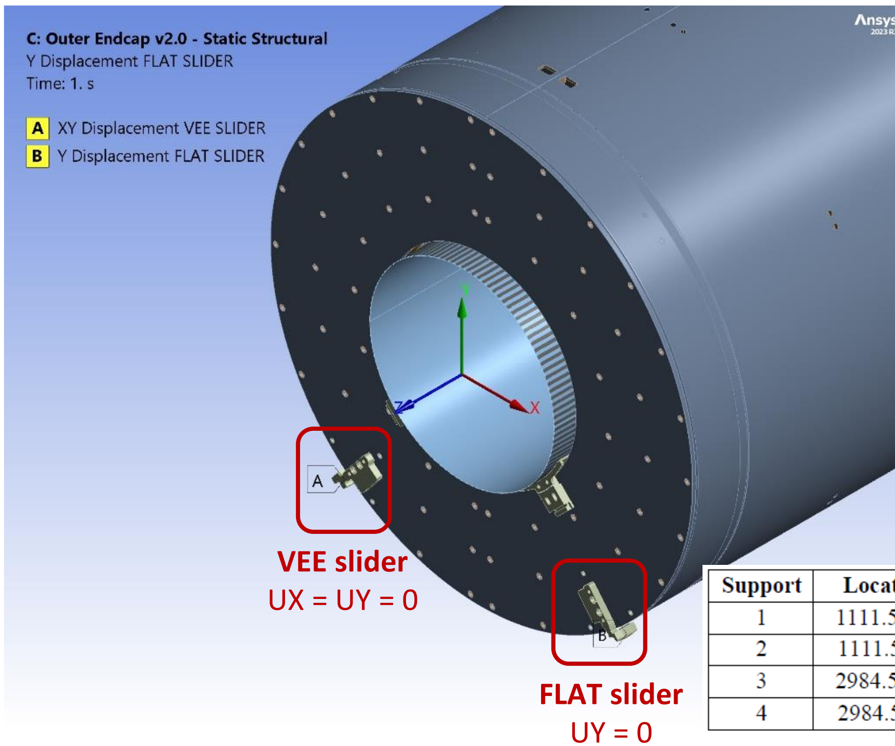

Support	Location Z/phi	Ux	Uy	Uz
1	1111.5mm / +39°	Free	0	Free
2	1111.5mm / -39°	0	0	Free
3	2984.5mm / +39°	Free	0	Free
4	2984.5mm / -39°	0	0	0

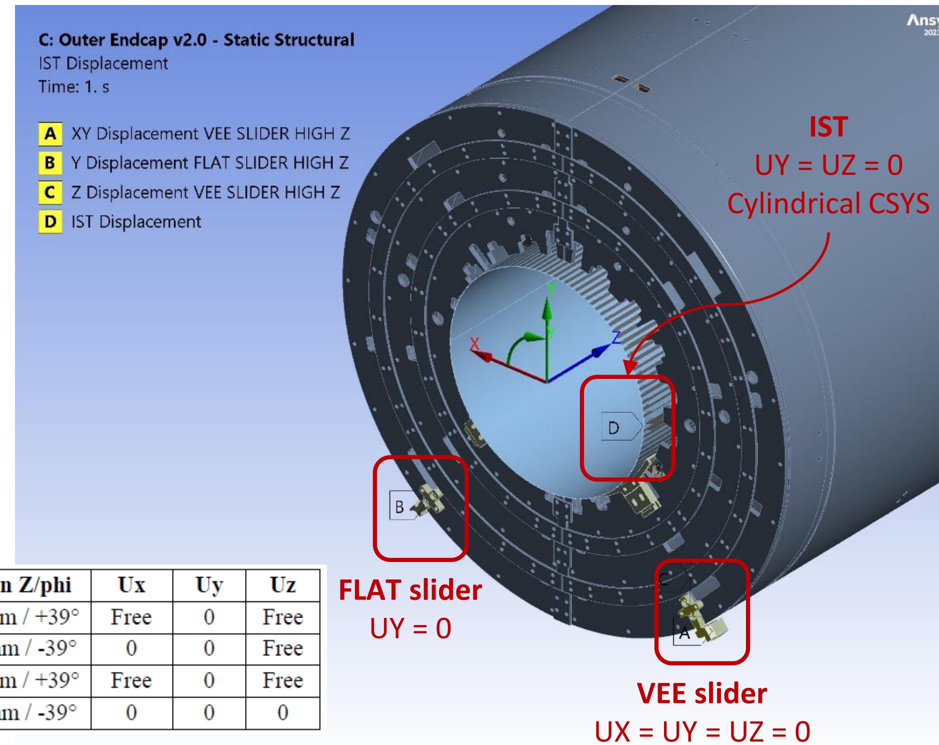

Figure 31a: Constraints of the OEC – front side.

Figure 31b: Constraints of the OEC – rear side.

A. Overall OEC FEA – Effect of Thermal gradient

- **Load step 1**: Gravity x 1.2 safety factor.
- **Load step 2**: Cooling down from +20°C: – 55°C (OEC bottom) ÷ -45°C (OEC top)

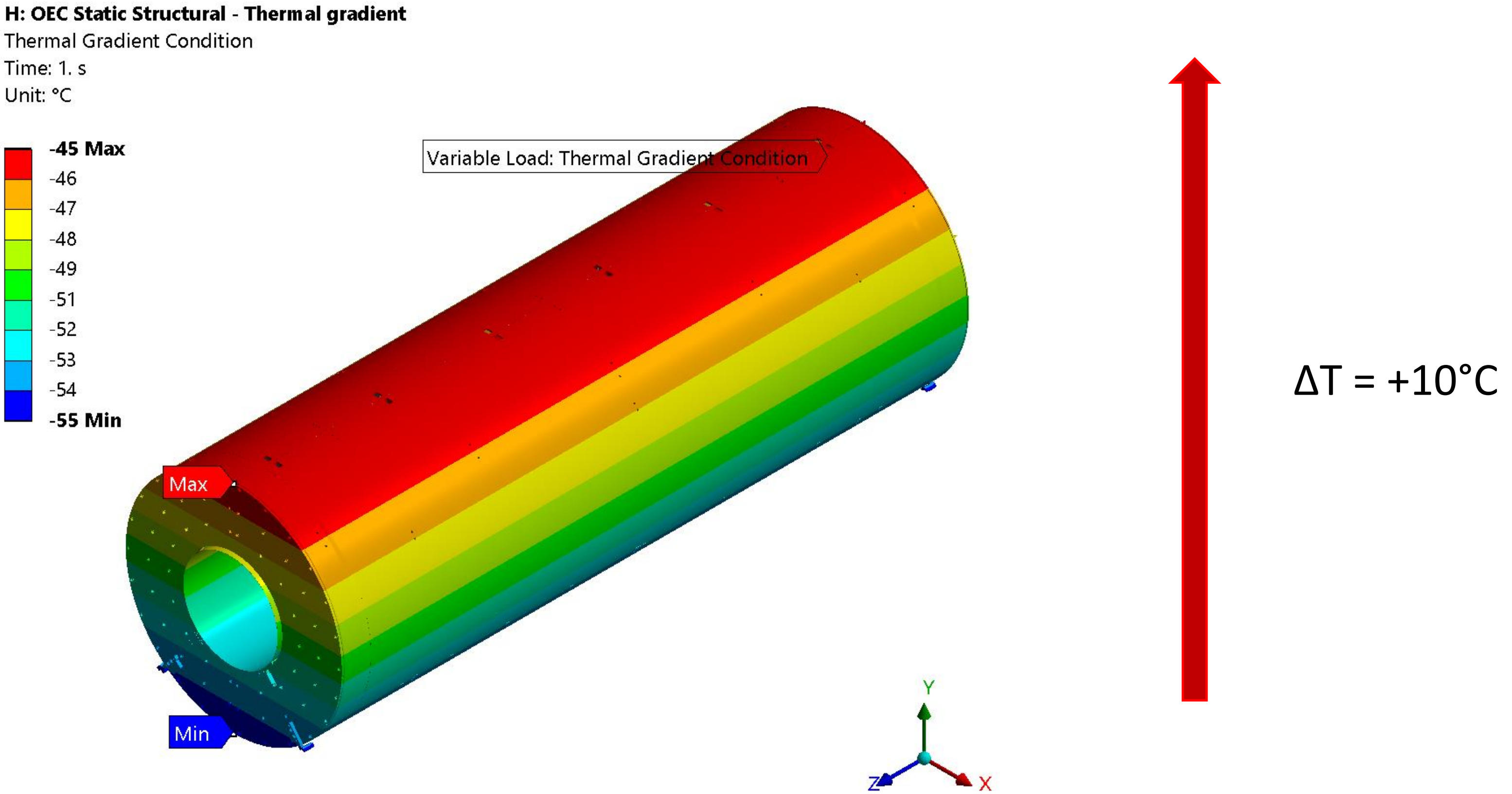

Figure 32: Thermal gradient applied to the OEC (ΔT = +10°C along vertical axis).

Overall OEC FEA – Effect of Thermal gradient

OEC Total deformation

Uniform T=-55°C, g x 1.2

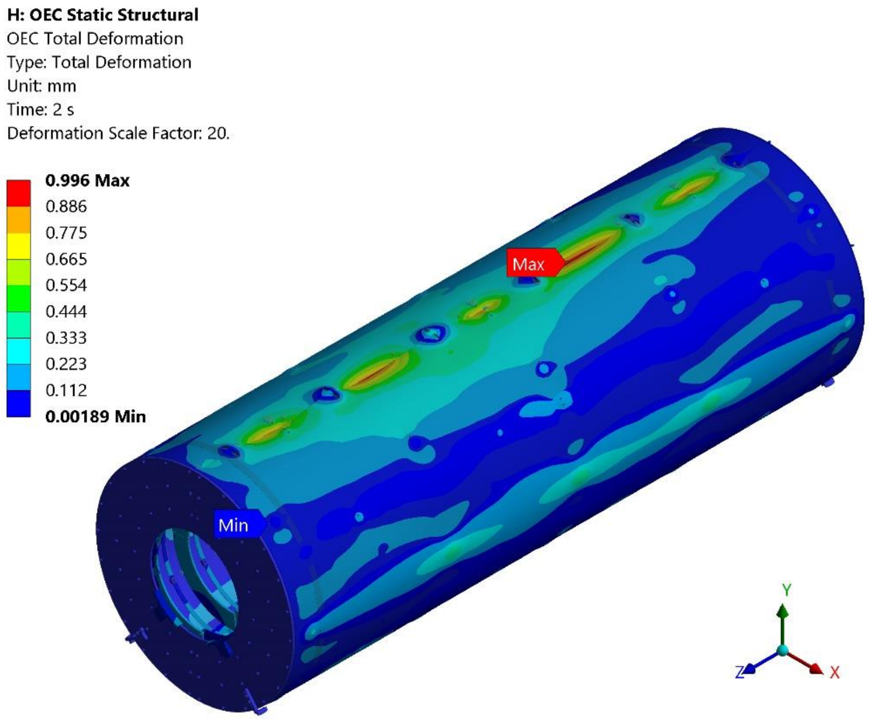

$USUM_{max}$ = 0.996 mm

Thermal gradient =-55/-45°C, g x 1.2

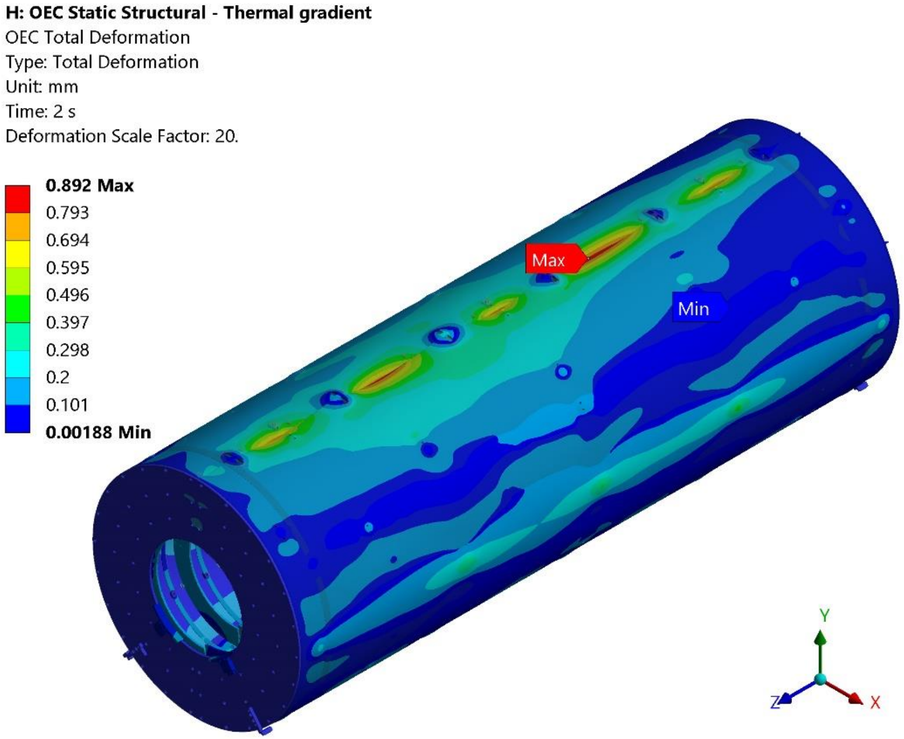

$USUM_{max}$ = 0.892 mm **-10%**

Figure 33: OEC Total deformation - left: uniform T -55°C, right: thermal gradient -55/-45°C.

OEC Envelope

AT2-IP-ES-0007 Rev. 4 - Section 6 [1] *- Performance Specifications:*
The design must ensure that the global support system envelope is never violated. *The envelopes include gravitational and thermal deformations over the OTR and with the load from the Design Values for the masses applied.*

The geometry of the ITk is controlled through the *ITk Envelope Drawing v2.0.0 -AT2-IC-EP-0001 v.2.0* [3].

The **radial envelope of the OEC** (fig.34) is **bounded by** the **outer envelope of the L4 half-shells** (**327 mm**), the **outer envelope of the IST** (143 mm) **plus a 2mm insertion clearance** (143 mm + 2 mm = **145 mm**).

At the interface to the IST the front and rear support both have a nominal inner radius of 146.0 mm, allowing a radial clearance of 1.0 mm to the inner endcap radial envelope.

The nominal outer radius of the L4 half-shell is 325.1 mm, leaving a radial clearance of 1.9 mm to the endcap outer radial envelope.

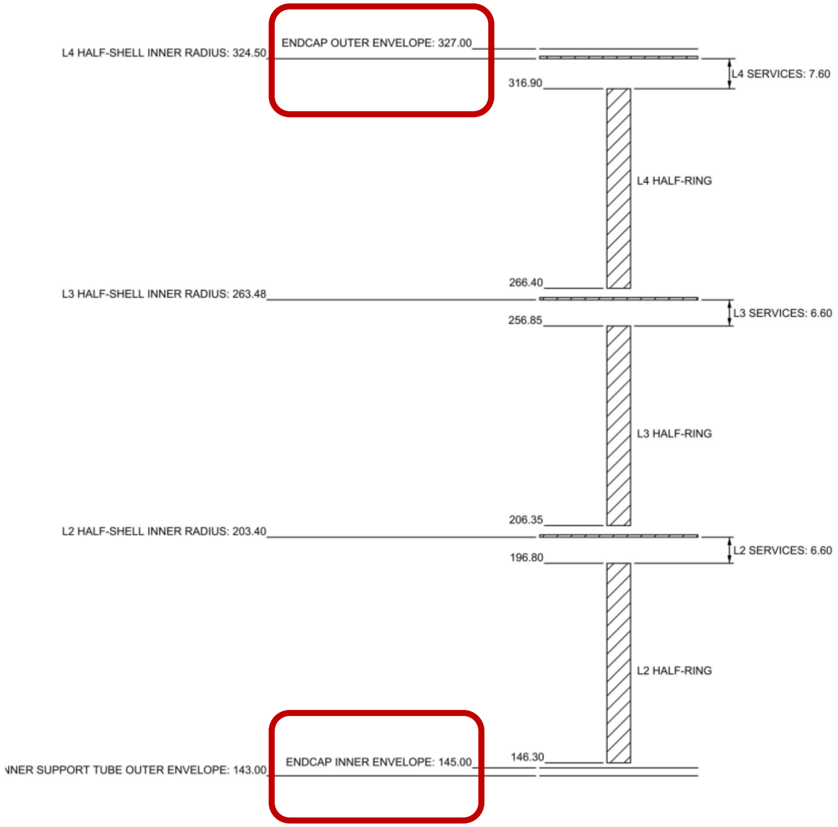

Figure 34: OEC nominal radial dimensions.

Overall OEC FEA – Effect of Thermal gradient

OEC Outer envelope: Radial deformation of L4 half-shells

Uniform T=-55°C, g x 1.2	Thermal gradient =-55/-45°C, g x 1.2

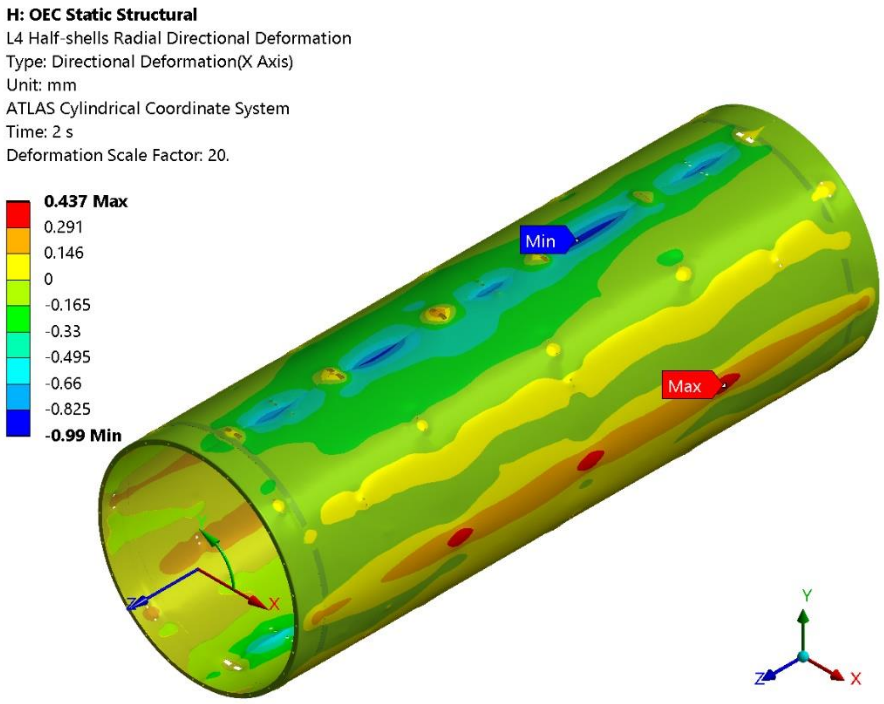

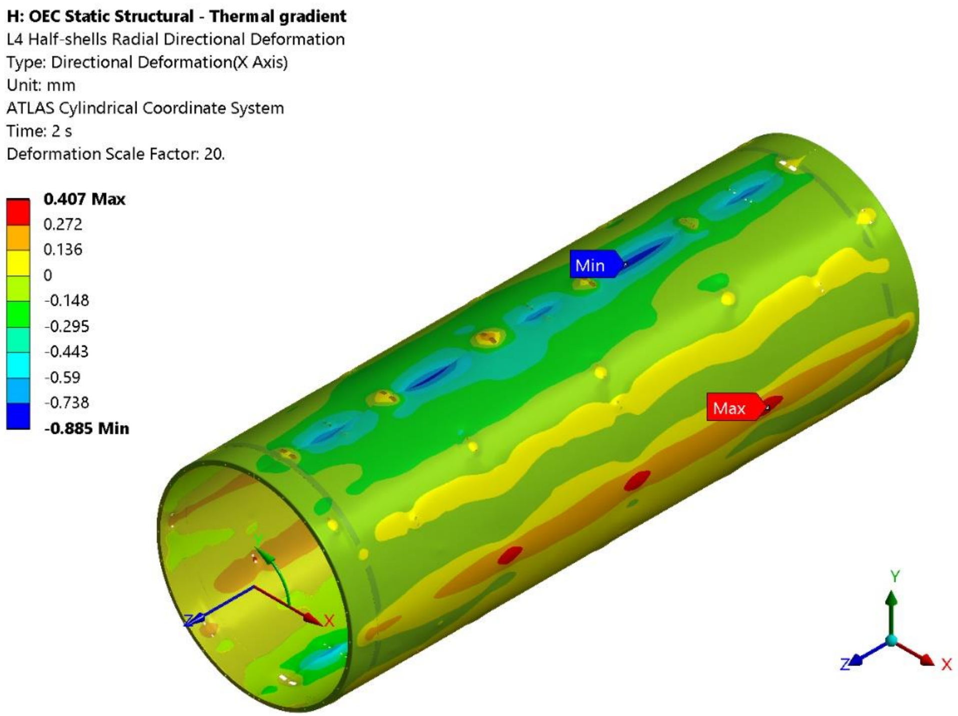

$UR_{O,max}$ = 0.437 mm

$UR_{O,max}$ = 0.407 mm **-7%**

Figure 35 : L4 half-shells Radial deformation - left: uniform T -55°C, right: thermal gradient -55/-45°C.

Overall OEC FEA – Effect of Thermal gradient

OEC Inner envelope: Radial deformation of Front/Rear supports

Uniform T=-55°C, g x 1.2

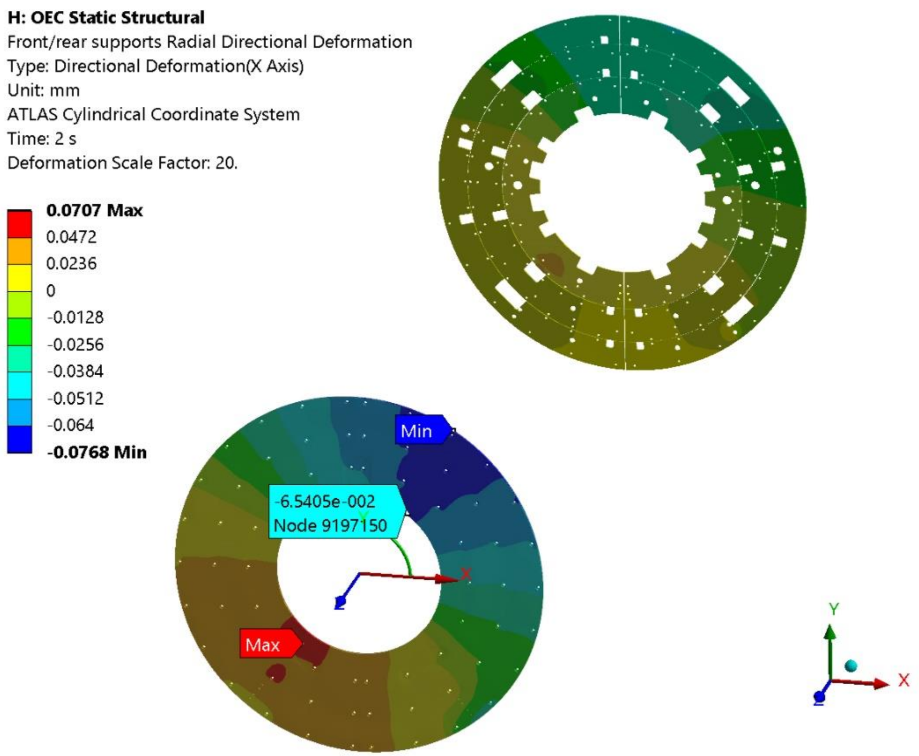

Thermal gradient =-55/-45°C, g x 1.2

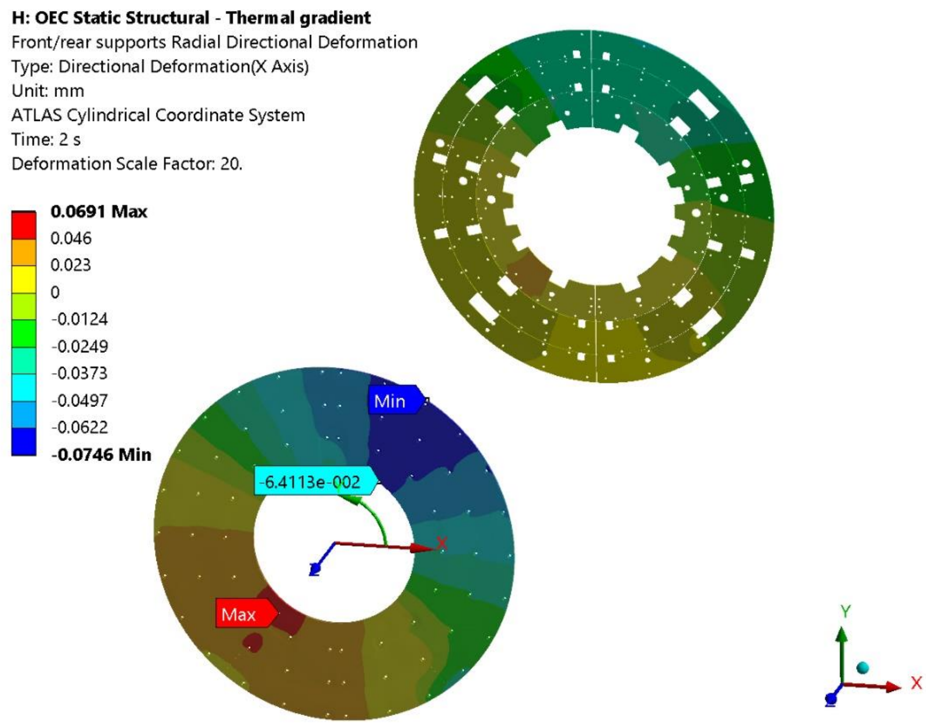

$UR_{I,min}$ = - 0.065 mm

$UR_{I,min}$ = - 0.064 mm **-2%**

Figure 36: Front/Rear support Radial deformation - left: uniform T -55°C, right: thermal gradient -55/-45°C.

Overall OEC FEA – Effect of Thermal gradient

OEC Inner envelope: Radial deformation of Front/Rear supports

Uniform T=-55°C, g x 1.2

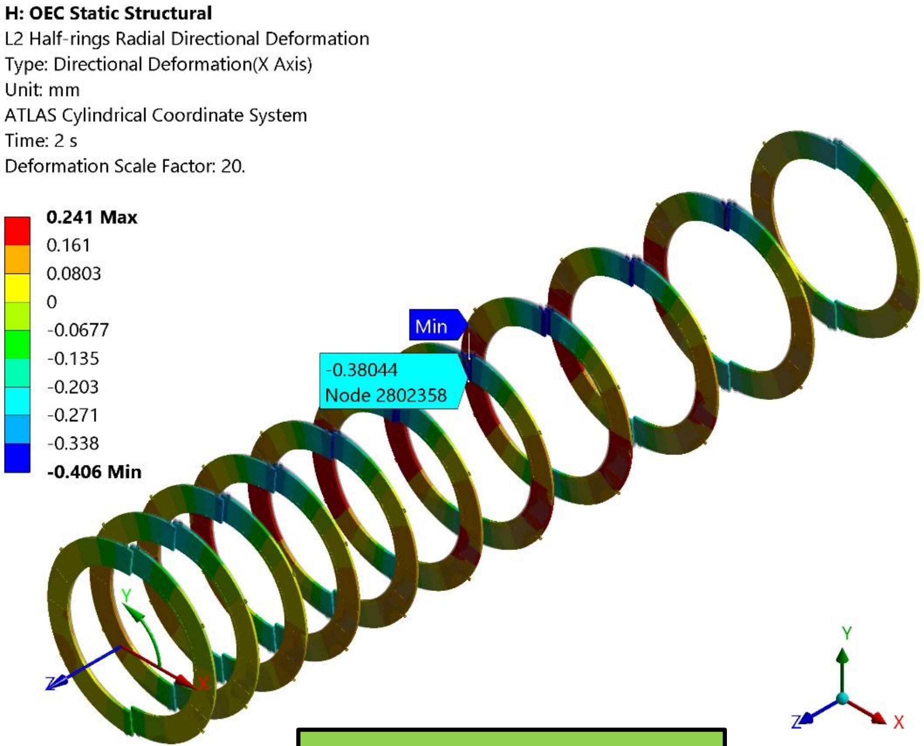

$UR_{I.min}$ = -0.380 mm

Thermal gradient =-55/-45°C, g x 1.2

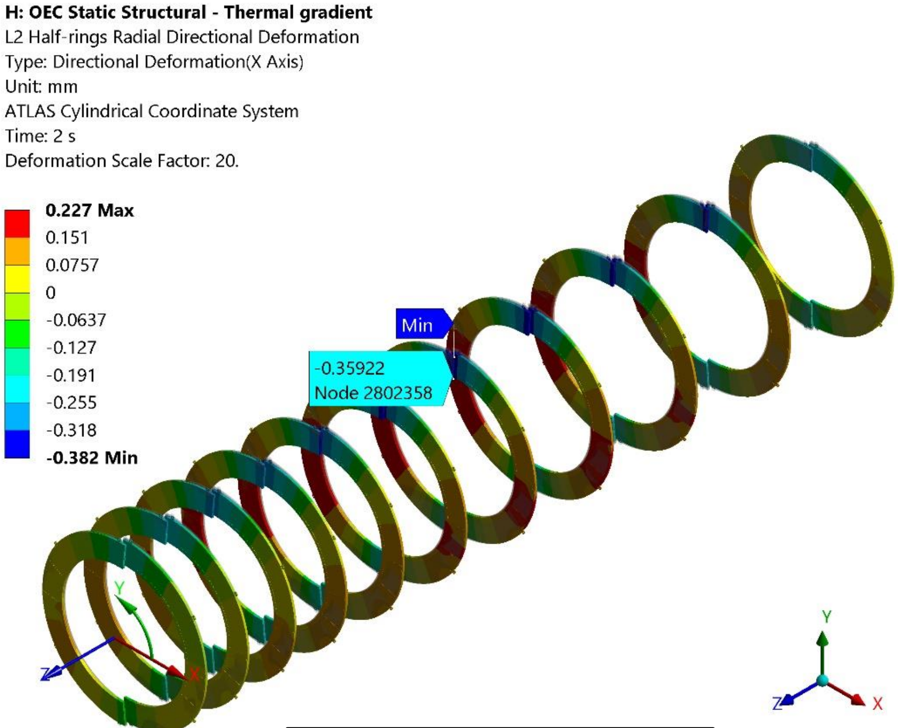

$UR_{I.min}$ = -0.359 mm **-5.6%**

Figure 37: L2 Half-rings Radial deformation - left: uniform T -55°C, right: thermal gradient -55/-45°C

Overall OEC FEA – Effect of Thermal gradient

In both cases, with or without thermal gradient, **FEA did not find radial violations of the OEC envelope.**

Table 10 below summarizes the results of the thermo-mechanical simulations concerning no envelope violation (updated FEM model).

STRUCTURE	FEATURE	NOMINAL RADIUS [mm]	MAXIMUM RADIAL DEFORMATION (FEA - T=-55°c) [mm]	MAX/MIN RADIUS AFTER DEFORMATION (FEA - T=-55°c) [mm]	OEC RADIAL ENVELOPE [mm]	RADIAL MARGIN [mm]
L4 HALF-SHELLS	outer diameter	**325.100**	**0.437**	**325.537**	**327.000**	**1.463**
FRONT/REAR SUPPORTS	inner diameter	**146.000**	**-0.065**	**145.935**	**145.000**	**0.935**
L2 HALF-RINGS	inner diameter	**146.300**	**-0.380**	**145.920**	**145.000**	**0.920**

Table 10: Results of OEC thermo-mechanical FEA @-55°C - No envelope violation.

Overall OEC FEA – Effect of Thermal gradient

L2 Half-shell - S_1 stress (top ply)

Uniform T=-55°C, g x 1.2

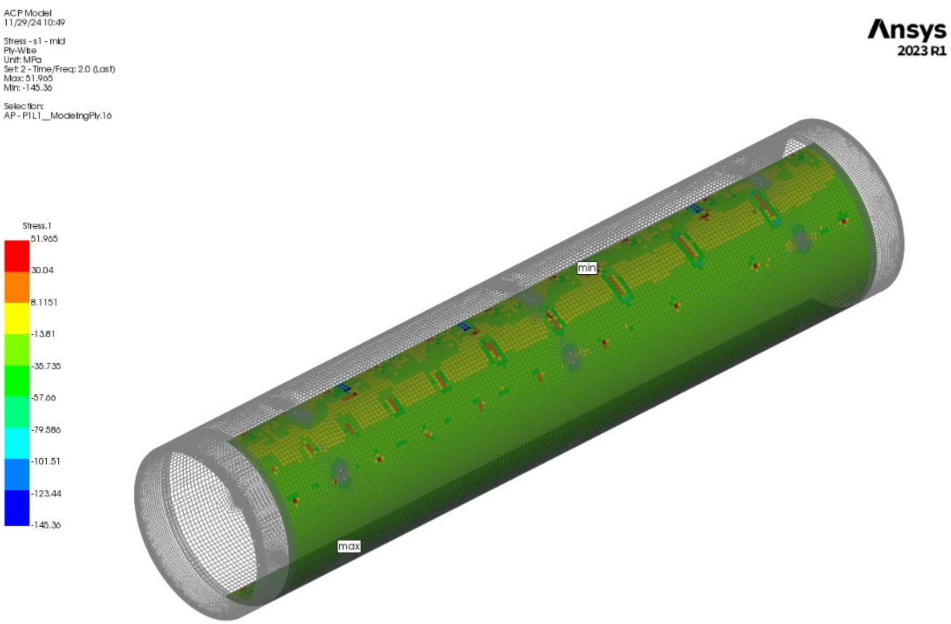

Thermal gradient =-55/-45°C, g x 1.2

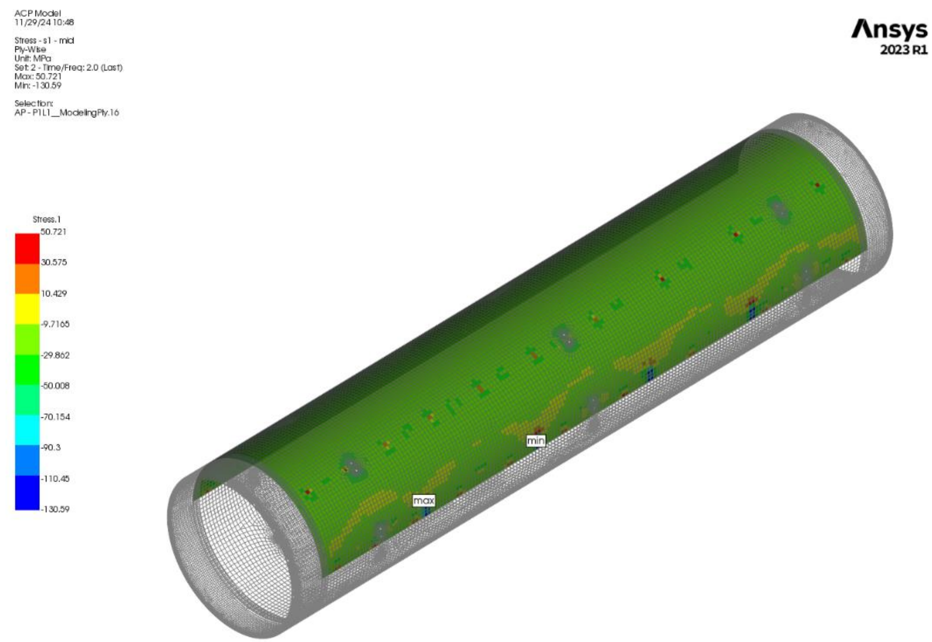

$S_{1,min}$ = -145.4 MPa

$S_{1,min}$ = -130.6 MPa **-10.2%**

Figure 38: L2 Half-shell -S_1 stress on top ply - left: uniform T -55°C, right: thermal gradient -55/-45°C.

Overall OEC FEA – Effect of Thermal gradient

L2 half-flange - S_1 stress (top ply)

Uniform T=-55°C, g x 1.2

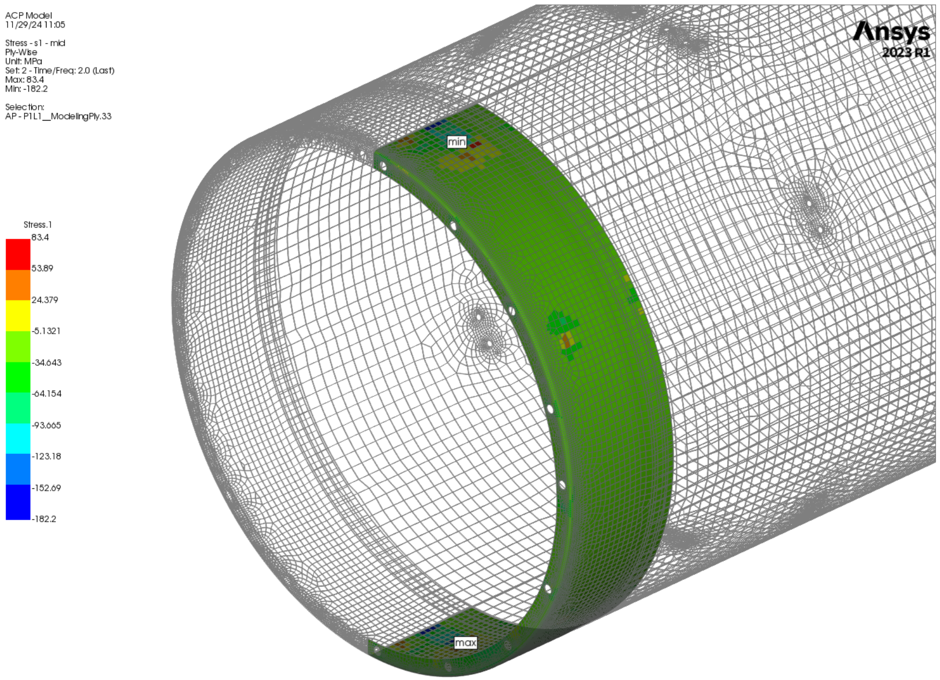

Thermal gradient =-55/-45°C, g x 1.2

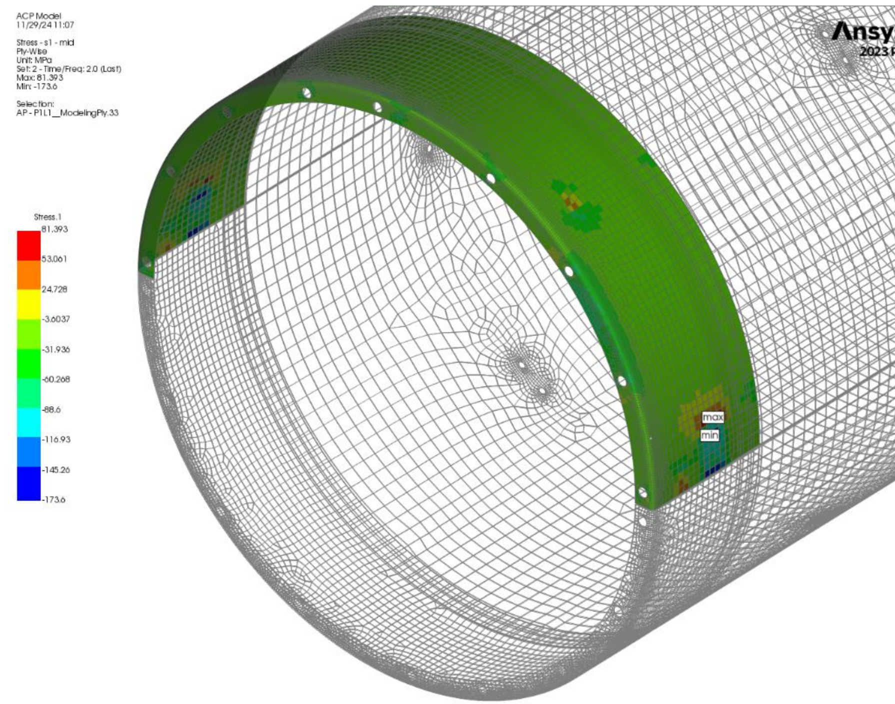

$S_{1,min}$ = -182.2 MPa

$S_{1,min}$ = -173.6 MPa **-4.7%**

Figure 39: L2 half-flange - S1 stress on top ply, left: uniform T -55°C, right: thermal gradient -55/-45°C.

ATLAS ITk

Overall OEC FEA – Effect of Thermal gradient

OEC Front Support - S_1 stress (bottom ply)

Uniform T=-55°C, g x 1.2

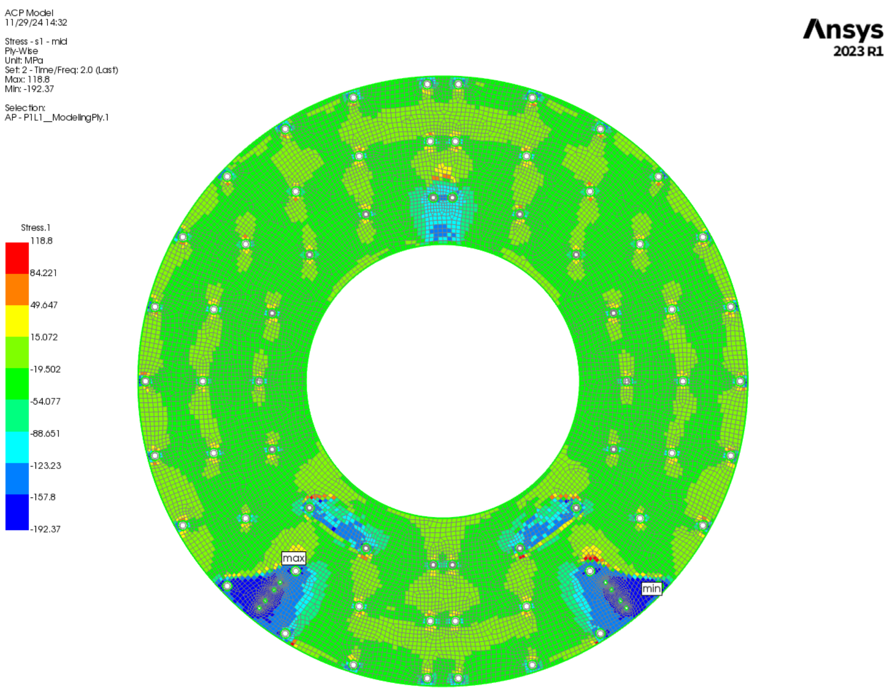

Thermal gradient =-55/-45°C, g x 1.2

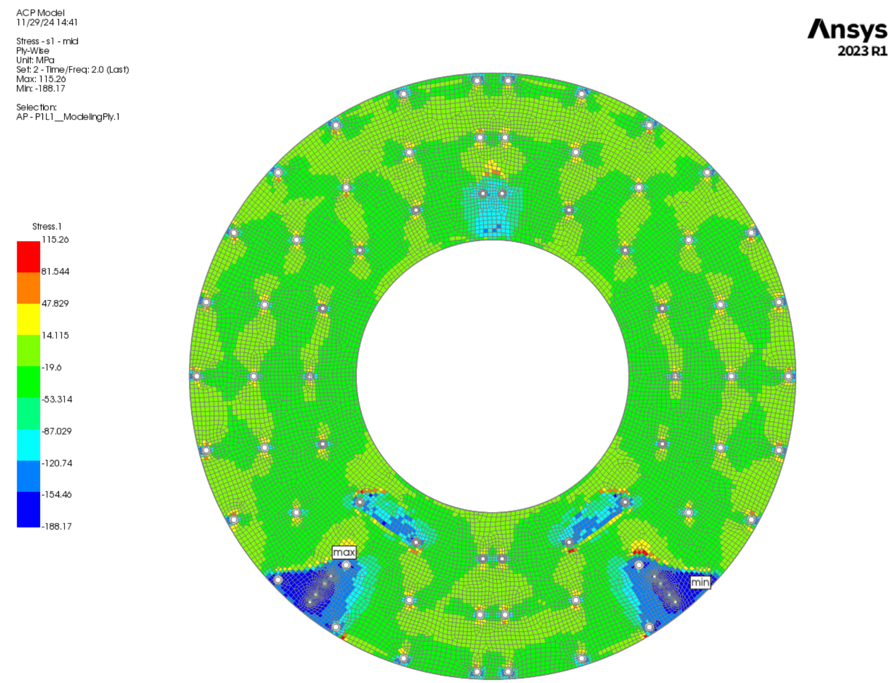

$S_{1,min}$ = -192.4 MPa

$S_{1,min}$ = -188.2 MPa

-2.2%

Figure 40: OEC Front Support - S_1 stress on top ply, left: uniform T -55°C, right: thermal gradient -55/-45°C.

B. Overall OEC FEA – Insertion load case

From the specification *AT2-IP-ES-0007 Rev. 4 - Section 4.8* [1] - *L.8 Insertion Load Case:*

Outer system insertion into the Strip detector will be a 5 wagons insertion. Two trollies will be necessary to hold services transition sectors *from end of the detector to PP1 and to Optoboxes for data cables.* ***The trolley will kinematicaly attached to the EC sector.***

The trolley tool + services extensions *(including connectors)* ***mass is less than 150Kg****. Trolley will slide on the PST pixel rails system.*

The insertion or extraction of the full pixel package will be done with a wire winch system by pulling.

The ***friction coefficient of the sliders on the rail system is set to 0.23****. A* ***safety factor of 1.5 will be applied on this parameter and the mass design values to evaluate the insertion forces****.*

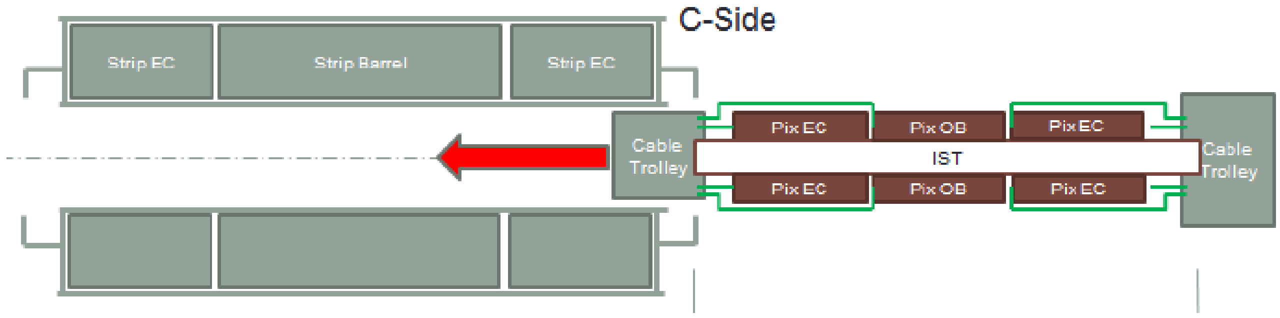

Figure 41: ITK Pixel insertion scheme

Overall OEC FEA – Insertion load case

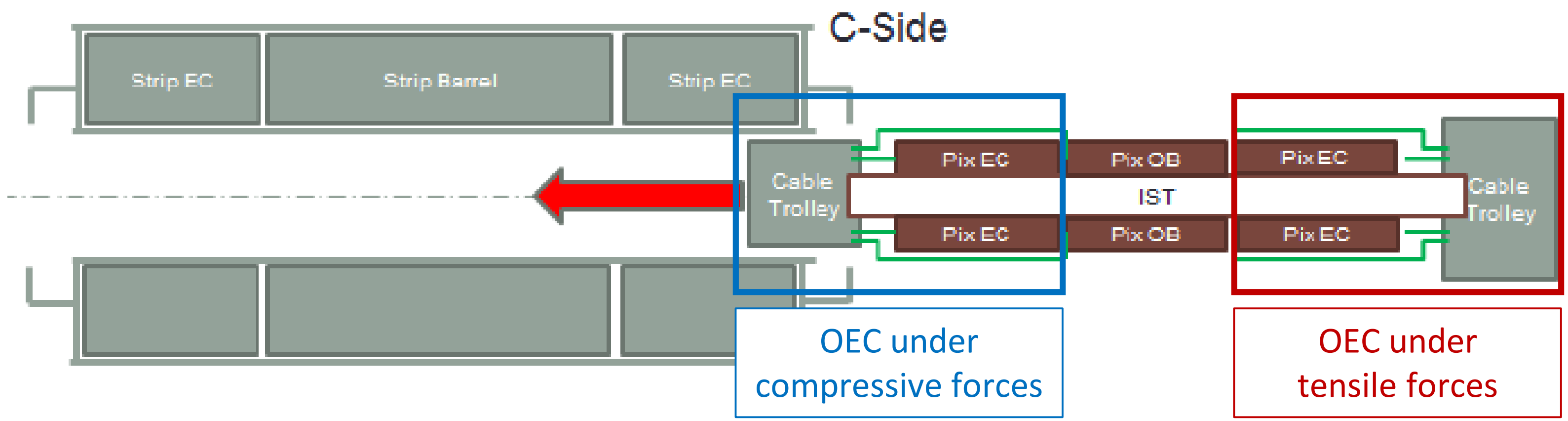

Compressive load is the worst structural case for the OEC because it can lead fibers buckling of the plies of the half-shells.

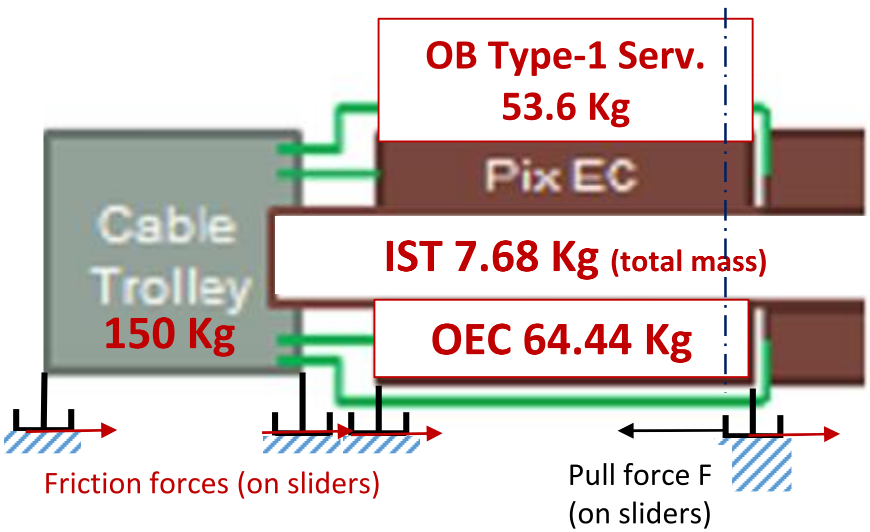

Masses are design values.

Compressive force:

Fc = (M x g x SF) x (μ x SF) =

=[(150+64.44/2+53.6/2+7.68/4) x 9.806 x 1.5] x (0.23 x 1.5)=

= **1071 N**

Overall OEC FEA – Insertion load case

Gravity x 1.2 SF has been applied along Y axis, in a preliminary load step 1.

Load step 2 simulates the insertion load case: a compressive force F_c = 1061 N has been applied on the sliders at low Z, while Z displacement has been blocked on the sliders at high Z.

VEE sliders: X,Y displacement blocked; Flat sliders: Y displacement blocked.

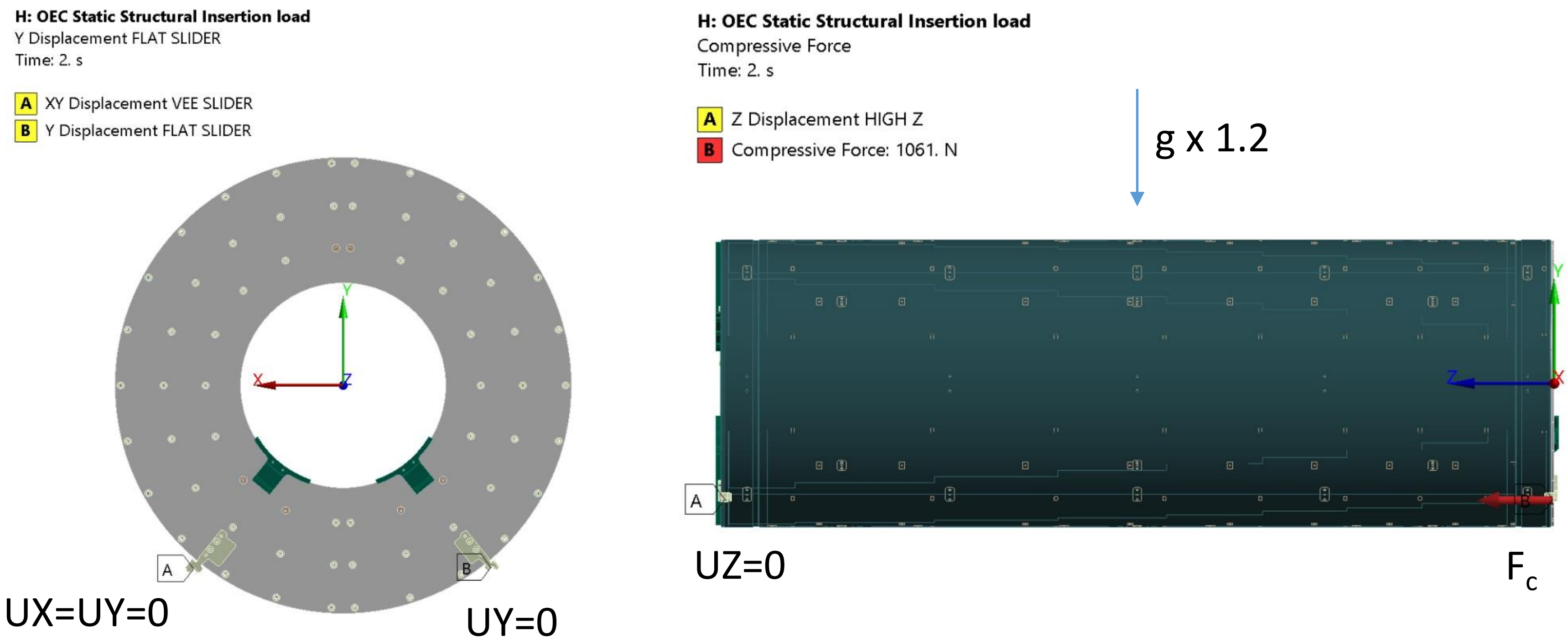

Figure 42: OEC insertion load case and constraints.

Overall OEC FEA – Insertion load case

Normal stress on the half-shells along Z axis

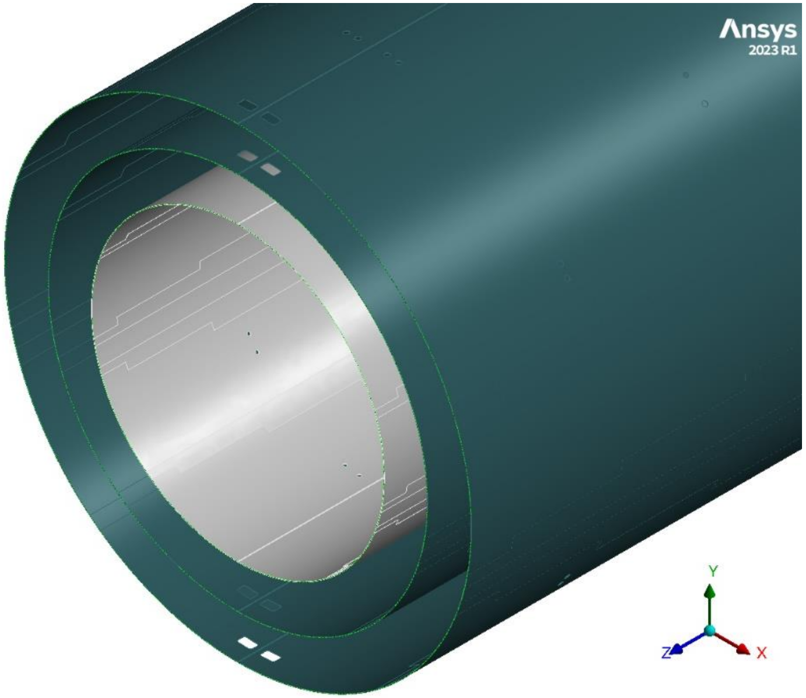

Half-shells cross section: A = 3211.4 mm^2

Compressive force: F_c = 1061 N

In the hypothesis of uniformly distributed compressive load on the three half-cylinder, the average compressive stress is:

$$\sigma_{Z,av} = \frac{F_c}{A} = \frac{1061\ N}{3211.4\ mm^2} = 0.33\ N/mm^2$$

Figure 43 : OEC cross section.

Overall OEC FEA – Insertion load case

OEC Total deformation

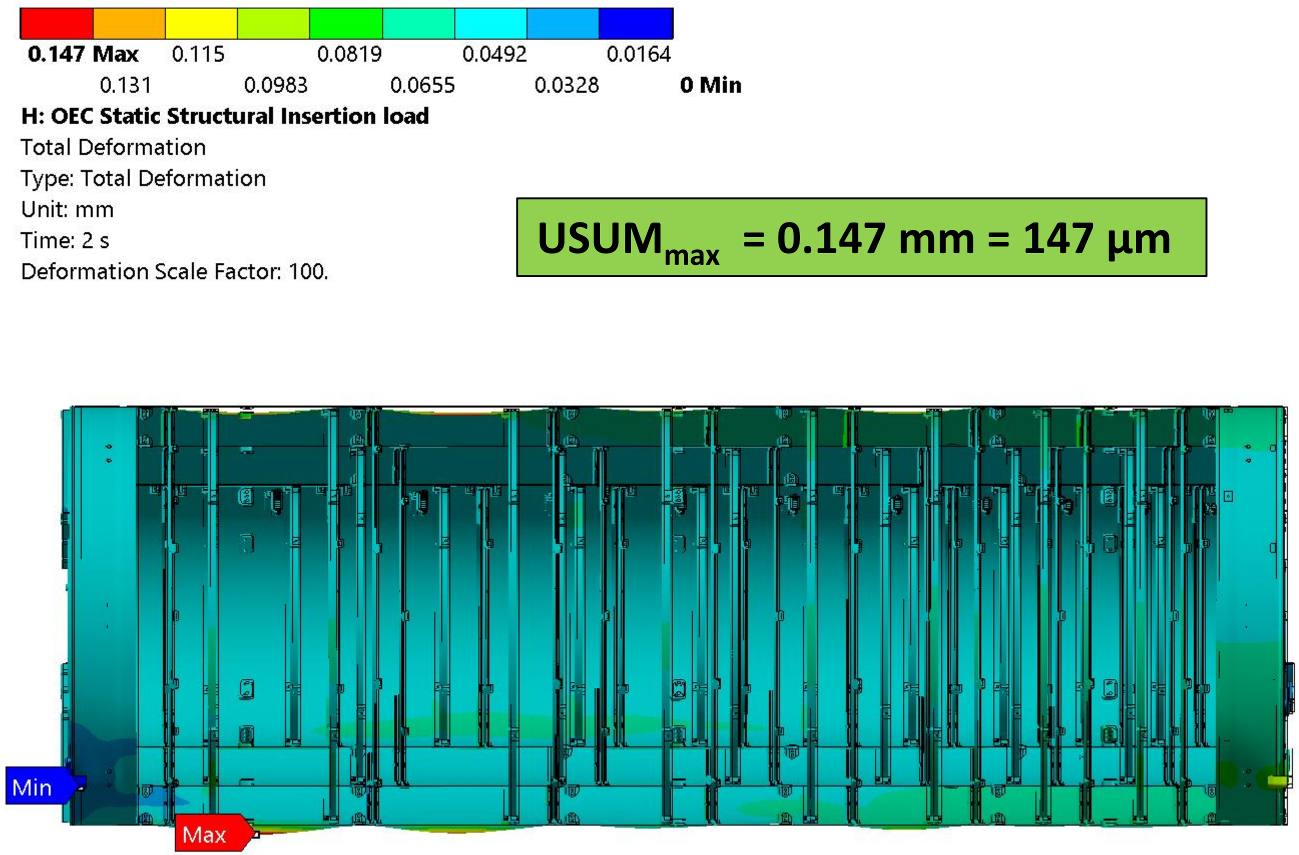

Figure 44: Insertion load case – OEC Total deformation.

Overall OEC FEA – Insertion load case

Normal stress along Z axis : L4,L3 (orthotropic) half-shells

To be verified with ANSYS ACP

L4 Half-shells

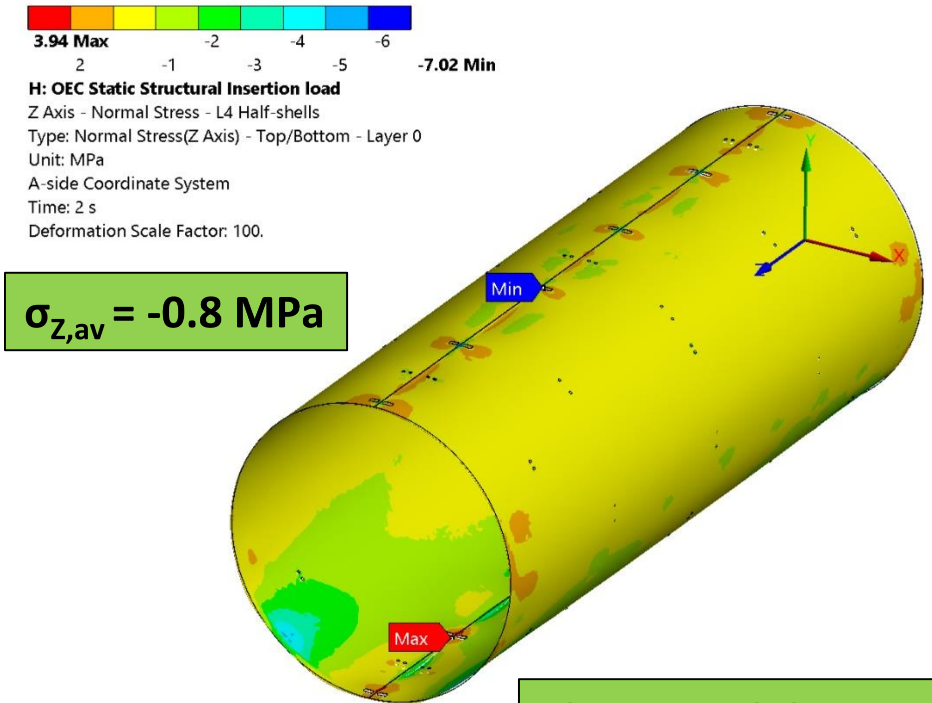

$\sigma_{Z,av}$ = -0.8 MPa

L3 Half-shells

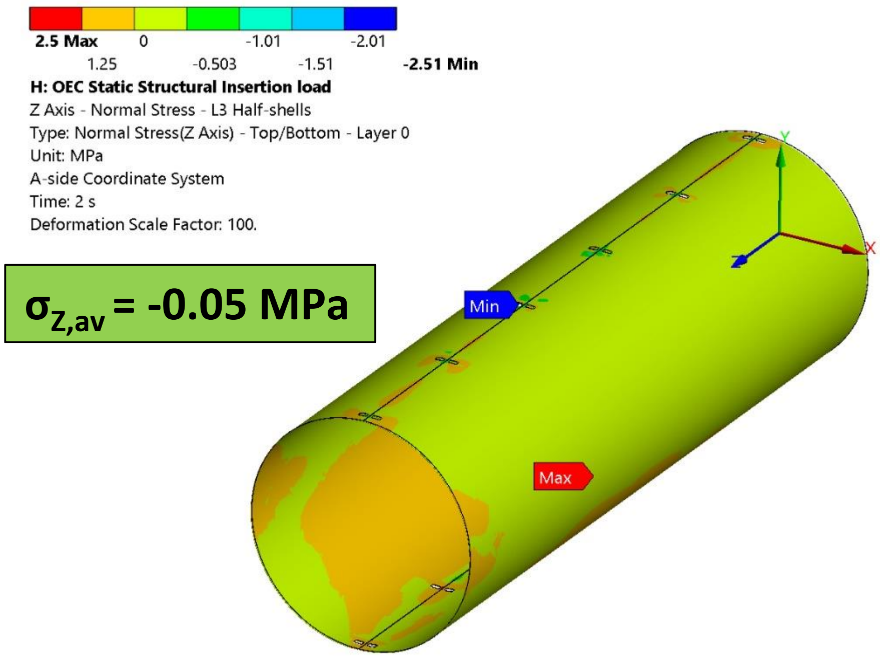

$\sigma_{Z,av}$ = -0.05 MPa

L2: $\sigma_{Z,av}$ = -0.01 MPa (ANSYS Workbench)

Figure 45: Insertion load case – L4 h-s (left) and L3 h-s (right) Normal stress along Z axis

Overall OEC FEA – Insertion load case

L2 Half-shells - S_1 stress (top ply)

L2 half-shells/flanges analysis in ANSYS ACP shows that S_1 maximum compressive stress is -4.69 MPa (middle ply with fibers oriented along 0°C). Comparison with compressive strength ($\boldsymbol{F_{1c,(46.5\%)}}$ = -**566 MPa**) gives **SF ≅ 120**. **Fibers buckling can be excluded.**

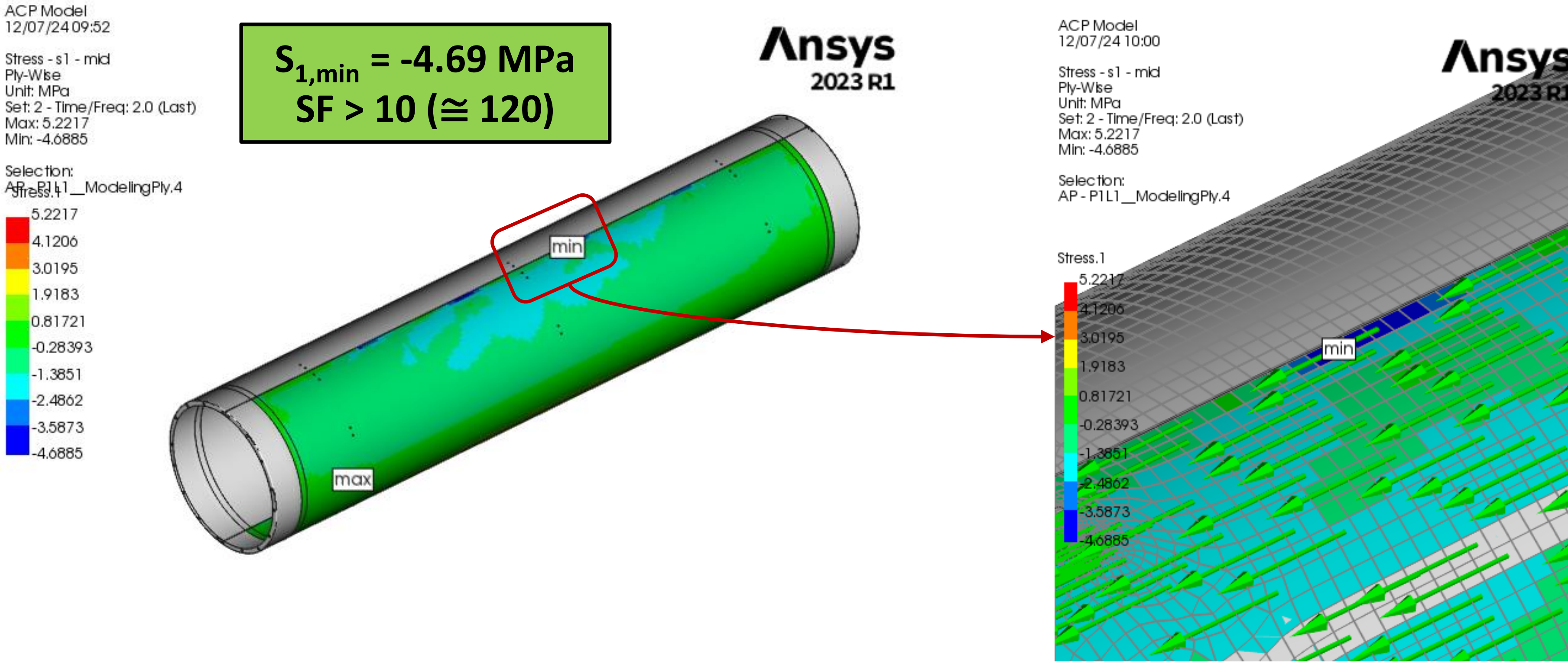

Figure 46: Insertion load case –Compressive S_1 stress along fibers of the middle ply

Overall OEC FEA – Insertion load case

Axial deformation of the front support

The deformation along the Z axis of the OEC Front Support is shown in figure below. Max deformation and stress concentration are clearly in the region of the Titanium inserts.

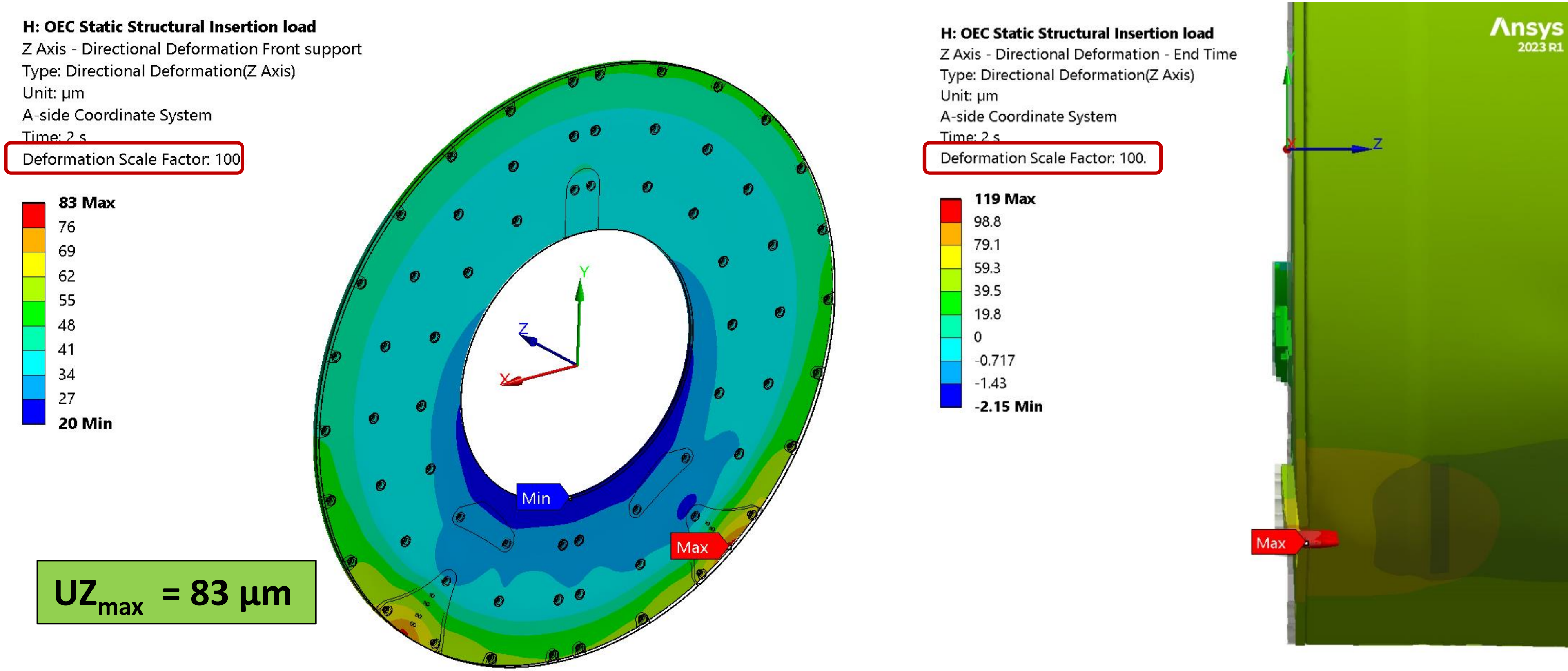

Figure 47: Insertion load case – Front Support deformation along Z direction.

Overall OEC FEA – Insertion load case

Front support stress analysis

Titanium inserts Von Mises stress

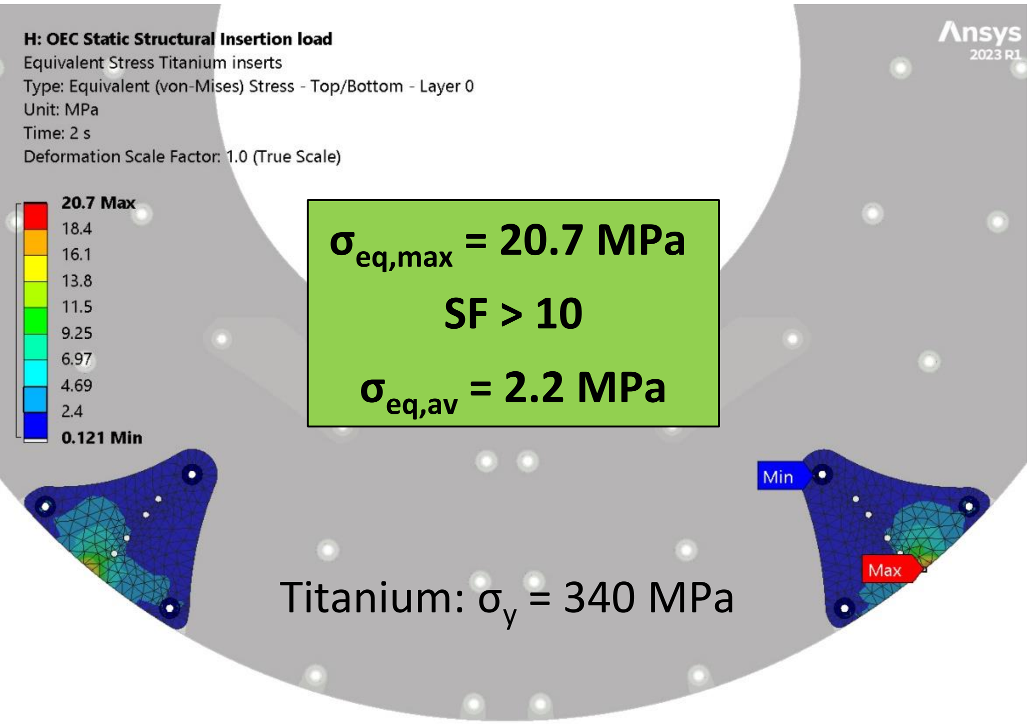

Maximum is clearly a peak on the edge

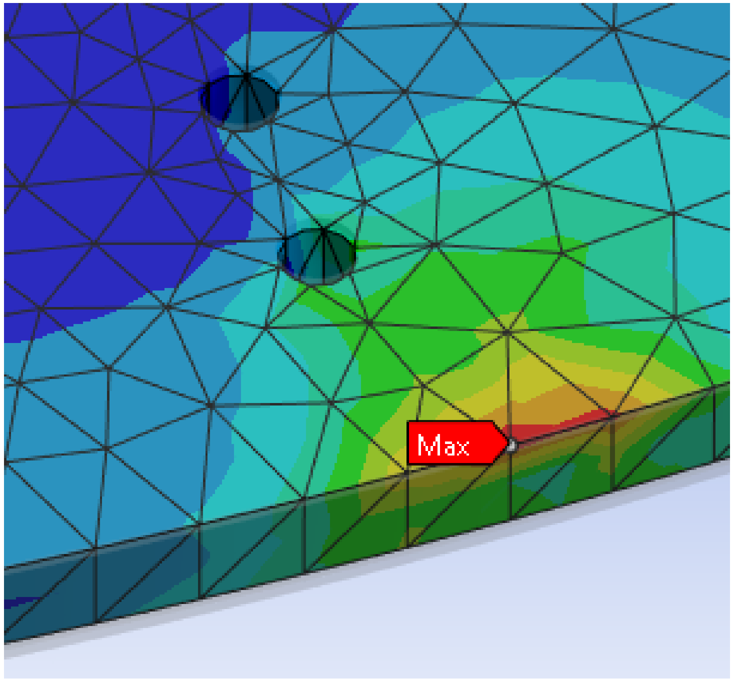

Figure 48: OEC insertion load case – Titanium inserts of the Front Support - Von Mises stress

Overall OEC FEA – Insertion load case

Front support stress analysis

Shear stress S_{13}, S_{23} over CFRP in contact with Titanium inserts (bottom ply).

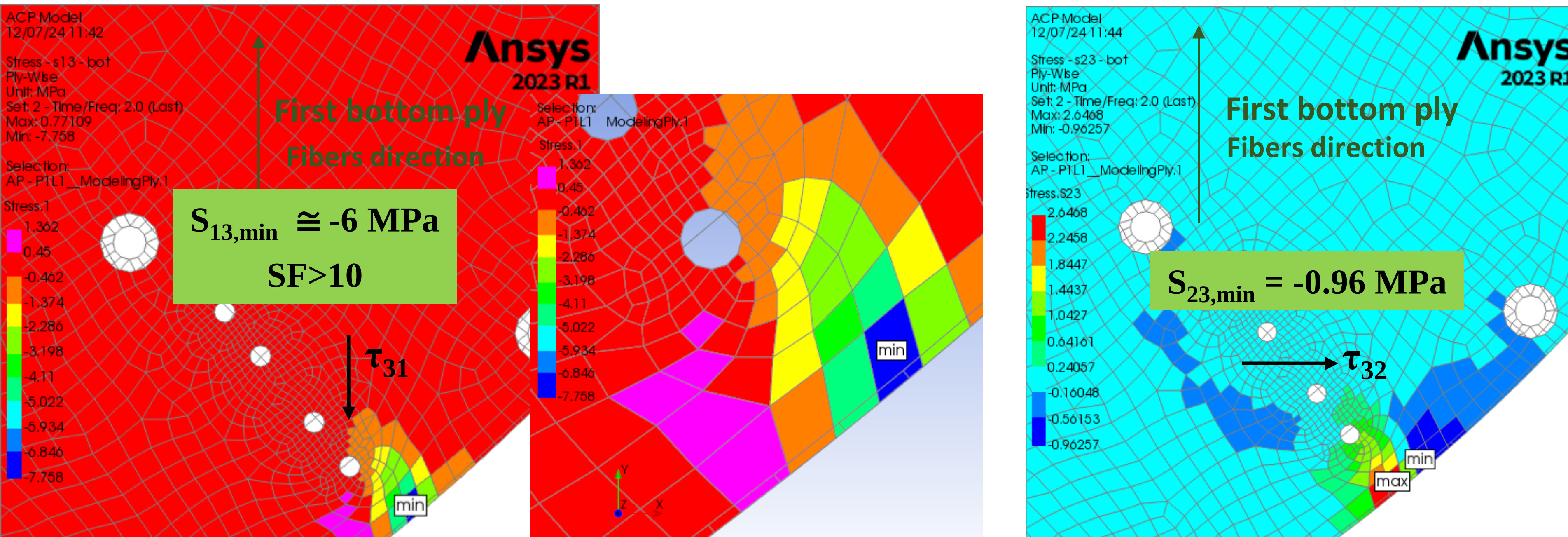

Figure 49: Insertion load case –Shear stress of CF skin on the interface with Titanium insert.

The peak of S_{13} Shear stress on the edge is a false value, the minimum can be conservatively set to -6 MPa, while the average value is very low (≈ 0.5 MPa). The interlaminar Shear Strength of unidirectional laminate M55J/EX15125is 62 MPa (Toray datasheet, Vf 60%) this implies a minimum SF > 10.

Overall OEC FEA – Insertion load case

Front support stress analysis

Compressive stress σ_Z (S_3) on the CFRP in contact regions with sliders (top ply).

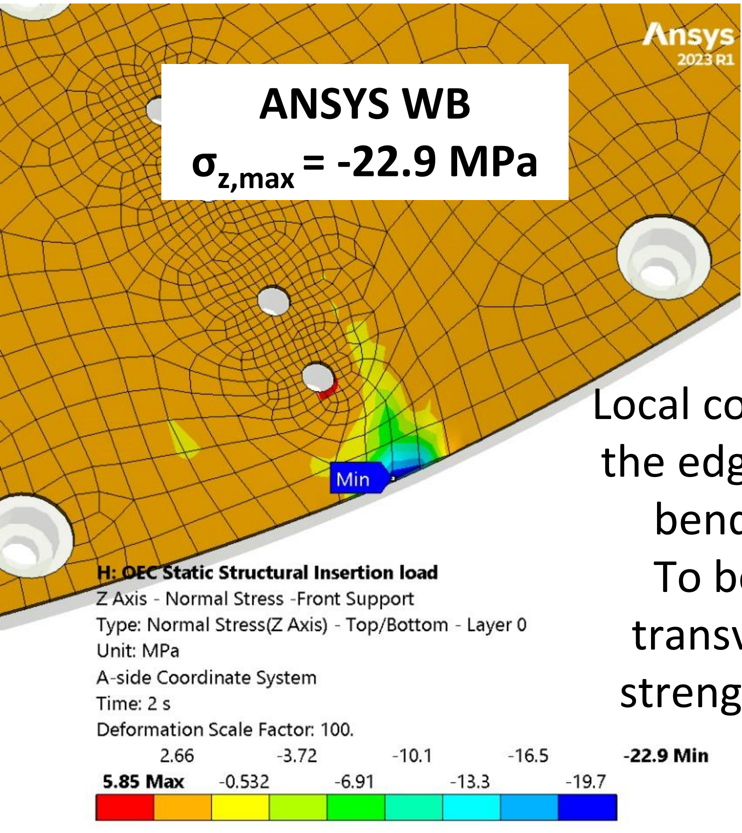

Local compressive stress on the edge due to the elastic bending of the slider.
To be compared with transverse compressive strength of the pre-preg.

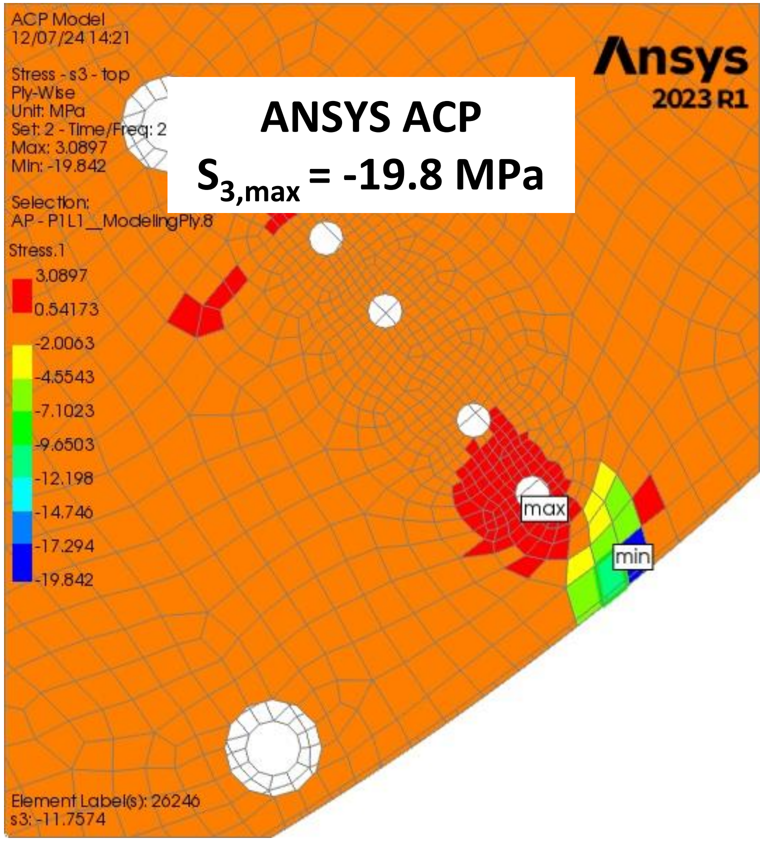

Figure 50: Insertion load case – Compressive stress of the top CFRP of the Front support

Overall OEC FEA – Effect of detector inclination

R-29: For all FEA simulations, the inclination of the ATLAS detector by 0.708° should be implemented (even if it is probably irrelevant for all practical purposes).

Static friction can be defined in terms of the maximum angle before which one of the items will begin sliding. This is called the angle of friction. It is defined as: $\tan\theta = \mu_s$ and thus: $\theta = \arctan \mu_s$ is the angle from horizontal and μ_s is the static coefficient of friction between the objects. So, in the case of the Pixel Detector:

$\tan(0.708°) = 0.012 < \mu_K = 0.23 < \mu_s$ (unknown)

Where $\mu_K = 0.23$ is the coefficient of kinetic friction *of the sliders on the rail system.*

The static friction forces take in place the detector, without any relevant axial action on the OEC of the C-side. Even considering zero the friction static forces, the axial action exerted on the C-side OEC would be $\cong 58\ \mathrm{N} \ll 1071\ \mathrm{N}$ suffered during insertion.

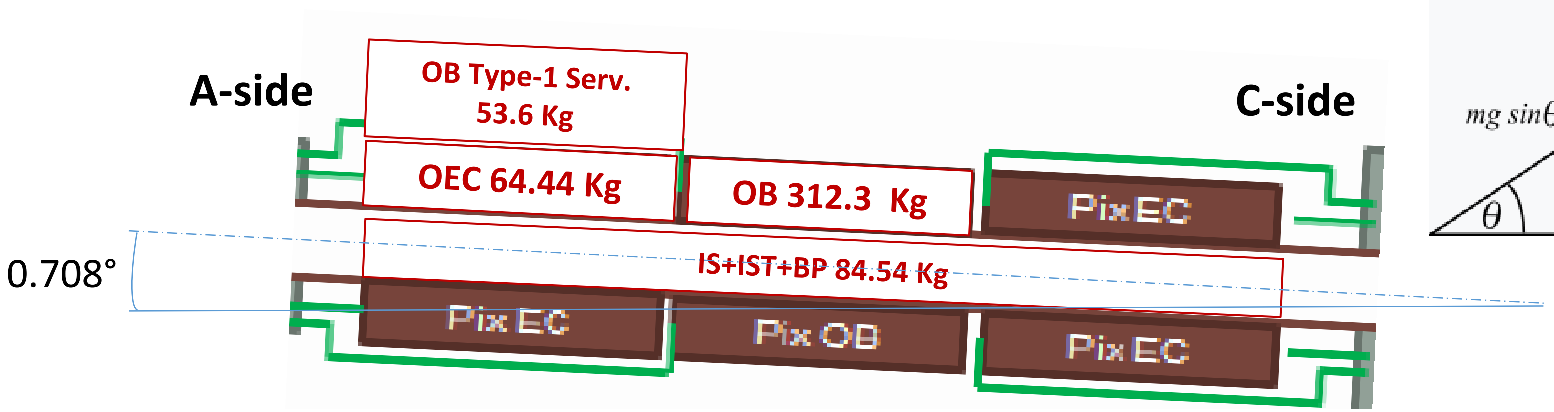

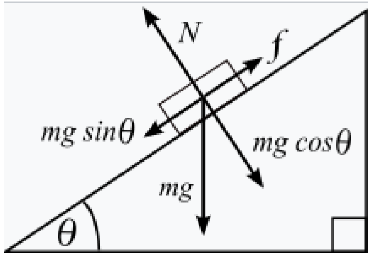

Figure 51: Evaluation of the effects of ITK Pixel Detector inclination

Overall OEC FEA

Conclusions

Responses of the thermo-mechanical and mechanical FEA of the overall OEC:

1. **A thermal gradient of 10°C along the OEC vertical axis (-55°C on the OEC bottom, -45°C on the OEC top), doesn't produce any worsening effects in deformations and stresses if compared with the total cooling down at uniform temperature (-55°C).** Maximum deformations and stresses of the Global Structures are reduced by 2÷10% applying the thermal gradient.

2. **The pull force during insertion of the Pixel Outer System into the Strip detector doesn't produce stresses that determine a safety factor of the OEC Global Structures below the expected value of 10 . Deformations are below 150 µm (less than those caused by cooling down).**

   However, possible local effects (stress concentrations) on the Front/Rear supports must be evaluated carefully after the finalization of the design.

3. **The effect of Pixel Detector inclination** (0.708°) **over the Global structures of the OEC after installation appears to be negligible**, because the friction forces are prevalent over a sliding that can produce an axial loading (which would be in any case lower than the axial load during the insertion into the Strip detector).

OEC FEA studies - references

[1] *ITk Pixel Global Supports Design Specifications* - AT2-IP-ES-0007 Rev. 4. https://edms.cern.ch/document/2016196/4.

[2] *ATLAS ITk Pixel ICD Between Outer Endcap and Global Mechanics Supports AT2-IP-MG-0013 rev. 4.* https://edms.cern.ch/document/2429049/2.

[3] *ITk Envelope Drawing* - AT2-IC-EP-0001 v.2.0. https://edms.cern.ch/document/1905419/2.0.

[4] *Production Readiness Review of Bare Local Supports for the ITk Pixel Outer Endcaps - AT2-IP-ER-0059 v.2 https://edms.cern.ch/document/2975996/2*

[5] *Description of the Global Mechanics and Integration Sequence for the Endcaps* AT2-IP-EN-0024 v.1

[6] *ITk Pixel Local Support Design Specifications* - AT2-IP-ES-0005 Rev. 5.1 https://edms.cern.ch/document/1534572/6.3

OEC FEA studies - references

[7] *Isaac M. Daniel, Ori Ishai Engineering Mechanics of composite materials, second edition, Oxford University Press 2006.*

[8] *Ryan Karkkainen, Oscar Martinez, Ply Strength Prediction of Unidirectional Continuous Carbon Fiber Composites, ORNL, 2023,* https://info.ornl.gov/sites/publications/Files/Pub204701.pdf

[9] https://www-eng.lbl.gov/~ecanderssen/PHENIX/Stave/M55J%2072gsm%2041.3%25%20 EX1515/M55J%20PrePreg%20 Calculations.xls

[10] https://www.toraytac.com/media/57c4813d-ce39-4b11-a5f4-11c3aaeeeef4/14xkyg/TAC/ Documents/Data_sheets/Thermoset/UD%20tapes%20and%20prepregs/EX-1515_Cyanate-Ester_PDS.pdf

[11] Sater J. Rigdon M., *Graphite-Reinforced Polycanate Composites for Space and Missile Applications*, Institute for Defense Analysis, 1801 N. Beauregard Street, Alexandria, Virginia 22311-1772" year 1993 Report, number AD-A285 509 https://apps.dtic.mil/sti/tr/pdf/ADA285509.pdf

OEC FEA studies

Backup slides

Overall OEC FEM model: half-rings

Each **half-ring assembly, in the FEM model includes**:

- Faceplates (CFRPs)
- Carbon foam
- Lugs
- Bus tape
- Cooling pipe (evaporator)
- Fittings and electrical breakers

Pixel modules are not directly modeled: footprints on CFRPs allow to apply their masses in the FEM model.

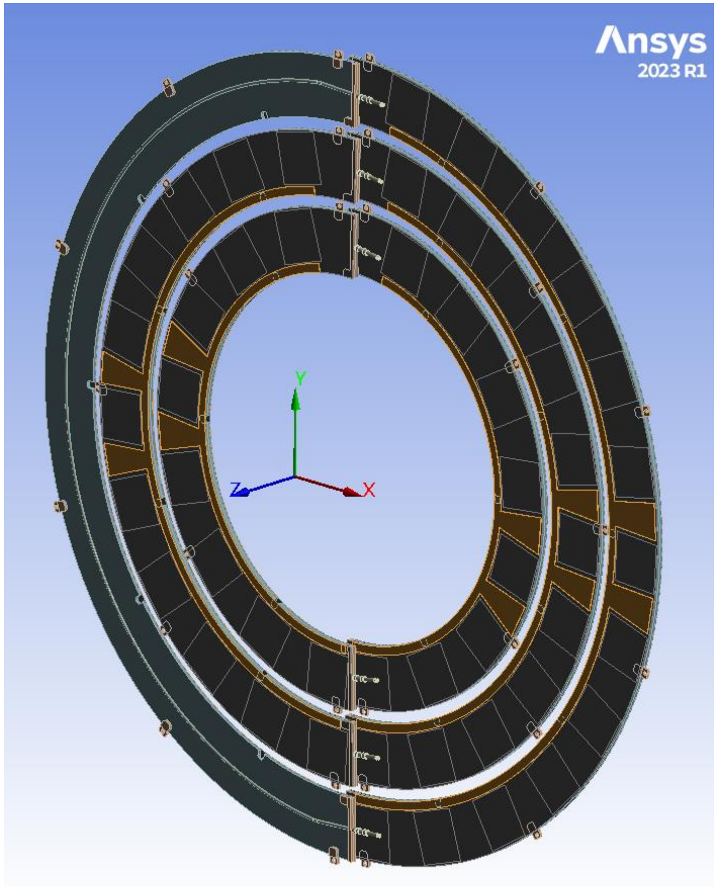

Figure: half rings assembly.

M55J/EX1515 pre-preg material properties

Toray datasheet refers to 60% fiber volume fraction, so the strength values must be scaled to 46.5% fiber volume fraction.

When the longitudinal fibers are in tension, the phase with the lower ultimate strain will fail first. For perfectly bonded fibers, the average longitudinal stress in the composite, $\boldsymbol{\sigma_1}$, is given by the rule of mixtures as [7]:

$$\boldsymbol{\sigma_1 = \sigma_f V_f + \sigma_m V_m} \quad \textbf{(1)}$$

Where

$\boldsymbol{\sigma_f, \sigma_m}$ = average longitudinal stresses in the fiber and matrix, respectively

$\boldsymbol{V_f, V_m}$ = fiber and matrix volume ratios, respectively.

Under the simple deterministic assumption of uniform strengths, in the case in which the ultimate tensile strain of the fiber is lower than that of the matrix , the composite will fail when its longitudinal strain reaches the ultimate tensile strain in the fiber. This is the case of the composite lamina **M55J/EX1515**: the strain at failure of the high modulus carbon fiber M55J is **0.8%.**

In this case, the longitudinal tensile strength of the composite can be approximated by the relation:

$$\boldsymbol{F_{1t} = F_{ft} V_f + \sigma'_m V_m} \quad \textbf{(2)}$$

Where

$\boldsymbol{F_{1t}}$ = longitudinal composite tensile strength

$\boldsymbol{F_{ft}}$ = longitudinal fiber tensile strength

$\boldsymbol{\sigma'_m}$ = average longitudinal matrix stress when ultimate fiber strain is reached.

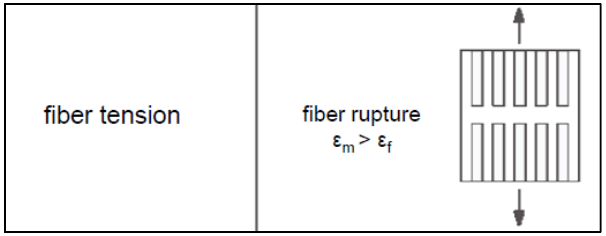

M55J/EX1515 pre-preg material properties

Assuming linear elastic behavior for the constituents and, being the fibers very stiff (E_f = 540 GPa $\gg$ E_m = 3.5 GPa), eq. (2) can be simplified as:

$$\boldsymbol{F_{1t} = F_{ft}V_f + E_m\varepsilon_{ft}V_m = F_{ft}\left(V_f + V_m\frac{E_m}{E_f}\right) \cong F_{ft}V_f} \quad \textbf{(3)}$$

which can be used to rescale the longitudinal tensile strength along fibers direction, from V_f= 60% to V_f= 46.5%:

$$\boldsymbol{F_{1t,(46.5\%)} \cong F_{1t(60\%)}\frac{0.465}{0.6}} \textbf{ = 1896 MPa} \cdot \boldsymbol{\frac{0.465}{0.6}} \textbf{ = 1469 MPa.}$$

Failure and strength of continuous-fiber composites under longitudinal compression is associated with microbuckling of the fibers within the matrix. A ply axial compressive strength ($\boldsymbol{F_{1c}}$) in a carbon–epoxy composite can be referenced from ply tensile strength ($\boldsymbol{F_{1t}}$), which must be decreased by a factor to include the effects of fiber anisotropy, kinking, misalignment, and buckling modes [8].

Referring to Toray **M55J/EX1515** datasheet (V_f= 60%) :

$$F_{1c}/F_{1t} = {}^{731\ MPa}/_{1896\ MPa} = 0.386$$

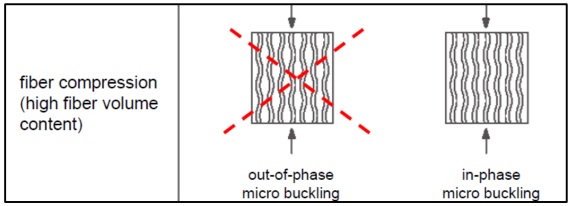

which can be used to calculate the longitudinal compressive strength along fibers direction for V_f= 46.5%:

$$|\boldsymbol{F_{1c,(46.5\%)}}| \cong \boldsymbol{0.386 \cdot F_{1t,(46.5\%)}} = 0.386 \cdot 1469 \text{ MPa} = \textbf{566 MPa.}$$

OEC thermo-mechanical FEA: Layer 2 results

Load step 1: Gravity x 1.2 safety factor

Vertical (Y axis) deformation

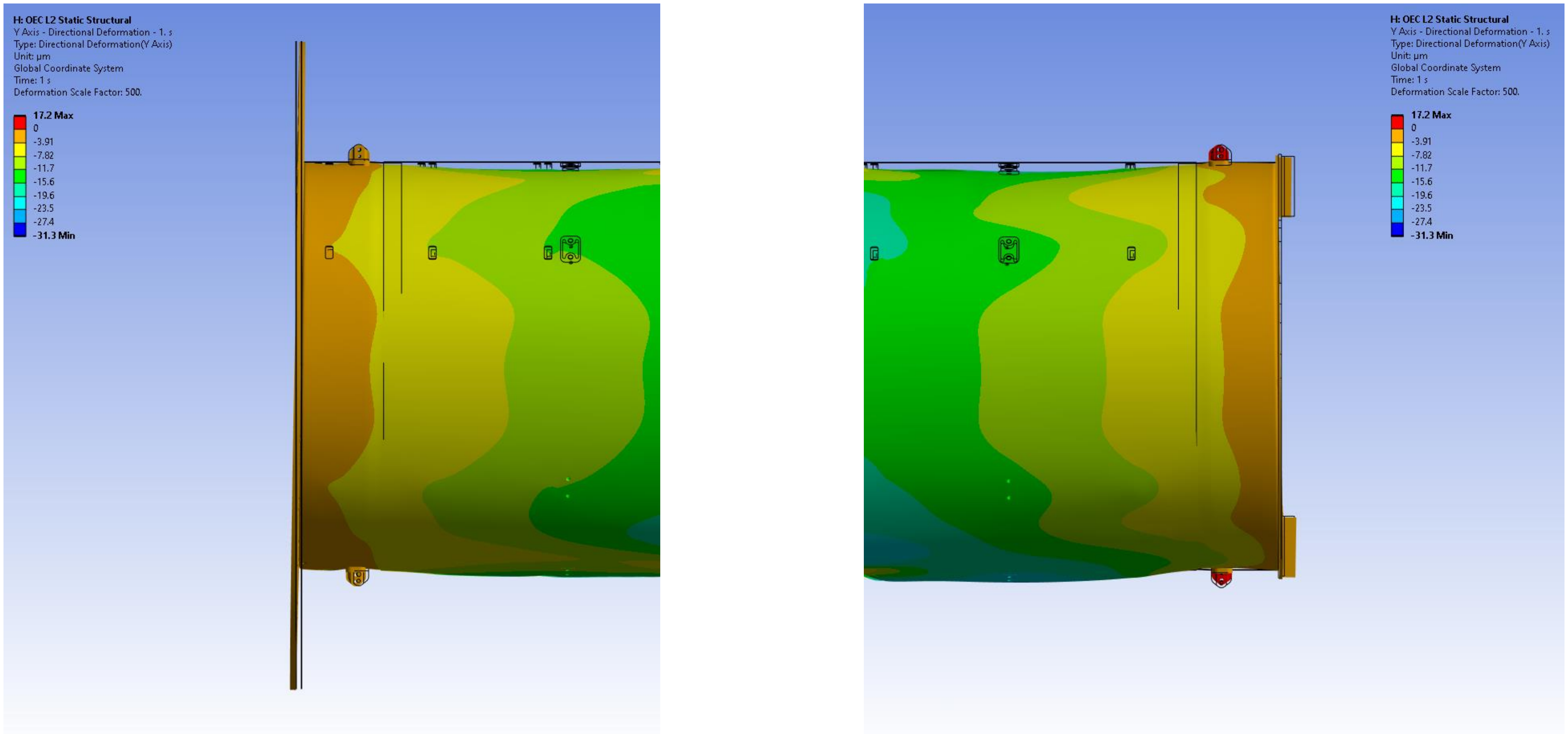

Figure: OEC L2 – Vertical deformation under gravity x 1.2 SF.

OEC thermo-mechanical FEA: Layer 2 results

Load step 1: Gravity x 1.2 safety factor

Vertical (Y axis) deformation

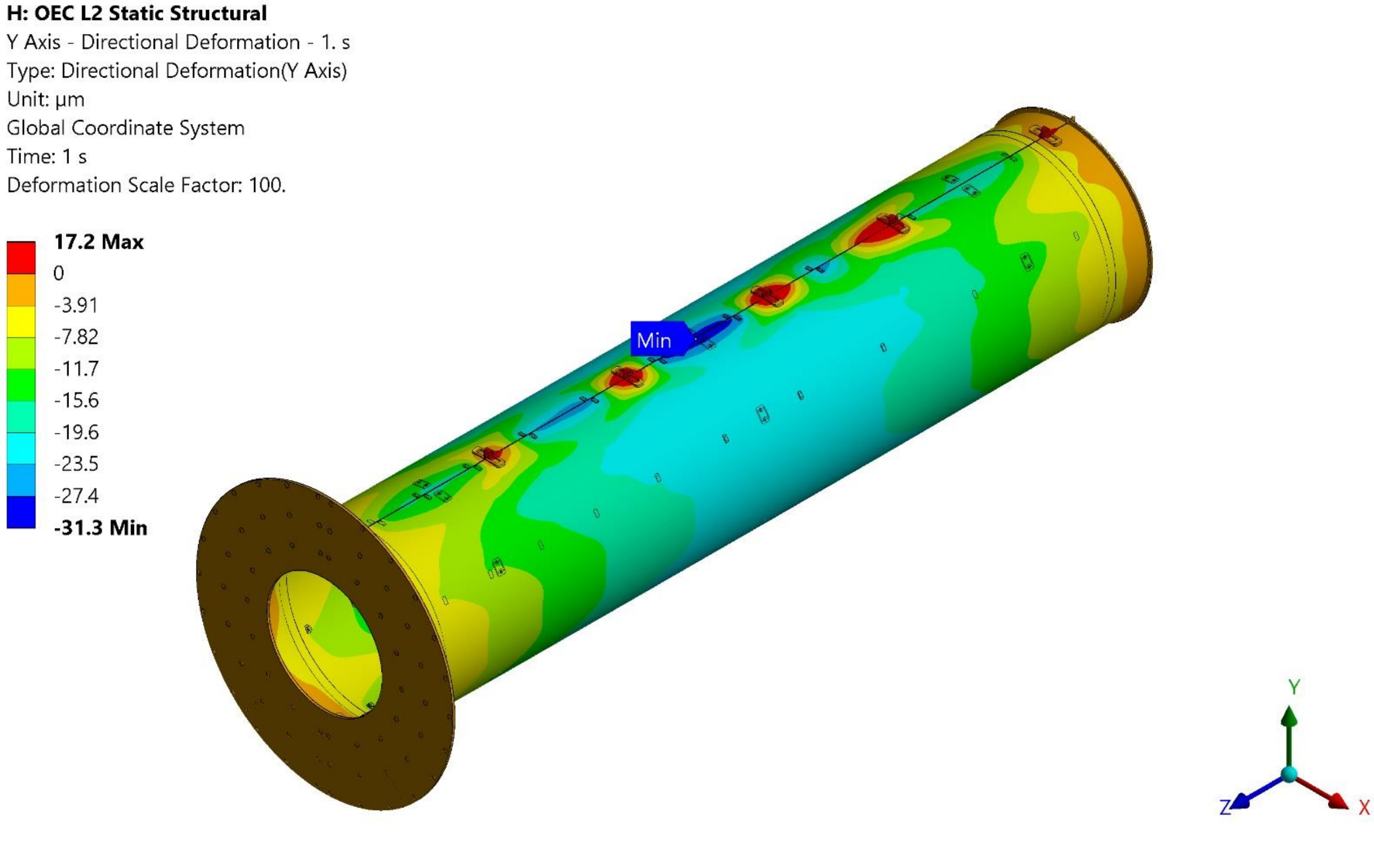

Figure: OEC L2 – Vertical deformation under gravity x 1.2 SF.

OEC thermo-mechanical FEA: Layer 2 results

Load step 2: Cooling down from +20°C to – 55°C

Total deformation

$USUM_{max}$ = 906 µm

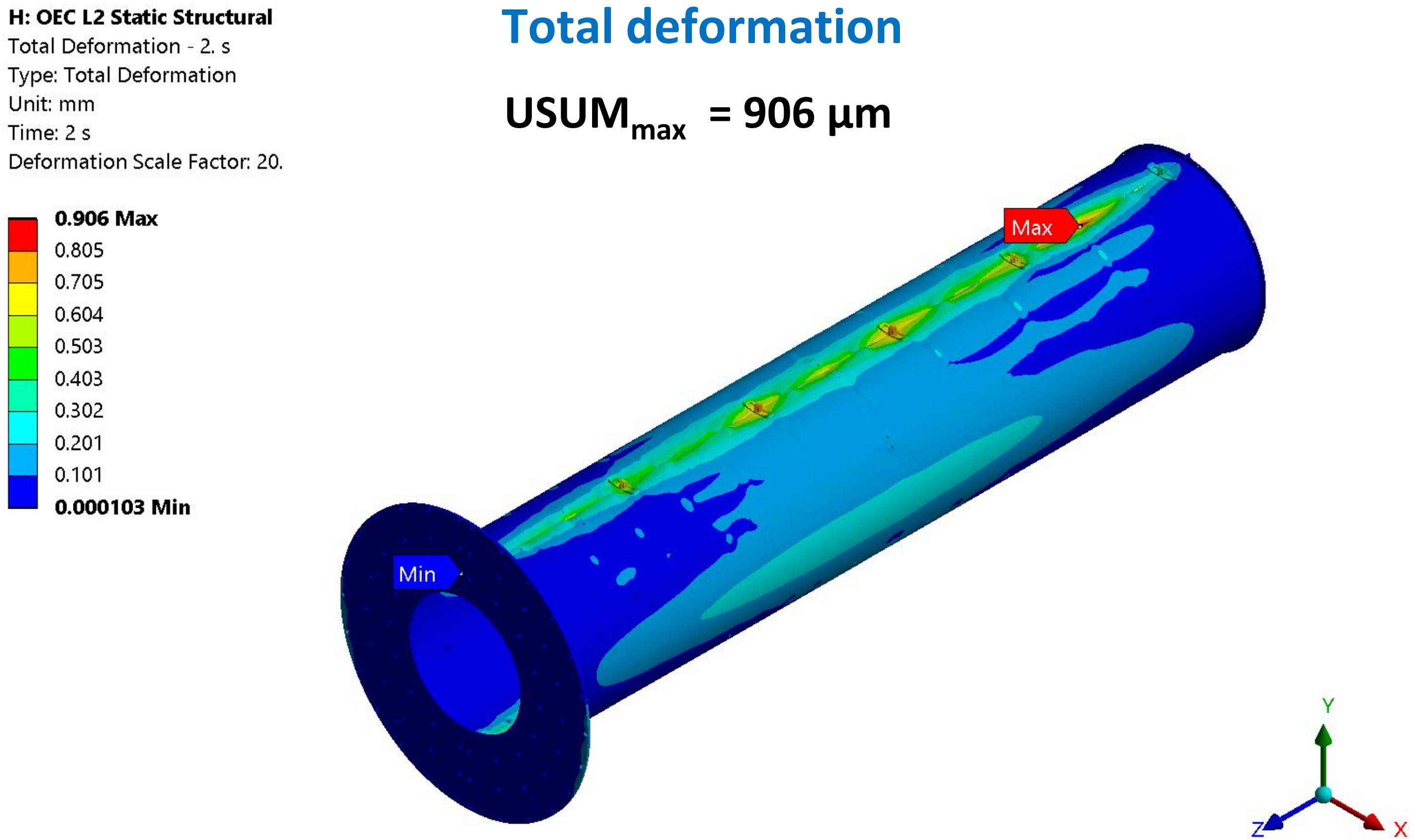

Figure: OEC L2 – Total deformation after cooling down @-55°C

OEC thermo-mechanical FEA: Layer 2 results

Load step 2: Cooling down from +20°C to – 55°C

L2 Half-shells Radial deformation

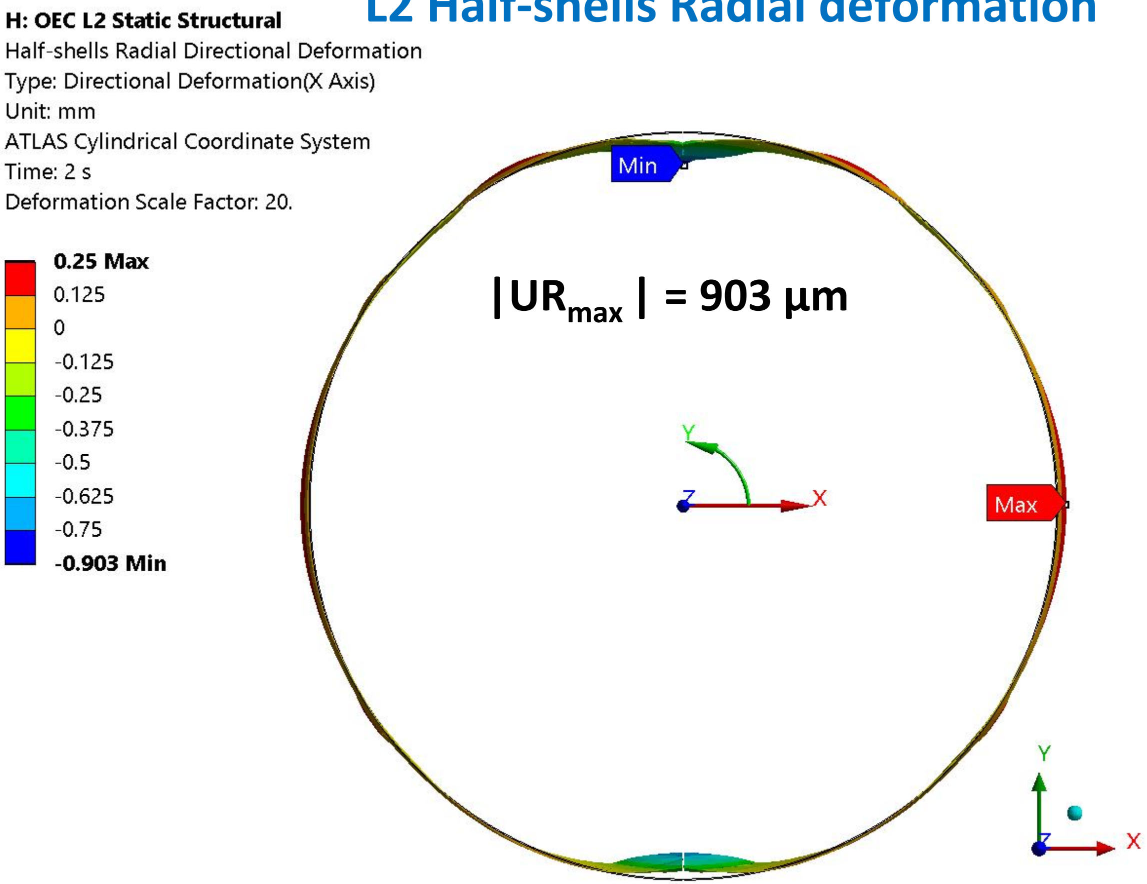

Figure: OEC L2 – Half-shells Radial deformation after cooling down @-55°C

OEC thermo-mechanical FEA: Layer 2 results

Load step 2: Cooling down from +20°C to – 55°C

L2 Half-shells Radial deformation

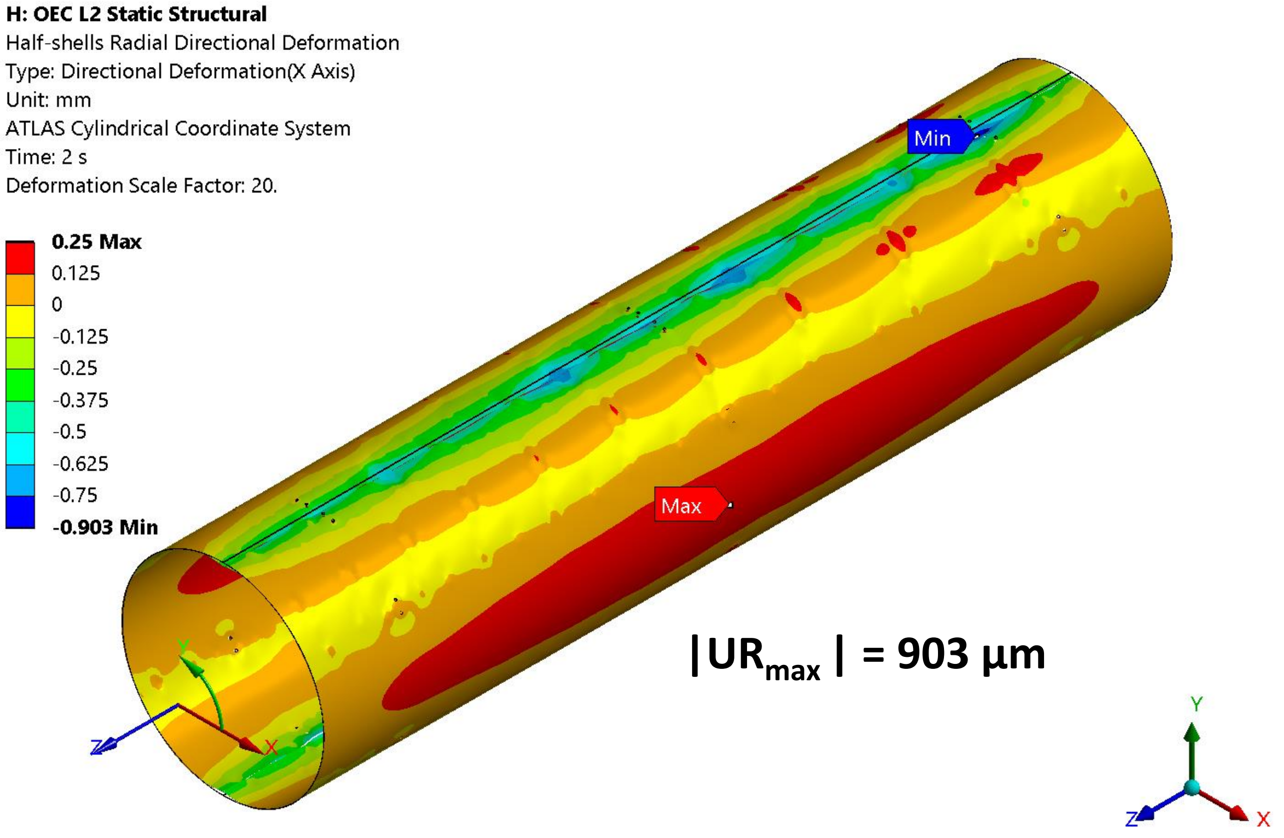

Figure: OEC L2 – Half-shells Radial deformation after cooling down @-55°C

OEC thermo-mechanical FEA: Layer 2 results

Load step 2: Cooling down from +20°C to – 55°C

Front/rear flanges Radial deformation

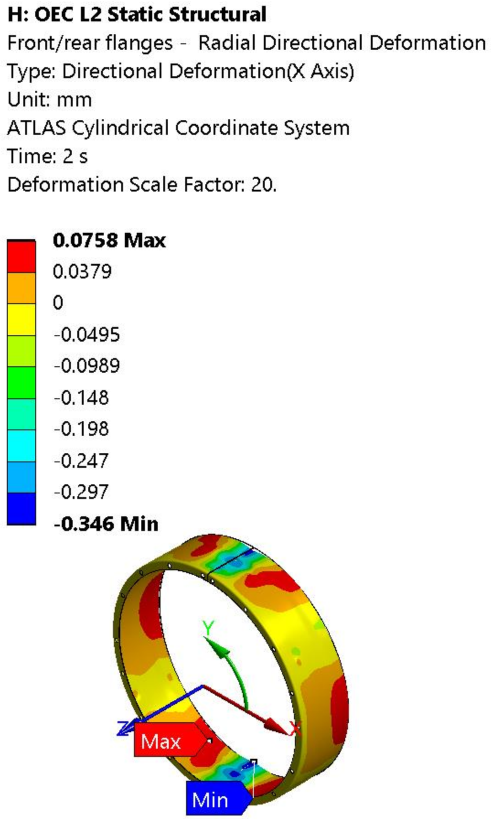

$|UR_{max}|$ = 346 µm

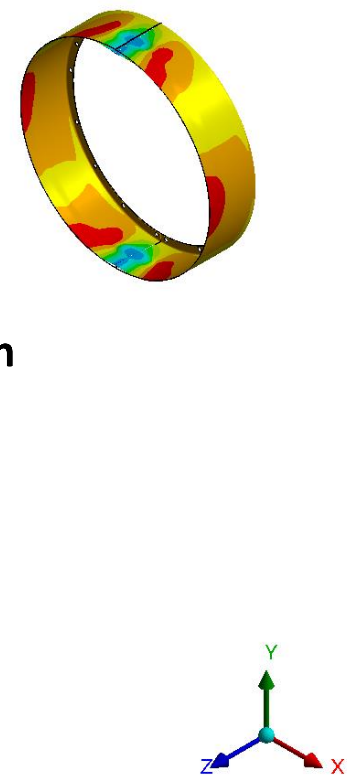

Figure: OEC L2 – Front/rear flanges Radial deformation after cooling down @-55°C

FEA results - Spec. ID S3.1: Gravitational sag

- Analysis with a single load step: applied gravity g = 9.8066 ms^{-2} along –Y axis.
- **Total mass of OEC** calculated via FEA model: **55.355 kg < 64.440 kg** (Design value [1]).
- **Maximum gravitational sag**: **$|UY|_{max}$ = 0.111 mm < 0.5 mm** (Spec. Range [1]).

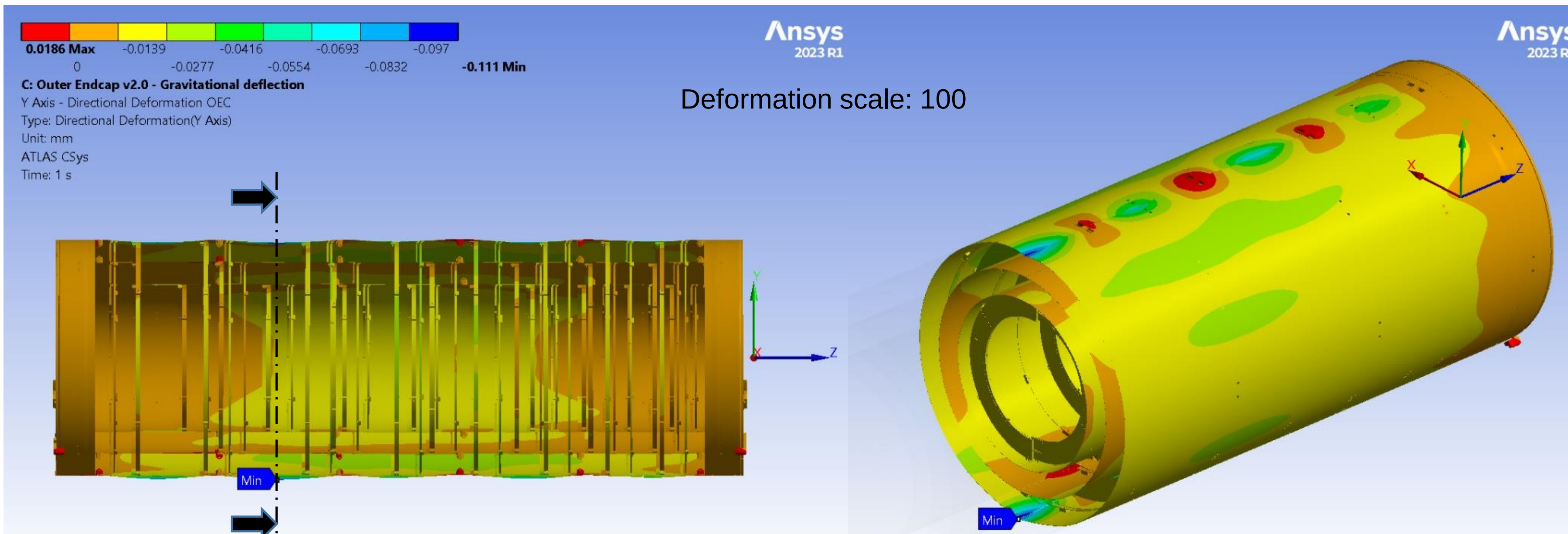

$|UY|_{max}$ = 0.111 mm < 0.5 mm

Figure: OEC gravitational sag.

FEA results - Spec. ID S3.2: First vertical modal frequency

AT2-IP-ES-007 Rev. 4 - Section 6 [1] *- Performance Specifications:*

S3.1 (Gravitational sag) & S3.2 (First vertical modal frequency)

Under the assumption that a structure behaves as a single degree of freedom simple harmonic oscillator, the gravitational sag (δ) and first vertical modal frequency (f) are related through the following expression:

$$f = \frac{1}{2\pi}\sqrt{\frac{g}{\delta}}$$

Expected theoretical value for the first vertical modal frequency of the OEC:

- Maximum OEC sag found by FEA: $\boldsymbol{\delta = |UY|_{max} = 0.111}$ **mm**
- g = 9806 mms^{-2}:

$$f = \frac{1}{2\pi}\sqrt{\frac{g}{\delta}} = \frac{1}{2\pi}\sqrt{\frac{9806}{0.111}} = \mathbf{47.3\ Hz}$$

FEA results - Spec. ID S3.2: First vertical modal frequency

- **First vertical modal frequency** found by FEA: $\mathbf{f_{1st,v}}$ **= 45.05 HZ > 25 Hz** (Spec. Range [1]).
- **Good agreement with the expected theoretical value based on gravitational sag.**

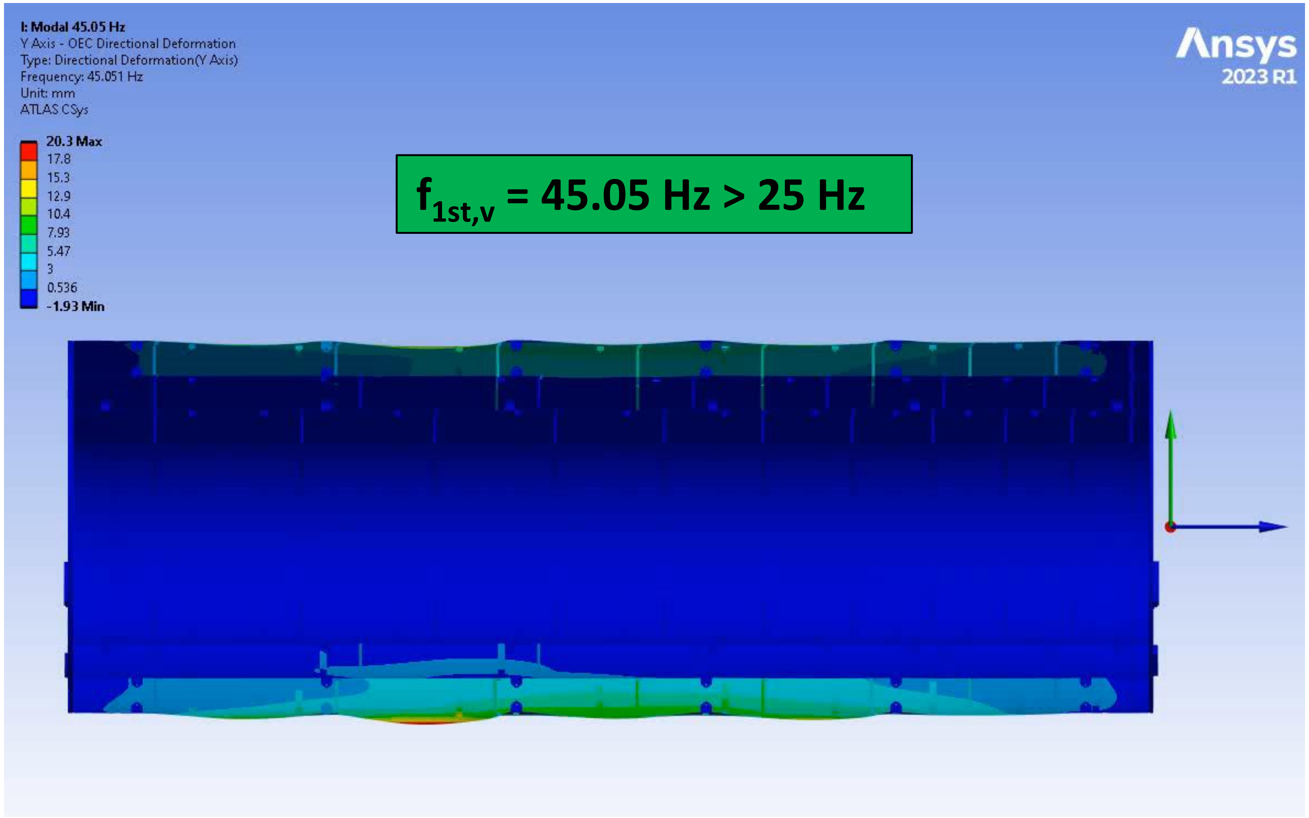

Animation: first vertical modal frequency of the OEC global structures .

FEA results - Spec. ID S3.3/S3.4: Short and Long term stability

AT2-IP-ES-007 Rev. 4 - Section 6 [1] *- Performance Specifications:*

The specifications for short and long-term stability are defined in the ITK alignment and stability requirements (ATY-SYS-ES-0027). This sets the specifications for the maximum allowable displacements of a module over a period of 1 day (short term) and 1 month (long term).

S3.3 - ***Short Term***

- *Variation in module power of 10%,*
- *Variation in evaporation temperature of +/- 1°C*

1-day stability period:

Target values: δR = ±14µm, δRφ=±3µm, δZ = ±30µm

S3.4 - ***Long Term***

- *Variation in the environmental relative humidity from 10% to 50%*
- *Variation in evaporation temperature of +/- 3°C*

1-month stability period:

Target values: δR = ±14µm, δRφ=±7µm, δZ = ±30µm

FEA results - Spec. ID S3.3/S3.4: Short and Long term stability

Stability FEA studies performed on a single L4 half-ring, connected to a portion of half-shell [4] (the worst condition for amplitude of the sensors displacements), clearly showed that:

- For the **short term stability, 10% change in power dissipation contributes less than 3.5% to sensors displacements**, compared to the contribution of 1°C change in CO_2 evaporation temperature.
- For the **long term stability, 40% change in moisture content of the CFRPs has a negligible effect to sensors displacements (less than 1%)**, compared to the deformation globally induced by the CTE, under a change in CO_2 evaporation temperature of 3°C.

For these reasons, performing the OEC stability FEA studies, the **displacements of the modules have been evaluated at the isothermal temperature of -45°C** (OTR lower limit) and then divided them by the $|\Delta T| = 65$°C, **to calculate the module displacements per Celsius degree** (the FEA analysis is completely linear).

The OEC contains 1,172 Pixel modules (468 on L4, 352 on L3, 352 on L2) so, for the GM&I FDR purposes, it has been decided to **evaluate the sensor displacements (R,rφ,Z) in the center of mass of the Pixel modules** (footprints on half-rings CFRPs with distributed massed applied).

[4] AT2-IP-ER-0010 v.3
2024-02-02_L4-Half-Ring_New_Thermo-Mechanical_Stability_FEA_studies_under_Flexible_B.C
https://edms.cern.ch/document/2474998/3.

FEA results - Spec. ID S3.3/S3.4: Short and Long term stability

L4 Pixel modules – displacements of the center of mass

- **No violations of the short term stability**, for all L4 modules.

- FEA detected **violations of the long term stability in R for 10 modules** (target value: δR = ±14μm)**, over a total of 468**. These modules are located at the top of the half-rings, mainly in the central region of the OEC. Table below, shows the details of the FEA results for the modules involved.

LAYER	HALF RING	MODULE	UR [μm]	Urφ [μm]	UZ [μm]	δR [μm/°C]	δrφ [μm/°C]	δZ [μm/°C]	δR [μm/°C]	δrφ [μm/°C]	δZ [μm/°C]
L4	LH HR3	M26	-322.9	56.2	-13.8	-5.0	0.9	-0.2	-14.9	2.6	-0.6
L4	RH HR3	M26	-374.7	-0.9	-5.6	-5.8	0.0	-0.1	-17.3	0.0	-0.3
L4	RH HR4	M26	-337.5	-9.4	119.2	-5.2	-0.1	1.8	-15.6	-0.4	5.5
L4	LH HR5	M26	-366.2	68.4	-3.1	-5.6	1.1	0.0	-16.9	3.2	-0.1
L4	RH HR5	M25	-330.2	-53.9	5.1	-5.1	-0.8	0.1	-15.2	-2.5	0.2
L4	RH HR5	M26	-421.1	-13.5	-4.4	-6.5	-0.2	-0.1	-19.4	-0.6	-0.2
L4	LH HR6	M26	-373.2	69.7	67.9	-5.7	1.1	1.0	-17.2	3.2	3.1
L4	RH HR6	M25	-333.4	-65.9	63.1	-5.1	-1.0	1.0	-15.4	-3.0	2.9
L4	RH HR6	M26	-431.9	-22.9	65.5	-6.6	-0.4	1.0	-19.9	-1.1	3.0
L4	RH HR7	M26	-346.6	-25.5	143.0	-5.3	-0.4	2.2	-16.0	-1.2	6.6

Table: L4 modules violating long term stability in R.

FEA results - Spec. ID S3.3/S3.4: Short and Long term stability

L4 Pixel modules – displacements of the center of mass

- **100% of the modules meet the short term specifications (R,rφ,Z).**
- **100% of the modules meet the long term specifications in rφ,Z.**
- **97.9% of the L4 modules meet the long term specifications in R.**

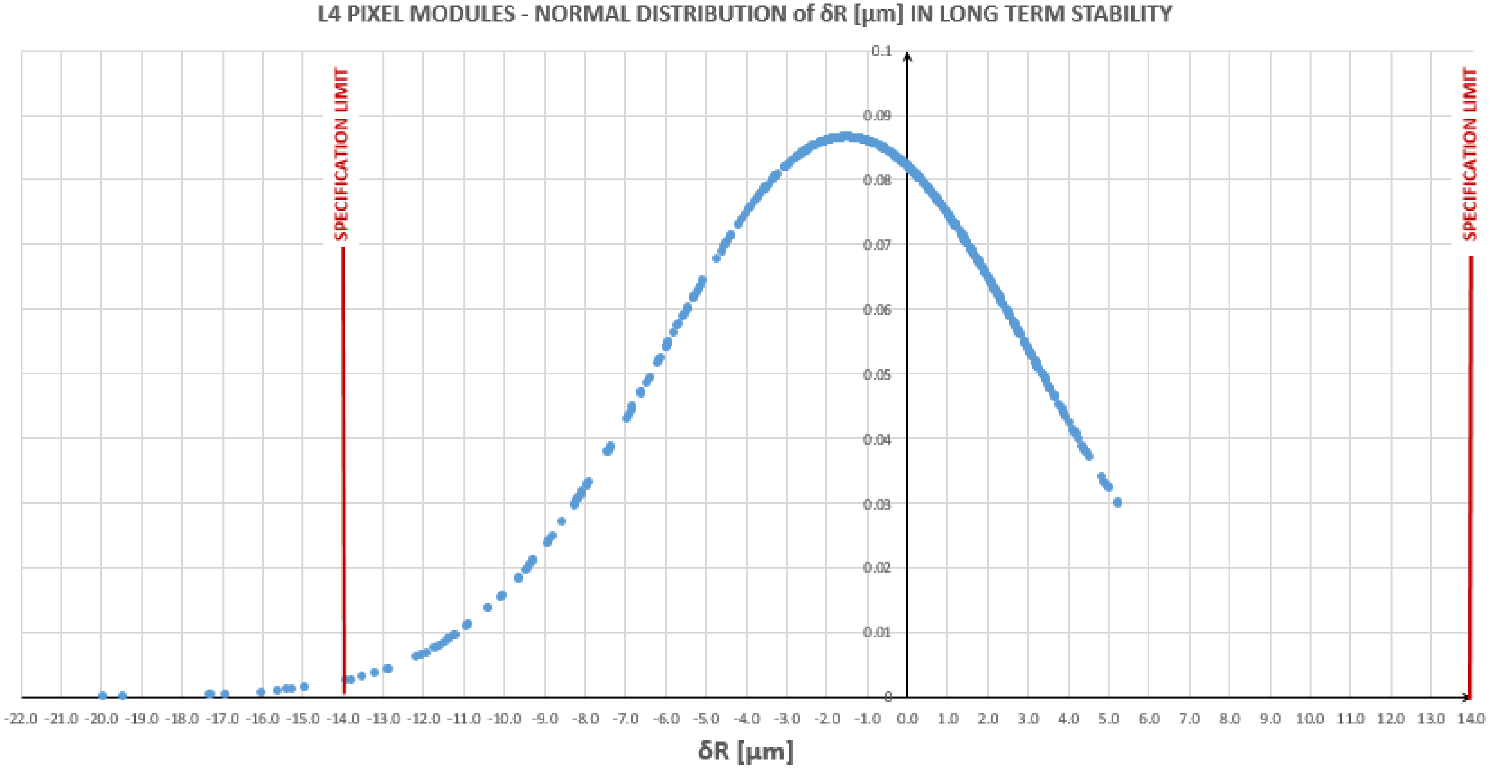

FEA results - Spec. ID S3.3/S3.4: Short and Long term stability

L3 Pixel modules – displacements of the center of mass

- **No violations of the short term stability**, for all L3 modules.
- FEA detected **violations of the long term stability for 16 modules (n.4 in R, n.12 in phi**, target values: δR=±14μm, δrϕ=±7μm) **over a total of 352**. These modules are mainly located at the top of the half-rings, in the central region of the OEC. Table below, shows the details of the FEA results for the modules involved.

L3	LH HR4	M19	-67.3	162.7	8.9	-1.0	2.5	0.1	-3.1	7.5	0.4
L3	LH HR4	M18	-15.6	160.0	6.1	-0.2	2.5	0.1	-0.7	7.4	0.3
L3	LH HR4	M20	-136.6	153.9	15.2	-2.1	2.4	0.2	-6.3	7.1	0.7
L3	LH HR5	M01	-306.5	-94.5	-79.7	-4.7	-1.5	-1.2	-14.1	-4.4	-3.7
L3	LH HR5	M17	41.0	173.0	-1.6	0.6	2.7	0.0	1.9	8.0	-0.1
L3	LH HR5	M19	-95.8	181.9	-17.9	-1.5	2.8	-0.3	-4.4	8.4	-0.8
L3	LH HR5	M16	90.4	157.6	6.5	1.4	2.4	0.1	4.2	7.3	0.3
L3	LH HR5	M18	-22.8	183.6	-9.7	-0.4	2.8	-0.1	-1.1	8.5	-0.4
L3	LH HR5	M20	-185.1	169.2	-21.6	-2.8	2.6	-0.3	-8.5	7.8	-1.0
L3	LH HR5	M22	-382.5	97.5	-35.7	-5.9	1.5	-0.5	-17.7	4.5	-1.6
L3	RH HR5	M22	-320.3	-66.0	-15.6	-4.9	-1.0	-0.2	-14.8	-3.0	-0.7
L3	LH HR6	M17	38.4	156.1	15.0	0.6	2.4	0.2	1.8	7.2	0.7
L3	LH HR6	M19	-70.5	168.5	21.6	-1.1	2.6	0.3	-3.3	7.8	1.0
L3	LH HR6	M18	-13.9	165.9	17.8	-0.2	2.6	0.3	-0.6	7.7	0.8
L3	LH HR6	M20	-145.3	158.5	29.1	-2.2	2.4	0.4	-6.7	7.3	1.3
L3	LH HR6	M22	-311.9	102.7	31.0	-4.8	1.6	0.5	-14.4	4.7	1.4

Table: L3 modules violating long term stability in R,rphi.

FEA results - Spec. ID S3.3/S3.4: Short and Long term stability

L3 Pixel modules – displacements of the center of mass

- **100% of the modules meet the short term specifications (R,rφ,Z).**
- **100% of the modules meet the long term specifications in Z.**
- **98.9% of the modules meet the long term specifications in R, 96.6% in rφ.**

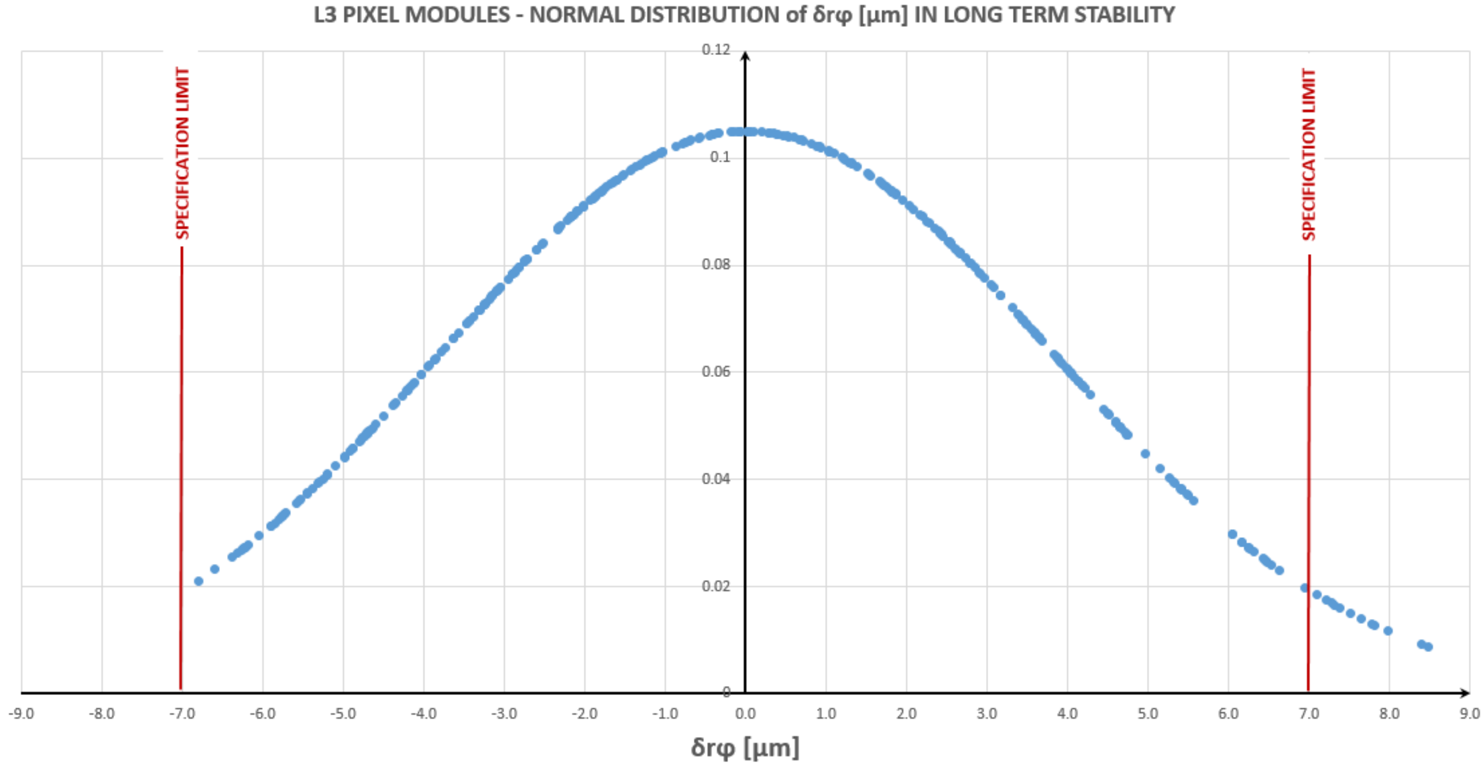

FEA results - Spec. ID S3.3/S3.4: Short and Long term stability

L2 Pixel modules – displacements of the center of mass

- **No violations of the short term stability**, for all L2 modules.

- FEA detected **violations of the long term stability for 15 modules in phi** (target value: δrϕ=±7µm) **over a total of 352**. These modules are mainly located located at the top of the half-rings, in the central region of the OEC. Table below, shows the details of the FEA results for the modules involved.

L2	LH HR5	M13	19.2	158.3	-6.8	0.3	2.4	-0.1	0.9	7.3	-0.3
L2	LH HR5	M14	-48.1	162.2	-1.6	-0.7	2.5	0.0	-2.2	7.5	-0.1
L2	LH HR6	M13	24.9	170.2	1.8	0.4	2.6	0.0	1.1	7.9	0.1
L2	LH HR6	M15	-137.6	161.0	10.4	-2.1	2.5	0.2	-6.4	7.4	0.5
L2	LH HR6	M14	-49.2	174.0	9.5	-0.8	2.7	0.1	-2.3	8.0	0.4
L2	LH HR7	M13	29.4	173.5	1.8	0.5	2.7	0.0	1.4	8.0	0.1
L2	LH HR7	M15	-136.2	165.4	9.6	-2.1	2.5	0.1	-6.3	7.6	0.4
L2	LH HR7	M12	88.2	154.2	-3.5	1.4	2.4	-0.1	4.1	7.1	-0.2
L2	LH HR7	M14	-45.5	178.1	9.2	-0.7	2.7	0.1	-2.1	8.2	0.4
L2	LH HR8	M13	29.2	170.8	11.0	0.4	2.6	0.2	1.3	7.9	0.5
L2	LH HR8	M15	-136.5	162.6	25.7	-2.1	2.5	0.4	-6.3	7.5	1.2
L2	LH HR8	M12	87.2	151.2	2.9	1.3	2.3	0.0	4.0	7.0	0.1
L2	LH HR8	M14	-46.5	174.8	21.3	-0.7	2.7	0.3	-2.1	8.1	1.0
L2	LH HR9	M13	23.8	154.5	13.2	0.4	2.4	0.2	1.1	7.1	0.6
L2	LH HR9	M14	-44.8	158.4	22.3	-0.7	2.4	0.3	-2.1	7.3	1.0

Table: L2 modules violating long term stability in rphi.

FEA results - Spec. ID S3.3/S3.4: Short and Long term stability

L2 Pixel modules – displacements of the center of mass

- **100% of the modules meet the short term specifications (R,rφ,Z).**
  - **100% of the modules meet the long term specifications in R,Z.**
  - **95.7% of the modules meet the long term specifications in rφ.**

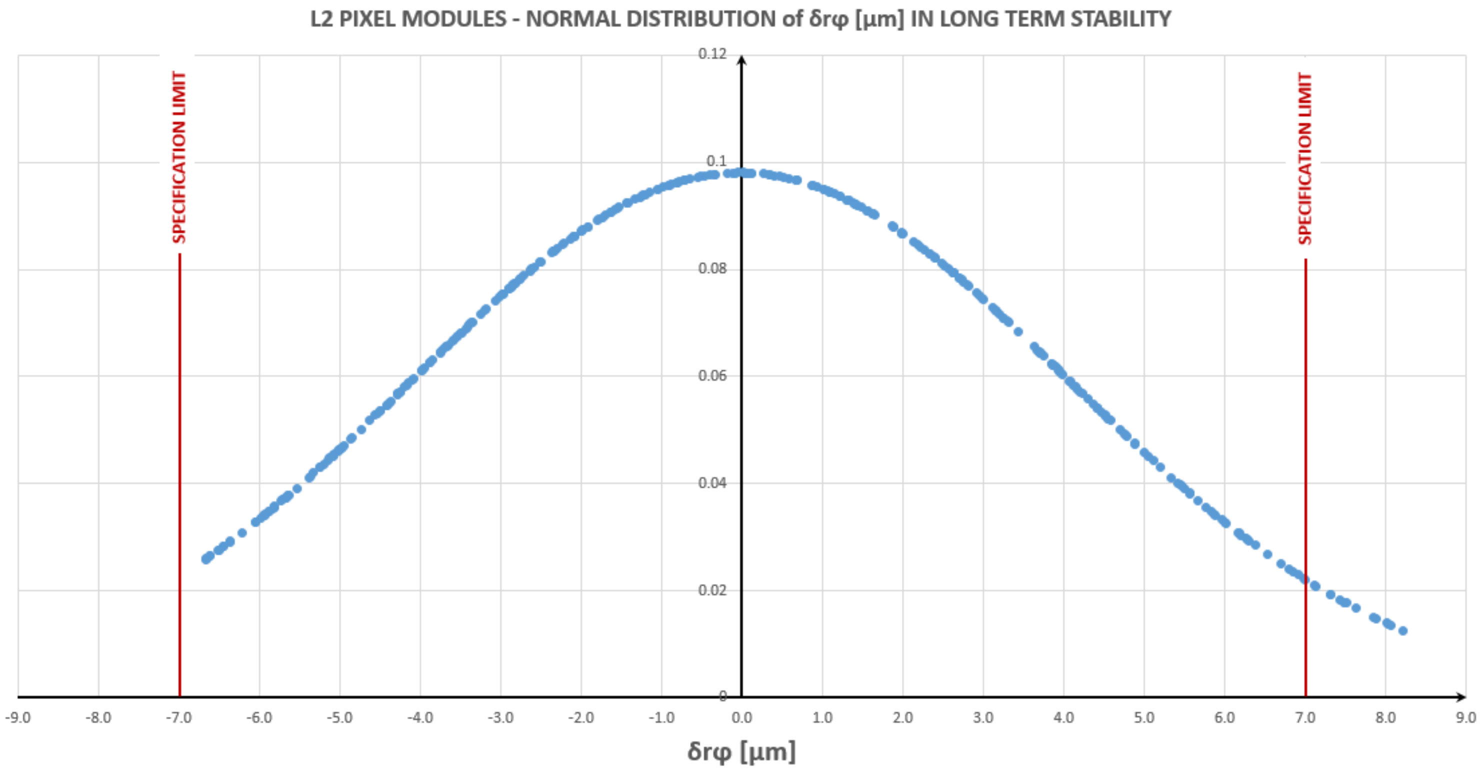

FEA results - Spec. ID S3.3/S3.4: Short and Long term stability

Summary Table of the OEC FEA Stability Studies

LAYER OF THE OEC	SHORT TERM STABILITY						LONG TERM STABILITY					
	SPECIFICATION LIMITS			SPECIFICATIONS VIOLATION			SPECIFICATION LIMITS			SPECIFICATIONS VIOLATION		
	δRmax [μm] ±14	δrφmax [μm] ±3	δZmax [μm] ±30	% OF PIXEL MODULES OVER THE TOTAL OF THE LAYER			δRmax [μm] ±14	δrφmax [μm] ±7	δZmax [μm] ±30	% OF PIXEL MODULES OVER THE TOTAL OF THE LAYER		
	FEA RESULTS						FEA RESULTS					
	δR_{max} [μm]	$\delta r\varphi_{max}$ [μm]	δZmax [μm]	R	rφ	Z	δR_{max} [μm]	$\delta r\varphi_{max}$ [μm]	δZmax [μm]	R	rφ	Z
L4	-6.6	2.3	2.6	0%	0%	0%	-19.9	6.9	7.9	2.1%	0%	0%
L3	-5.9	2.8	-1.2	0%	0%	0%	-17.7	8.5	-3.7	1.1%	3.4%	0%
L2	-3.9	2.7	1.0	0%	0%	0%	-11.7	8.2	3.0	0%	4.3%	0%

Table 10: summary of the results of the short and long term Stability FEA studies.

OEC FEA studies conclusions -1

The results of the structural and thermo-mechanical FEA, performed to assess the compliance of the global structures of the OEC to the performance specifications of the *ITk Pixel Global Supports Design Specifications - AT2-IP-ES-0007 Rev. 4* [1], give these responses:

1. No violation of the OEC envelope by the structures involved (L4 half-shells for outer envelope, front/rear supports and L2 half-rings for inner envelope), after a cooling down to the limit of the Design Temperature Range (-55°C), applying a safety factor of 1.5 to the masses.
2. Maximum gravitational sag of the OEC found by FEA (UY = -0.111 mm) within the specification limit of 0.5 mm, by a factor 4.5.
3. First vertical modal frequency of the OEC global structures, found by FEA ($f_{1st,v}$ = 45.05 Hz) is greater than the minimum specification value (25 Hz).
4. Evaluating the displacements of the Pixel modules in their center of mass, at the OTR limit (-45°C) and applying the gravity (g=9.806 ms^{-2}), all the modules meets the short term specification requirements (δR, δrφ, δZ). Long term stability violations (δR for L4, δR, δrφ for L3, δrφ for L2) involve a marginal number of Pixel Modules in the central region of the OEC, mainly at the top of the half-rings, in any case over 2σ limits (95.5%) of a Normal Distribution of the δ displacements.

OEC FEA studies conclusions -2

5. The preliminary stress analysis performed on isotropic parts made in ULTEM 1000, at the lower Design Temperature Range limit and under gravity (without mass safety factor), shows that both interlinks and mounting lugs are safe, because Von Mises stress is always lower than $\boldsymbol{\sigma_{adm}}$ by, at least, a factor 2 This conclusion assumes that the local peaks of Von Mises Stress stress, located on the edges, are not reliable, being affected by false Shear Stress values.

   The stress analysis will be repeated after the implementation of the composite parts, in the FEA model, with ANSYS ACP (mainly the half-shells).